ENHANCING INHIBITOR- AND ENZYME-BASED STRATEGIES FOR PROPHYLAXIS AGAINST ORGANOPHOSPHATE TOXICITY

By

KIRSTIN PAIGE HESTER

Bachelor of Science in Cell & Molecular Biology
Oklahoma State University
Stillwater, Oklahoma
2015

Submitted to the Faculty of the
Graduate College of the
Oklahoma State University
in partial fulfillment of
the requirements for
the Degree of
DOCTOR OF PHILOSOPHY
December, 2019

ENHANCING INHIBITOR- AND ENZYME-BASED STRATEGIES FOR PROPHYLAXIS AGAINST ORGANOPHOSPHATE TOXICITY

Dissertation Approved:

Dr. Carey Pope

Dissertation Adviser

Dr. Joshua Ramsey

Dr. Pratul Agarwal

Dr. Guangping Chen

ACKNOWLEDGEMENTS

This work would not have been possible without the contributions of many. I want to extend my sincere gratitude to my advisor, Dr. Carey Pope, for his constant guidance, encouragement, and support. The remaining members of my committee, Dr. Pratul Agarwal, Dr. Guangping Chen, and Dr. Josh Ramsey have all served as excellent mentors during my development as a scientist, and I thank them for their time and insight. I am truly grateful to have worked with such wonderful people during my time at OSU.

I would also like to express my appreciation for my fellow lab members, Tim Anderson and Stacey Herriage, for their apt assistance and kind advice. Their friendship truly enriched my time as a graduate student. Additionally, I would like to acknowledge members of the Graduate Society for Interdisciplinary Toxicology for their fellowship.

To my husband, Dustin, thank you for your unwavering support, understanding and encouragement throughout this process, I love you. Thank you to my wonderful parents, John and Karen Poindexter, who shaped me into the person I am today. While my dad is not here to celebrate this achievement with me, he instilled in me a love for learning, and the belief that I can achieve anything I set my mind to. Without him I would not be where I am today. I am lucky to have received so much support from family and friends during this process, which was as an invaluable outlet during times of both success and difficulty. I hope that one day I may return the favors that you have given me.

Finally, I want to acknowledge the financial support I have received from the department of Physiological Sciences, the Interdisciplinary Toxicology Program and the Graduate College which have allowed me to pursue this research.

Name: KIRSTIN PAIGE HESTER

Date of Degree: DECEMBER, 2019

Title of Study: ENHANCING INHIBITOR- AND ENZYME-BASED STRATEGIES FOR PROPHYLAXIS AGAINST ORGANOPHOSPHATE TOXICITY

Major Field: VETERINARY BIOMEDICAL SCIENCES

Abstract: Countermeasures against organophosphorus (OP) anticholinesterases (organophosphates) have been extensively investigated. One means of safeguarding against exposure to OP compounds is use of a prophylactic agent, which can be either enzyme- or inhibitor-based. Butyrylcholinesterase (BChE) has been shown to completely protect against OP intoxication by binding to toxicant molecules before reaching the target enzyme (acetylcholinesterase) in tissues. Its use, however, is limited due to the large amount of enzyme needed for effective protection. Reduction of the enzyme dose necessary for long-term use may be achieved by pharmacokinetic or pharmacodynamic means. The effects of 1) poly-l-lysine grafted poly(ethylene glycol) copolymer complexation and 2) re-engineering of enzyme surface loops on BChE related to prophylactic capacity (e.g. substrate and inhibitor kinetics, *in vitro* enzyme inactivation) were investigated. Complexation with PLL-g-PEG resulted in a decreased turnover number (k_{cat}) with butyrylthiocholine (BTChI), but relatively similar bimolecular rate constants (k_i) with paraoxon (7-12%). More extensive reductions in k_i were noted with other inhibitors (up to 60%). Copolymer-complexed enzymes were also less sensitive to heat and protease-mediated enzyme inactivation. While PLL-g-PEG complexation may improve the *in vivo* pharmacokinetics of BChE, we also investigated a pharmacodynamic approach. A catalytic variant of BChE, G117H, has been previously developed, though its interaction with OP compounds is too slow to be toxicologically relevant. Five $BChE_{G117H}$ mutants were produced with a 3-residue insertion into an identified hypermobile surface loop on $BChE_{G117H}$ (278-285). While loop mutants displayed decreased catalytic activity against BTChI, one loop mutant (ENA variant) had a slight but significant increase in the enzyme's reactivation rate (k_3) with paraoxon (a 50% increase). In addition to enzyme-based strategies, we also investigated the inhibitor-based prophylactic drug pyridostigmine bromide (PB). PB is effective when used in conjunction with standard antidotes, though its pharmacokinetics are suboptimal. We 3) studied the ability of nanocrystalline cellulose hydrogel formulations (NCC-PB) as an oral PB delivery vehicle for enhanced dosing logistics. *In vitro* and *in vivo* evaluations of four NCC-PB formulations suggested that the time course of cholinesterase inhibition may be extended in comparison to free PB. Overall, these studies highlight a range of approaches aimed at improving both available and developing prophylactic agents against organophosphate toxicity.

.

TABLE OF CONTENTS

Chapter Page

LIST OF TABLES viii

LIST OF FIGURES ix

I. INTRODUCTION 1

II. REVIEW OF LITERATURE 6

2.1 CHOLINERGIC SYSTEM 6
2.1.1 Butyrylcholinesterase 12
2.1.1.1 BChE Structure and Mechanism 14
2.2 ORGANOPHOSPHATES 16
2.2.1 Chemical Properties of OP Compounds 18
2.2.2 Kinetic Scheme of Cholinesterase Inhibition 18
2.2.3 Toxicity from OP Compounds 21
2.2.4 Post-Exposure Treatment 24
2.2.5 Sequelae of Toxicity 26
2.3 PRE-EXPOSURE PROPHYLAXIS 27
2.3.1 Carbamates 27
2.3.2 Bioscavengers 30
2.3.2.1 Stoichiometric 31
2.3.2.2 Catalytic 33

III. CHARACTERIZATION OF THE RELATIVE IN VITRO ENZYME ACTIVITY, INHIBITOR INTERACTION, OP BIOSCAVENGING CAPACITY, AND STABILITY OF FREE AND COPOLYMER-COMPLEXED BCHE 36

3.1 INTRODUCTION 36
3.2 MATERIALS AND METHODS 39
3.2.1 Chemicals 39
3.2.2 Copolymer-Complexation of BChE 40
3.2.3 Colorimetric BChE Assay 41
3.2.4 Choline Substrate Kinetics 41
3.2.5 Inhibitor Kinetics 42

3.2.6 Sequestration (Bioscavenging *In Vitro*) 43
3.2.7 Heat Inactivation 44
3.2.8 Protease Inactivation 45
3.2.9 Native BChE Activity Gels 45
3.2.10 Statistical Methods 46
3.3 RESULTS 47
3.3.1 Catalytic Activity of free rhBChE and C-BCs 47
3.3.2 Sensitivity of free rhBChE and C-BCs to Inhibition 53
3.3.3 *In Vitro* Scavenging Capacity of C-BCs Against Paraoxon 61
3.3.4 Sensitivity to Inactivation by Proteases and Heat 67
3.4 DISCUSSION 74

IV. EVALUATION OF SURFACE PEPTIDE NETWORKS ASSOCIATED WITH CATALYSIS IN A VARIANT ($BCHE_{G117H}$) FOR RE-ENGINEERING 81

4.1 INTRODUCTION 81
4.2 MATERIALS AND METHODS 83
4.2.1 Chemicals 83
4.2.2 Molecular Simulations of $BChE_{G117H}$ 84
4.2.3 Expression of Selected Recombinant Loop Mutants 85
4.2.4 Choline Substrate Kinetics 86
4.2.5 Paraoxon Hydrolysis Assay 86
4.2.6 Resistance to Inhibition Assay 87
4.2.7 OP Reactivation Assay 87
4.2.8 Statistical Methods 88
4.3 RESULTS 89
4.3.1 Molecular Dynamics Studies 89
4.3.2 Activity of Loop Mutants with BTChI as Substrate 91
4.3.3 Resistance to Inhibition 95
4.3.4 Reactivation of Loop Mutants 100
4.3.5 Paraoxon Hydrolysis 107
4.4 DISCUSSION 110

V. *IN VITRO* AND *IN VIVO* EVALUATION OF TOXICOKINETICS/TOXICODYNAMICS OF FREE PYRIDOSTIGMINE AND PYRIDOSTIGMINE IN NANOCRYSTALLINE CELLULOSE HYDROGELS 114

5.1 INTRODUCTION 114
5.2 MATERIALS AND METHODS 116
5.2.1 Chemicals 116
5.2.2 Animals 117
5.2.3 Radiometric Cholinesterase Assay 117
5.2.4 *In Vitro* Time Course of ChE Inhibition 118
5.2.5 *In Vivo* Pharmacodynamic Evaluation 118

5.2.6 Statistical Methods 120
5.3 RESULTS 120
5.3.1 *In Vitro* Evaluation of NCC-PB 120
5.3.2 *In Vivo* Evaluation of NCC-PB0 128
5.4 DISCUSSION 135

VI. CONCLUSIONS 139

REFERENCES 142

LIST OF TABLES

Table Page

3-1 Substrate kinetic parameters (k_{cat}, K_M, and k_{cat}/K_M) for free rhBChE and C-BCs. ... 52
3-2 Bimolecular rate constants (k_i) of free rhBChE and C-BCs 60

4-1 Substrate kinetic parameters (k_{cat}, K_M, and k_{cat}/K_M) for $BChE_{G117H}$ and loop mutants..... 94
4-2 Enzyme reactivation of $BChE_{G117H}$ and loop mutants with DFP..... 105
4-3 Comparison of the substrate kinetics parameters of $BChE_{G117H}$ and loop mutants using PO..... 109

LIST OF FIGURES

FIGURE PAGE

2-1 Actions at the cholinergic synapse 11
2-2 Interaction of OP compounds and AChE 20

3-1 Activity of rhBChE after dilution with PBS or PBS+BSA 49
3-2 Activity of free rhBChE and C-BCs 50
3-3 Concentration-dependent hydrolysis of BTChI by free rhBChE and C-BCs 51
3-4 Concentration- and time-dependent inhibition of free rhBChE by PO, DFP, PB, and EthP 55
3-5 Concentration- and time-dependent inhibition of LMW C-BCs by PO, DFP, PB, and EthP 56
3-6 Concentration- and time-dependent inhibition of MMW C-BCs by PO, DFP, PB, and EthP 57
3-7 Concentration- and time-dependent inhibition of HMW C-BCs by PO, DFP, PB, and EthP 58
3-8 Secondary plots for bimolecular rate constant (k_i) determination 59
3-9 CarbE sensitivity to inhibition by paraoxon 63
3-10 Sensitivity of CarbE and BChE to ethopropazine 64
3-11 *In vitro* inactivation of paraoxon by free rhBChE and C-BCs 65
3-12 *In vitro* sequestration capacity of free rhBChE and C-BCs 66
3-13 Heat inactivation of free rhBChE and C-BCs 70
3-14 Time course of heat inactivation of free rhBChE and C-BCs 71
3-15 Protease-mediated inactivation of free rhBChE and C-BCs 72
3-16 Native activity gels of free rhBChE and MMW C-BCs following physical and biochemical inactivation 73

4-1 Average distance of substrate molecules to the active site of $BChE_{G117H}$ 90
4-2 Activity of $BChE_{G117H}$ and loop mutants with BTChI as substrate 92
4-3 Concentration-dependent hydrolysis of BTChI by $BChE_{G117H}$ and loop mutants 93
4-4 BChE sensitivity to inhibition by PO, DFP, and EthP 97
4-5 Preliminary range finding assays for resistance to inhibition of $BChE_{G117H}$ and loop mutants 98
4-6 Comparative resistance to inhibition of $BChE_{G117H}$ and loop mutants following a 10-min exposure to paraoxon (50 µM final), DFP (5 µM final) or EthP (100 µM final) 99
4-7 Recovery of $BChE_{G117H}$ and loop mutant activity following exposure to PO 102
4-8 Recovery of $BChE_{G117H}$ and loop mutant activity following exposure to DFP 103

FIGURE PAGE

4-9 Recovery of $BChE_{G117H}$ and loop mutant activity following exposure to EthP 104
4-10 Reactivation rates (k_3) of $BChE_{G117H}$ and loop mutants following exposure to 10 mM of an OP compound (PO, DFP or EthP). 106
4-11 Concentration-dependent hydrolysis of PO by $BChE_{G117H}$ and loop mutants 108

5-1 *In vitro* time course of intestinal ChE inhibition by PB or NCC-PB 123
5-2 *In vitro* time course of whole blood ChE inhibition by PB or NCC-PB 124
5-3 Comparison of intestinal ChE inhibition by PB or NCC-PB at selected time points 125
5-4 Comparison of whole blood ChE inhibition by PB or NCC-PB at selected time points. 126
5-5 Comparison of whole blood ChE inhibition by PB or TEMPO-PB at 24 hours 127
5-6 Comparison of acute toxicity following treatment with PB or NCC-PB0 130
5-7 Comparison of whole blood ChE inhibition following *in vivo* exposure to 0.5 MTD of PB or NCC-PB0 131
5-8 Comparison of whole blood ChE inhibition following *in vivo* exposure to 0.3 MTD of PB or NCC-PB0 132
5-9 Twenty-four-hour time course of ChE inhibition following oral PB or NCC-PB0 .. 133
5-10 Twenty-four-hour body weight comparison of animals treated with PB or NCC-PB0 134

CHAPTER I

INTRODUCTION

Organophosphorus (OP) compounds are a diverse class of chemicals both utilized as pesticides and exploited as agents of chemical warfare and terrorism. OP compounds share a common mechanism of action by inhibition of acetylcholinesterase (AChE) and subsequent overstimulation of the cholinergic system. During WWII several new OP compounds were developed, and their high human toxicity was quickly recognized [1]. These highly toxic OP compounds became known as nerve agents. Chemical warfare and terrorism attacks with nerve agents have been reported since the 1980s, with recent recognition due to their use in the murder of Kim Jong Nam (the former heir apparent to North Korea) and the attempted murder of former Russian spy Sergei Skripal in 2017 and 2018, respectively [2-4]. While efforts to prevent the use of nerve agents have been largely effective, recent history suggests the threat of a nerve agent attack persists.

Anticholinesterase toxicity manifests as excess salivation, gastrointestinal upset, muscle tremors and fasciculations, and difficulty breathing, with seizures and death occurring in more severe exposures [5]. Treatments are available to manage signs and symptoms of toxicity, though there is evidence that long-term neurological deficits persist following exposure, even when current treatments are administered [6]. Moreover, it is

important to recognize that severe exposures (with some compounds, milligram amounts) can cause death in less than 10 minutes. During a realistic exposure scenario, in these cases it is dubious that potentially life-saving treatments would be delivered within the necessary time frame. As a result, there is a need for countermeasures which can reliably prevent both lethality and neurological sequelae from severe OP intoxications.

One approach for improving the consequences of OP toxicity are prophylactic agents, which would be taken in cases when there is a perceived threat of nerve agent exposure. It is likely that this approach would only be utilized in individuals deemed high-risk for exposure, for example soldiers and military physicians. Despite this, highly effective prophylactic agents could conceivably improve outcomes during a civilian attack, as temporary resistance to OP toxicity in first responders could facilitate the emergency response.

Prophylaxis against OP toxicity can be carried out *via* acetylcholinesterase inhibitor- (e.g., a carbamate anticholinesterase) or enzyme- (e.g., butyrylcholinesterase) based strategies. Both types have demonstrated efficacy, though both face challenges relating to their pharmacokinetic and/or pharmacodynamic properties. We hypothesized that systematic modulation of inhibitor- and enzyme-based strategies by nanomaterial-based formulation and computer modeling-driven protein re-engineering can improve their respective prophylactic properties. This project was divided into three aims, wherein three different strategies for improvement of prophylactic agents were evaluated.

Butyrylcholinesterase (BChE), a close relative of AChE, has been extensively investigated as a prophylactic agent. BChE stoichiometrically binds all OP compounds. Therefore, when BChE is present in large amounts it acts as a molecular sponge,

removing toxicant molecules from the circulation before reaching synaptic AChE molecules. Injected BChE is both safe and effective at preventing **all** adverse effects of OP exposure when administered in sufficient doses [7, 8]. Despite its effectiveness, there are economic barriers to the implementation of BChE as a prophylactic agent. One potential mechanism to overcome this barrier is development of modifications which prolong the circulation of BChE, thereby decreasing the necessary dosing frequency and total protein amount needed.

The goal of Aim 1 was to evaluate enzymatic properties of BChE in complex with a biodegradable poly-l-lysine graft poly(ethylene glycol)(PLL-g-PEG) copolymer of three different sizes. Modification of BChE with a PLL-g-PEG copolymer has the potential to improve pharmacokinetic properties of the enzyme [9, 10]. However, previous studies have demonstrated that PEG conjugation alone may alter enzymatic properties such as catalytic activity, protease sensitivity, and heat tolerance [11-13]. As these characteristics could have an impact on BChE's prophylactic efficacy, we investigated the effect of PLL-g-PEG on these properties. Moreover, enzyme modifications aimed at improving the pharmacokinetic profile of BChE must not significantly hinder the enzyme's ability to bind OP compounds. We therefore performed inhibitor kinetics and an *in vitro* scavenging assay to inform our final conclusions.

While complexation with PLL-g-PEG was aimed at improving BChE's pharmacokinetic properties, the next approach was focused on improving pharmacodynamic interactions. Due to the stoichiometric nature of the reaction between BChE and OP compounds, a severe exposure to an anticholinesterase can overcome the protection provided by BChE. Therefore, enzyme prophylactics which are catalytically

active towards OPs would be superior, as they would require less total protein and are not consumed as a result of interaction with the OP. A single nucleotide mutant of BChE, G117H, has been previously developed and shown to hydrolyze multiple OP compounds; however, the turnover rate against OP molecules is too slow to be physiologically relevant [14]. Aim 2 sought to improve the turnover rate of $BChE_{G117H}$ using a molecular dynamics-based re-engineering strategy. The conceptual framework for this approach was based on previous findings that manipulation of catalysis-linked dynamic surface loops can increase enzymatic activity [15]. In this study, we identified a promising surface loop and produced mutant enzymes which contained a three-residue insertion in the sequence of interest. It was postulated that increasing the length of a dynamic peptide loop with hydrophilic residues could increase energy transfer from the solvent to the active site. These loop mutants were evaluated for catalytic activity against the model substrate butyrylthiocholine and selected OP anticholinesterases. Resistance to inhibition and enzyme reactivation assays were also performed to further elucidate the effect of our three-residue insertion on OP hydrolysis.

The final aim of this study focused on the inhibitor-based prophylactic, pyridostigmine bromide (PB). Pyridostigmine was used by soldiers as a prophylactic agent during the Persian Gulf War of 1991, and has been found to increase resistance to organophosphate-induced lethality by 40 times [16]. Importantly, however, if an individual is exposed to an OP compound while using PB protection, it is still necessary to seek traditional post-exposure treatments. This is in contrast to enzyme-based strategies which can work independently. Despite this drawback, inhibitor-based strategies are the only prophylactic agents currently approved for human use, and they are

a much more affordable option. While PB is given orally, it faces similar pharmacokinetic issues as BChE (i.e. a relatively short duration of action). Cellulose-based hydrogels have been previously used to extend drug release in oral delivery systems [17, 18]. For our study, four nanocrystalline cellulose-PB formulations were produced and evaluated. Cholinesterase inhibition over time was used as a mechanism to evaluate the efficacy of the cellulose formulations to extend the release of PB, both *in vitro* and *in vivo*.

CHAPTER II

REVIEW OF LITERATURE

2.1 CHOLINERGIC SYSTEM

The cholinergic system, of which acetylcholine (ACh) is the endogenous neurotransmitter, is a major signaling pathway in many organisms, including humans. In the 1920's, Otto Loewi proved that synaptic signaling was mediated by chemical transmission. He demonstrated that fluid collected from a bath in which a heart-vagus nerve preparation was stimulated to slow the heart, could be transferred to a denervated heart in a separate bath and reduce that heart's rate. Later Dale identified the substance in the fluid that reduced heart rate as acetylcholine. Both received the Nobel Prize for their contributions. Thus acetylcholine was the first identified neurotransmitter [19].

In the central nervous system, cholinergic activity influences learning and memory, addiction, motor coordination, respiration, and thermoregulation, among other functions [20-23]. ACh also acts at the neuromuscular junction, where it is responsible for the stimulation of somatic muscle fibers [24]. Furthermore, the autonomic nervous system, which is split into the opposing sympathetic (i.e. flight-or-fight) and parasympathetic (i.e. rest and digest) branches, primarily uses cholinergic neurons to

innervate parasympathetic end organs [25]. Activation of the parasympathetic branch, mediated by cholinergic signaling (by both preganglionic and postganglionic neurons), results in decreased heart rate, miosis, increased gastrointestinal secretions and motility, urination, and many other effects. In contrast, only the preganglionic neurons of the sympathetic branch are cholinergic, with postganglionic signaling mediated by adrenergic neurons (i.e. norepinephrine-releasing). An exception to this is the eccrine sweat glands, whose postganglionic neurons are actually cholinergic. When sympathetic tone predominates, individuals experience increased blood pressure, adrenal stimulation, and diaphoresis, in addition to effects opposite those above (e.g. increased heart rate, mydriasis, inhibition of digestive functions, etc.).

The general features of ACh synthesis and metabolism are the same in the central and peripheral systems. First, acetylcholine is synthesized from choline and acetyl-CoA in the presynaptic nerve terminal by choline acetyltransferase. Much of the choline needed for ACh synthesis is recycled following ACh hydrolysis, *via* a high affinity choline uptake transporter. Uptake of choline into the nerve terminal is the rate limiting step of ACh synthesis [26]. Following synthesis, ACh is concentrated into vesicles by the vesicular ACh transporter and an energy-dependent pump [27]. Vesicle exocytosis is triggered by calcium entry into the nerve terminal following the arrival of an action potential and opening of voltage-gated calcium channels. ACh released from the cholinergic neuron diffuses across the nerve synapse where it can stimulate postsynaptic

and, in some cases, presynaptic receptors. ACh binds and activates two classes of receptors, nicotinic and muscarinic, though it displays different affinities ($K_D \sim 30$ nM for muscarinic and ~ 30 μM for nicotinic) [28]. The duration of activation resulting from ACh release is controlled by the enzyme acetylcholinesterase (AChE), which rapidly hydrolyzes unbound ACh molecules. AChE is one of the most efficient enzymes known, with a k_{cat}/K_M (10^8 x M^{-1} sec^{-1}) which approaches the diffusion-controlled limit [29]. In fact, ACh degradation occurs on a faster time scale than the receptor activation cascade, preventing receptors from being activated more than once per release [25]. As a result, cholinergic receptor activation is rapid and sensitive, able to distinguish between sequential nerve impulses, a feature particularly important at the neuromuscular junction. Figure 2-1 summarizes the general features of a cholinergic synapse.

Muscarinic acetylcholine receptors (mAChRs) are named after muscarine, a toxin produced by the mushroom *Amanita muscaria* which is an agonist at the aforementioned receptors [30]. MAChRs belong to the G protein-coupled receptor family, characterized by seven transmembrane regions and intracellular responses mediated by G proteins [30]. There are five subtypes of muscarinic receptors, M_1 - M_5, which differ in their sensitivity to pharmacological agents and participation in downstream functions. Odd numbered subtypes (M_1, M_3, M_5) facilitate cell excitation through activation of phospholipase C, while even numbered subtypes (M_2, M_4) suppress cellular excitability through adenylyl cyclase inhibition and potassium channel activation [31]. In general, M1 receptors are concentrated in the central nervous system, M_2 receptors are prominent in their modulation of cardiac function, M_3 receptors are typically responsible for parasympathetic end organ responses, and all five receptor subtypes can be found in the

brain [32, 33]. However, much overlap occurs in the overall distribution of mAChR subtypes.

Nicotinic acetylcholine receptors (nAChRs) were first identified for their sensitivity to the snake venom α-bungarotoxin, though they became known for their response to the agonist nicotine [34]. Unlike mAChRs, nAChRs are ligand-gated ion channels whose activation increases cation permeability (mainly Na^+ and K^+) to induce an excitatory reaction. A variety of nAChR subtypes exist as there are seventeen potential subunits (α1-10, β1-4, γ, δ, and ε) and individual receptors are pentamers organized around a central pore. Receptors are often heteromeric containing both α and β subunits, but some homomeric receptors have been identified. Mature skeletal muscle contains primarily $(\alpha1)_2\beta1\delta1\varepsilon1$ nAChRs, while autonomic ganglia receptors frequently occur in a $(\alpha)_2(\beta)_3$ configuration [35, 36]. Receptor subtypes found in the brain are formed from a variety of α/β combinations (e.g. $(\alpha4)_2(\beta2)_3$, $(\alpha7)_5$, $(\alpha9)_2(\alpha10)_3$, etc.), and are often located presynaptically where they modulate the release of other neurotransmitters (e.g. glutamate or dopamine), though postsynaptic nAChRs also have functional importance [37-39].

Unsurprisingly, due to its pervasiveness, the cholinergic system has considerable medical relevance. In the peripheral nervous system, cholinesterase inhibitors have been used for the management of glaucoma and myasthenia gravis. In glaucoma, locally applied cholinesterase can facilitate movement of aqueous humor and decrease ocular pressure [40]. Myasthenia gravis, characterized by muscular weakness and fatigue, is typically caused by autoantibodies against nAChRs in the neuromuscular junction, resulting in reduced receptor density which can be countered with a cholinesterase

inhibitor [41]. In the central nervous system, certain neurodegenerative and neuropsychiatric conditions may be treated *via* cholinergic modulation. Alzheimer's disease is characterized by the formation of β-amyloid plaques and neurofibrillary tangles, progressing to neuronal shrinkage and loss. Treatment with cholinesterase inhibitors (e.g. donepezil, rivastigmine) improves cognitive function in patients, though it does not slow disease progression [42, 43]. Tremors associated with Parkinson's disease may also be improved by treatment with centrally-acting muscarinic antagonists [44]. More recently, it has been suggested that receptor agonists for $(\alpha 7)_5$ nAChR and M_1 and M_4 mAChRs may be effective treatments for schizophrenia [45]. Other psychiatric conditions, including depression and bipolar disorder, may also be affected by cholinergic modulation [46].

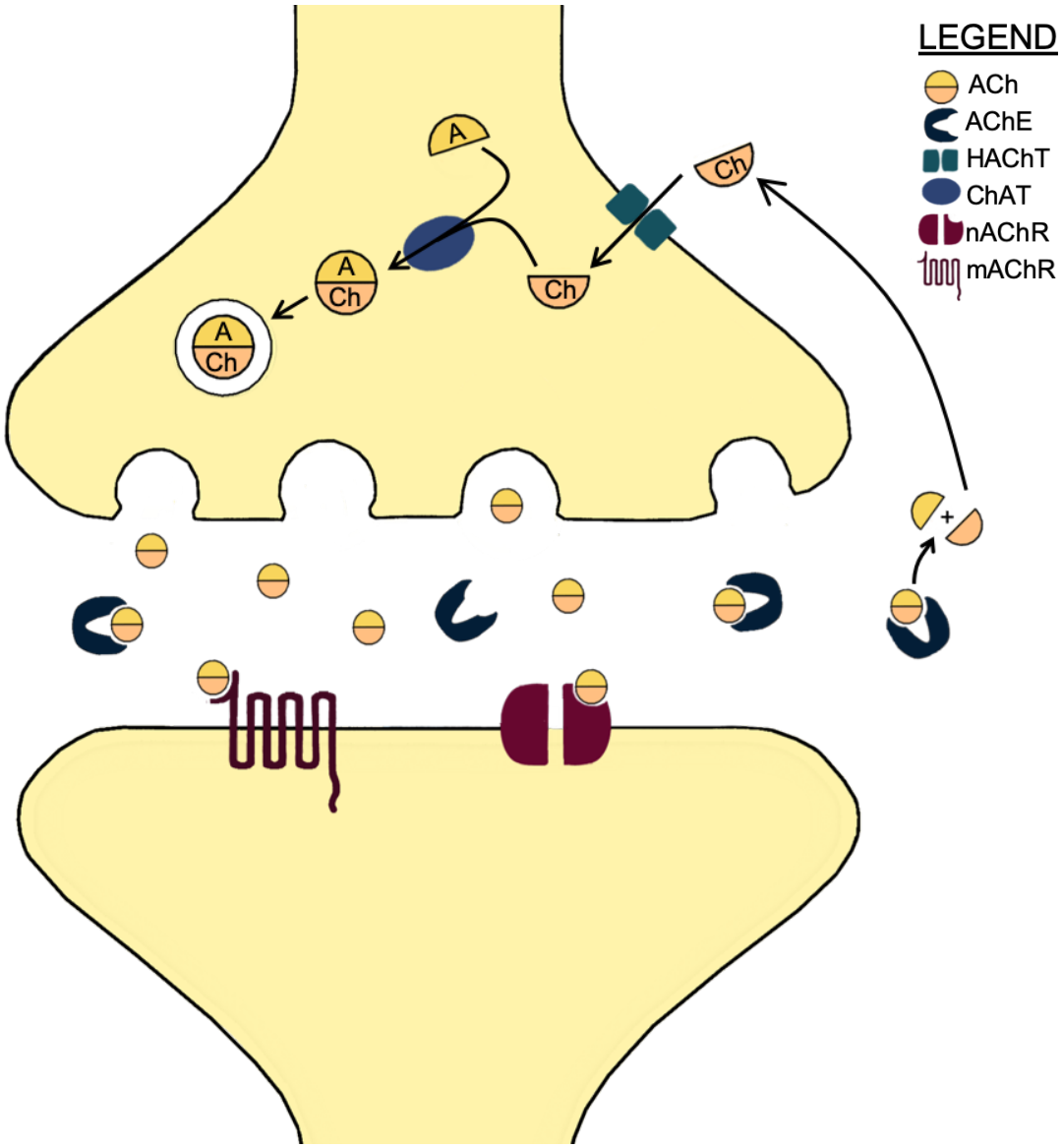

Figure 2-1. Actions at the cholinergic synapse. Acetyl-CoA (A) and choline (Ch) are synthesized into acetylcholine (ACh) by the enzyme choline acetyltransferase (ChAT), and transported into release vesicles. Following release into the synapse, ACh binds to muscarinic and/or nicotinic acetylcholine receptors (mAChR & nAChR). Acetylcholinesterase (AChE) is present in the synapse to hydrolyze ACh, and choline generated from this reaction is taken into the pre-synaptic terminal by a high affinity choline uptake transporter (HAChT).

2.1.1 Butyrylcholinesterase

Butyrylcholinesterase (BChE) is serine hydrolase that is closely related to acetylcholinesterase. It was first distinguished from AChE in the 1940s on the basis of substrate selectivity and distribution [47-49]. Originally, BChE was named pseudocholinesterase for its capacity to hydrolyze both choline and non-choline esters and its absence in brain tissue, which made it unlikely to function like the "true" cholinesterase, AChE [50].

Further research has refined the notion that BChE is not involved in cholinergic neurotransmission. While the highest levels of BChE are in the plasma and liver, it can in fact be found in the brain, skeletal muscle, and other cholinergic tissues [51, 52]. Studies in AChE knockout mice have shown that BChE can hydrolyze ACh *in vivo,* acting as a substitute for AChE, albeit a poor one [53]. Additionally, BChE knockout mice experience higher toxicity following exposure to the AChE-specific inhibitors donepezil and huperzine A [54]. These studies suggest that BChE may function to hydrolyze ACh in cholinergic synapses, under certain conditions.

In addition to its role as a "backup" for AChE, BChE has long been implicated in the metabolism of ester drugs and toxicants. In the 1950's it was recognized that the muscle relaxant succinylcholine (often used during anesthesia) caused prolonged apnea in some patients, an effect attributed to low plasma BChE activity [55]. BChE also plays a role in the metabolism of drugs such as aspirin (detoxification), cocaine (detoxification), and heroin (activation) [56-58]. The asthma prodrug bambuterol is converted by BChE into terbutaline [59]. BChE also interacts with organophosphorus toxicants similarly to

AChE [60]. This interaction is considered detoxifying, as BChE-bound OP compounds cannot thereafter interact with AChE.

Recently, a role for BChE in ghrelin metabolism has also been examined. Ghrelin is a peripherally produced peptide hormone which is implicated in meal initiation, fat accumulation, rewarding/addictive behaviors and anxiety, among a host of other effects [61-63]. BChE converts active acyl-ghrelin to inactive desacyl-ghrelin, an effect seen both *in vitro* and *in vivo* [64-66]. Studies have shown that BChE knockout mice become obese on a high-fat diet due to an abnormal increase in adiposity, an effect that can be prevented by BChE gene transfer [66-68]. In contrast, mice given a cocaine-hydrolyzing variant of BChE weekly (1 mg/kg, iv) were shown to gain less weight on a high-fat diet as compared to controls [69]. Manipulation of BChE levels through gene transfer and genetic modification have also been shown to decrease aggressive behaviors in mice [70]. Further studies are necessary to elucidate the importance of BChE on ghrelin signaling. Such metabolic effects of BChE may have relevance, however, in its use as a prophylactic agent.

Despite this array of functions, BChE activity is not considered essential. Mice completely lacking the BChE gene are indistinguishable from wild type mice under normal conditions [71]. This observation is also supported in humans. While mutations in AChE occur with low frequency, BChE mutations are relatively common. It is estimated that 35% of the American/European population has at least one mutated BChE allele, and the most frequent mutation, the K-variant, results in 33% reduced BChE activity [51, 72]. Furthermore, certain populations have been found with completely “silent” BChE activity. Studies of these individuals have revealed no abnormalities in regards to health,

fertility, and body weight [73]. Little is known, however, regarding how these individuals would react to challenges to cholinergic and ghrelin signaling pathways.

2.1.1.1 BChE Structure and Mechanism

The BChE monomer is a globular protein composed of 574 amino acids, nine N-linked glycosyl groups, and three intra-chain disulfide bonds [74]. While these monomers are catalytically independent, BChE is primarily found in the tetrameric form. The BChE tetramer is considered a dimer of dimers; BChE dimers are formed though inter-chain disulfide bonds at Cys571, and these dimers assemble *via* non-covalent interactions at the C-terminus [75, 76]. C-terminal alpha helices form a superhelical structure surrounding a proline-rich peptide to yield the tetramer [77, 78]. The native tetramer has a molecular weight of 340 kDa, of which carbohydrates contribute 24% [79]. This unique structure contributes to the long plasma half-life of human BChE (~ 11 days) [80-82].

The main structural feature of BChE is a ~20 Å long gorge protruding halfway into the protein, termed the "active site gorge" [83, 84]. Within this gorge there are several distinct regions which contribute to enzymatic function. Near its entrance, the peripheral anionic site (Asp70 and Tyr332) is responsible for initial binding of positively charged substrates (e.g. choline esters) [85, 86]. This site is also implicated in the non-Michaelian behavior of BChE (i.e. substrate activation) [87]. Ester hydrolysis occurs near the bottom of this gorge *via* a catalytic triad (Ser198, Glu325, and His438) with assistance from a nearby oxyanion hole (Gly116, Gly117, and Ala199) [83]. Two additional sites near the catalytic triad, the acyl binding pocket (Leu286, Val288, and Trp231) and the choline binding site (Trp82; sometimes called π-cation site) aid in proper substrate orientation [83, 88]. While both AChE and BChE contain these domains, the

volume of BChE's gorge is 200 Å larger than AChE due to fewer aromatic amino acids [89]. This space disparity is the basis for substrate/inhibitor selectivity, as the AChE gorge is too small to accommodate larger molecules (e.g. butyrylcholine, succinylcholine, ethopropazine, iso-OMPA) [90].

Substrate catalysis by BChE and AChE is carried out with an active site triad *via* an Ordered Uni Bi reaction mechanism (i.e. one substrate, two products). Mutations in these residues can produce an incorrectly folded enzyme with no enzyme activity [91]. During acylation, Ser198 carries out a nucleophilic attack on the carbonyl carbon, aided by a general acid-base catalytic element provided by the imidazole ring on His438. A tetrahedral intermediate is formed as a result of this attack. Proton transfer from the imidazole ion on His438 initiates the expulsion of a leaving group (product 1; e.g. choline) leading to the formation of the acylated enzyme [59]. The deacylation step begins with a nucleophilic attack by water, and results in the regenerated enzyme and product 2 (e.g. butyric acid) [92]. In the case of phosphylated adducts, altered stereochemistry results in impaired general base function of His438 during the dephosphylation step (i.e. reactivation) and consequently inhibited function [93, 94]. The last member of the catalytic triad, Glu325, does not directly participate in catalysis, but instead stabilizes the tetrahedral intermediates and transition states *via* electrostatic interactions [95]. The oxyanion hole serves a similar role, as its NH peptidic backbone stabilizes the partial negative charge which develops on the carbonyl oxygen [92, 95, 96]. Knowledge of BChE's structure and mechanism at a molecular level has enabled both past and present enzyme mutagenesis studies aimed at improving catalysis of certain substrates and hemi-substrates of BChE (e.g. OP compounds, cocaine).

2.2 ORGANOPHOSPHATES

OP compounds have a wide range of uses and applications. Due to their potent anticholinesterase activity, they have been used for over half a century as insecticides in agricultural, residential and commercial settings worldwide. In 2012, 20 million pounds of OP insecticides (accounting for 33% of U.S. insecticide market) were applied on cotton, fruit, vegetable, and orchard grape crops, among others [97]. Their market share in low-income and developing nations is even higher [98]. OP compounds can also be used as flame retardants, plasticizers, and lubricants, useful for industry and as additives in a number of household products [99, 100].

Unfortunately, these compounds were quickly recognized for their potential to be used for nefarious purposes. During a search for better insecticides in the mid-1930s, the German chemist Gerhard Schrader developed a highly potent organophosphorus compound he named tabun (ethyl dimethylamidocyanophosphate; GA) [101]. While it was too toxic to be used as an insecticide, the Nazi government took interest in the chemical as a potential warfare agent in the looming World War. By the end of the war, Germany had stockpiled between 10,000-30,000 tons of tabun, and German scientists had developed more OP warfare agents including sarin (isopropyl methylphosphonofluoridate; GB) and soman (pinacolyl methylphosphonofluoridate; GD) [5]. This class of ultra-potent OPs became known as "nerve agents" which grew to include cyclosarin (*O*-cyclohexyl methylphosphonofluoridate; GF), VX (*S*-(2-diisopropylaminoethyl) *O*-ethylmethylphosphonothiolate), and others in the proceeding decades. VX is considered the most potent nerve agent with a LCt_{50} of 10 mg(min)/m^3, which is 500-times that of cyanide [5].

While nerve agents were never deployed in WWII, they have been used in other military conflicts such as the Iraq-Iran Civil War (1980s) and the Syrian Civil War (2013), killing thousands [2, 102-104]. Sarin was used by Aum Shinrikyo, a Japanese terrorist group, to carry out attacks in Matsumoto, Japan (1994) and the Tokyo Subway (1995), which together claimed the lives of 19 individuals and hospitalized hundreds [5]. In 2017, the former heir apparent to North Korea, Kim Jong Nam, was murdered at a Malaysian airport using VX [3]. Most recently, a nerve agent was used in the attempted murder of former Russian spy Sergei Skripal and his daughter in England [4]. In the case of the Skripals, it has been reported that a Russian "Novichok" agent was used in the attack. Little is known about Novichok agents as they remain classified, but it is thought that they are even more potent than VX [105].

In 1997 a multinational treaty regarding chemical weapon use, called the Chemical Weapons Convention, was enacted. Signatory nations agreed to cease production of chemical weapons and destroy current chemical stockpiles. Originally there were 165 signatory states, and in subsequent years 28 additional states have acceded to the treaty [106]. Syria acceded to the treaty following international pressure as a result of the 2013 nerve agent attack. Subsequently, the OPCW (the governing body for the treaty) established a program to destroy Syria's remaining chemical weapons [107]. The OPCW estimates that 97% of declared chemical weapons have been destroyed [108]. As of 2019, however, three states have not acceded to the treaty: Egypt, North Korea, and South Sudan. Additionally, while Israel was one of the original signatory states, it has never ratified the treaty. Concern remains, though, that some signatory nations may have

undeclared chemical weapons [109]. Moreover, possession of chemical weapons by violent non-state actors cannot be ruled out, as evidenced by the attacks in Japan.

2.2.1 Chemical Properties of OP Compounds

Most OPs are derivatives of phosphoric, phosphonic, or phosphinic acid, containing a characteristic phosphorus-oxygen double bond. OP insecticides are often organophosphorothioates which contain a P=S group in place of P=O. These compounds must be metabolically activated (*via* oxidative desulfuration) to the "oxon" form (P=O) prior to exerting potent anticholinesterase activity [110]. In contrast, nerve agents do not require metabolic activation to exert toxicity.

OP insecticides are generally lipophilic with low volatility [111]. While these characteristics are desirable for agricultural use, exposure to highly lipophilic OP compounds may result in fatty tissue distribution and prolonged toxicity. In general, nerve agents have relatively lower lipophilicity, in most cases higher volatility (especially sarin), and higher vapor density [112]. These characteristics make aerosol formulations of nerve agents particularly hazardous (other than VX, which is primarily a contact hazard). Moreover, nerve agents are colorless and odorless which, combined with their high toxicity, make them an insidious threat [112].

2.2.2 Kinetic Scheme of Cholinesterase Inhibition

The reaction of cholinesterases (ChEs) with OP compounds follows the general outline shown in Figure 2-2. An important distinction between the two lies in the deacylation/dephosphylation step. While acylated enzymes rapidly deacylate *via* hydrolysis to regenerate the free enzyme, phosphylated enzymes do not. Because of this,

OP compounds are generally considered irreversible inhibitors; spontaneous reactivation of ChEs may occur slowly in humans (hours to days), though not at a clinically relevant rate [113-115]. In some cases, the phosphylated enzyme undergoes a further dealkylation reaction, termed aging, which results in a truly irreversibly inhibited enzyme [116]. Common nerve agents have an *in vitro* aging half-time between three minutes (soman) and 36 hours (VX) [117, 118].

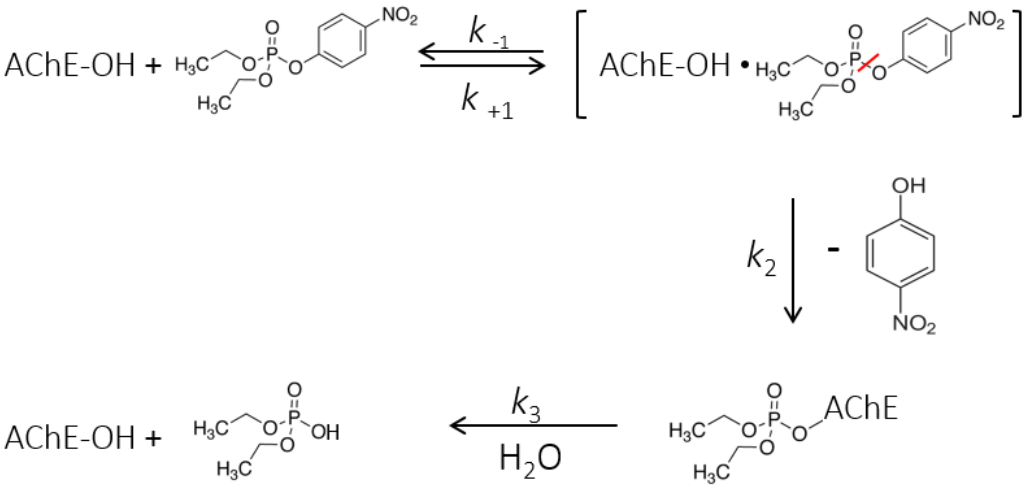

Figure 2-2 Interaction of OP compounds and AChE. First, the OP compound and AChE form a reversible Michaelis-complex (k_1/k_{-1}), however, the bond quickly progresses through this step and is phosphorylated (k_2). Following phosphorylation, the compound may go through two different pathways. The OP can reactivate, either spontaneously or through the use of nucleophilic agents (e.g. oximes, fluoride salts) at a rate of k_3. Some agents go through a dealkylation reaction prior to the k_3 step, resulting in an aged compound which cannot be reactivated.

2.2.3 Toxicity from OP Compounds

Though nerve agent exposure is the focus of much research, including herein, most acute OP compound exposures are the result of intentional insecticide poisonings. Recent data suggest that pesticide self-poisoning causes 170,000 deaths annually, accounting for about 20% of global suicides [119]. Prospective studies on hospitalized self-poisoning patients demonstrated that OP compounds were the most commonly used pesticide class (~30-60%), though increased regulations on them seem to be decreasing their prevalence over time [120-122]. Overall lethality associated with OP ingestion is around 10% for treated individuals, though it varies greatly based on the specific compound and formulation and can be up to 60% [120-123]. The variability in mortality following OP insecticide exposure is confounded by many variables including delays in treatment and treatment mismanagement.

While acute toxicity from OP compounds works primarily though inhibition of AChE, interestingly, there is some evidence that suggests differential toxicity of certain organophosphates could be due to effects on secondary targets, including acetylcholine synthesis, direct binding to receptors, and others [124]. Furthermore, some OPs inhibit other hydrolases including carboxylesterase, fatty acid amide hydrolase, and monoacylglycerol lipase [125]. As a result, the following discussion describes the typical effects of acute exposure to OP compounds. However, unique effects of certain organophosphates should not be ignored. For example, some OP compounds (e.g. tri-*o*-cresyl phosphate, leptophos, mipafox) cause delayed neurotoxicity as a result of secondary interactions with the enzyme neurotoxic esterase [126]. Further discussion of

the toxicological relevance of secondary targets of OP compounds is contained in the cited reviews [60, 127-129].

The general toxidrome resulting from overstimulation of the peripheral nervous system by OP compounds includes a variety of signs and symptoms. In the parasympathetic system, inappropriate stimulation of secretory glands induces salivation, rhinorrhea, bronchorrhea and lacrimation, while overstimulation at smooth muscle receptors results in miosis, bronchospasm, diarrhea, nausea/vomiting, and urinary incontinence. Though parasympathetic effects generally predominate, signs arising from sympathetic overstimulation also occur. Recall that eccrine sweat glands are the only sympathetic endpoint with postganglionic cholinergic neurons. As a result, excessive sweating (i.e. diaphoresis) is present in about one in four patients seen for toxicant ingestion [130, 131]. Cardiovascular effects may present as sympathetically or parasympathetically driven. In six studies of humans exposed to OP insecticides (354 patients between 1974 - 2010), an abnormal heart rate was detected in 48% of patients on admission, with 72% of those affected presenting with tachycardia [130-135]. Furthermore, patients with abnormal blood pressure (23%) were more often hypertensive (66%). These effects may arise due to increased activity in the autonomic ganglia acting to increase postganglionic adrenergic activation or adrenal stimulation and subsequent catecholamine release. It could also reflect overstimulation and failure of cholinergic signaling such that vagal input is overall reduced, leading to relative sympathetic overstimulation. Signs resulting from prolonged stimulation at the neuromuscular junction include fasciculations, weakness and flaccid paralysis, usually presenting in more severely intoxicated individuals. Victims determined to have moderate to severe

poisoning from the Tokyo Subway attack frequently presented with fasciculations (25%) and muscle weakness (35%) [136].

In the central nervous system, cholinergic overstimulation causes tremors, ataxia, respiratory depression, seizures, and coma. These effects generally only occur in severe intoxications, with respiratory failure being the most common cause of death [137]. Loss of central respiratory drive appears to be the predominant factor in organophosphate-induced respiratory failure, though peripheral effects contribute (e.g. bronchorrhea, bronchospasm, diaphragm contraction, etc.) [138, 139]. This effect is likely mitigated by mAChRs, supported by findings that centrally-acting muscarinic antagonists (e.g. atropine) mitigate respiratory effects, while peripheral muscarinic antagonists (e.g. methylatropine, glycopyrrolate) do not [140, 141]. Similar studies have also suggested mAChRs are the primary receptor type involved in organophosphate-induced seizures [142]. Though seizure initiation seemingly results from mAChR overstimulation, a three-phase model of seizure progression has been proposed, wherein other neurotransmitter systems (e.g. glutamatergic) are recruited [143].

Clinical presentation of anticholinesterase toxicity is dependent on many factors, including the molecular structure of the OP molecule, absorbed dose and route of exposure [144]. In the case of OP nerve agents, exposure is most likely to occur through the dermal and inhalation routes. Following a dermal exposure, symptom onset is delayed and will initially present as diaphoresis and fasciculations at the site of exposure. In moderate poisonings, toxicity will progress to systemic parasympathetic symptoms [5]. In contrast, inhalation of vapors or aerosols results in rapid onset of toxicity, peaking only minutes after exposure [145]. Miosis is the most sensitive endpoint during mild vapor

exposures followed by mild wheezing and difficulty breathing. Moderate exposures will become systemic, with respiratory and ocular signs becoming more pronounced [5]. Data collected during the Tokyo Subway attack (inhalation of sarin vapor) showed that miosis, headache, dyspnea, nausea and eye pain were most commonly experienced in hospitalized victims, which supports the previous notion [136]. The same study found that in severely intoxicated individuals (n=4) recovery of red blood cell AChE activity into the normal range took approximately two months.

2.2.4 Post-Exposure Treatment

Management of OP intoxication involves several therapies aimed at different aspects of the toxidrome. A centrally-acting muscarinic receptor antagonist, usually atropine, is given to suppress muscarinic effects in the parasympathetic and central nervous systems [146]. Other mAChR antagonists including glycopyrrolate and scopolamine have been studied with some success, though the recommendation for atropine is unlikely to be revised [147, 148]. Conversely, effects at the neuromuscular junction (i.e. fasciculations, paralysis) are managed indirectly *via* intubation/mechanical ventilation and oximes [5, 149]. Some researchers have suggested that pharmacological intervention at nAChRs may be beneficial, though a recent clinical trial of rocuronium (a nAChR antagonist) failed to find beneficial outcomes with its use [150, 151].

Oximes (e.g., pralidoxime, obidoxime) are strong nucleophiles which can reactivate phosphylated AChE, restoring catalytic activity and thus decreasing the accumulation of acetylcholine in cholinergic synapses [152]. Unfortunately, aging of the OP-enzyme adduct renders oximes ineffective so the value of this treatment is highly dependent on the identity of the OP compound and the timing of oxime administration.

Because of this, the practical benefit of oxime administration is debated. Meta-analyses and clinical studies on patient outcomes following oxime treatment have not come to a shared conclusion, with some suggesting that it is beneficial while others find no benefit [153-156]. A reactivating agent that is effective on aged OP-AChE adducts may solve this issue, though development of such an agent is mechanistically difficult, and attempts have not yet been successful [157-159].

While atropine and oximes are the principal treatments, other management strategies may also be employed when appropriate. Benzodiazepines (e.g. diazepam and midazolam) are used to suppress seizure activity [160]. As severe toxicity may result in loss of consciousness and/or flaccid paralysis, seizure activity may be difficult to recognize. Thus, it is appropriate to administer anticonvulsants until the absence of seizure activity can be confirmed. Gastrointestinal decontamination (i.e. lavage or charcoal administration) is sometimes performed following OP ingestion, though the benefit of such treatments is dubious due to the rapid absorption of the toxicant from the stomach [161, 162]. Alternatively, in cases of percutaneous or vapor exposure, skin decontamination (i.e. clothing removal and alkaline rinse) may be important to halt further chemical absorption as well as prevent secondary exposures.

In addition to those discussed above, a variety of adjunctive treatments have demonstrated positive effects in laboratory studies, though they have little, if any, clinical evidence. Administration of glutamate receptor antagonists (e.g. gacyclidine, caramiphen) aid in seizure attenuation, improving survival and recovery when given up to 45 minutes after intoxication and standard antidotes [163-166]. The anti-epileptic drug levetiracetam has also been shown to further enhance anti-seizure effects when given in

conjunction with anticholinergic and antiglutamatergic drugs [167]. Another study found that a combination of procyclidine and propofol are also able to terminate seizures long after onset, though this regimen could not be administered outside of a hospital setting [168]. Brief isoflurane administration may also have neuroprotective effects when given between 20-30 minutes following exposure [169]. Nebulized ipratropium bromide, a medication commonly used in COPD, has also been used to counteract bronchospasm [170].

2.2.5 Sequalae of OP Toxicity

Even with successful treatment, exposure to OP compounds can result in a wide variety of persistent neurological consequences [171]. Seizures resulting from OP intoxication can induce extensive neuronal damage, including cell death [172]. However, there is evidence that neuropathological changes may occur even when seizures are prevented or rapidly terminated [173-176]. Neuropathological changes following OP toxicity have been correlated with persistent behavioral deficits in animal models [177-181].

While neuropathology cannot currently be determined in humans, neurobehavioral and neurophysiological effects of OP toxicity have been studied. One year after the Tokyo Subway attack, exposed individuals showed a decrease in event-related potential and visual-evoked potentials, which reflect cognitive and visuomotor function respectively [182, 183]. In another study, victims reported continued ocular symptoms (18.5%), fatigue (12%) and headache (8.6%), among other symptoms one-year post-exposure [184]. In a seven-year follow-up, exposed individuals had significantly decreased performance on tests of psychomotor function (finger tapping test) and

working memory (backward digit span test) compared to the reference population [185]. Pesticide applicators may also be unintentionally exposed to OP compounds [186-188]. Compared to non-farmworkers, these populations showed decreased scores on a variety of cognitive and neurobehavioral tests (verbal abstraction, visuomotor speed, memory, attention) [189-193]. These studies show that there continues to be a need for developing effective strategies to prevent and treat OP compound intoxication.

2.3 PRE-EXPOSURE PROPHYLAXIS

2.3.1 Carbamates

While post-exposure therapy is the only option for civilians involved in an unexpected attack, militaries employ carbamates for prophylaxis against nerve agent threats. Carbamates are a class of chemicals that bind to and inhibit AChE, but with much shorter duration than OP compounds. It was first reported in 1946 that administration of the carbamate physostigmine protected animals against the toxic effects of the organophosphate DFP [194]. Superficially, it seems illogical that protection against OP anticholinesterases can be achieved by preadministration of another anticholinesterase. The mechanism of carbamate pretreatment is two-fold. First, carbamates transiently occupy the AChE active site thereby preventing binding by a more persistent OP inhibitor. Second, over the course of an exposure, carbamylated enzymes spontaneously reactivate (half-life of 15-30 minutes *in vitro*) [195]. This provides a steady source of catalytically active AChE, consequently reducing the effects of OP toxicity. It is important to note, however, that the efficacy of carbamate pretreatment is dependent on receiving the standard post-exposure therapy following exposure. When animals are

exposed to OP inhibitors but not given the standard antidotes, carbamate pretreatment does not influence the toxic outcome [196-198].

Pyridostigmine bromide (PB) is the most commonly used carbamate for nerve agent prophylaxis. The U.S. military first utilized PB as a prophylactic agent during the Persian Gulf War (1990-1991), and it remains the only FDA-approved carbamate pretreatment. In rhesus monkeys exposed to soman, PB pretreatment demonstrated a protective ratio (PR; factor by which the LD_{50} of untreated group is increased) of greater than 40 when used in conjunction with standard antidotes. For comparison, the standard therapy alone had a PR of 1.6 [16]. When pre-exposure PB is given in addition to the standard antidotes against tabun, the PR is increased from 4.4 to 12.1 (in guinea pigs) and 1.3 to 2.1 (in mice) [199]. While the inclusion of PB is beneficial with soman and tabun exposures, PB does not increase the PR against sarin and VX exposures [16, 199]. The efficacy of standard antidotes with sarin (PR=34.6) and VX (PR=58.8) is much better than with soman and tabun, which may contribute to the relative lack of effect of PB [199]. The presence of PB, however, has been shown to have no or minimal effect on survivability of guinea pigs following exposure to sarin or VX [200].

Ideally, peripheral AChE activity including AChE in blood should be inhibited 20-40% by the carbamate pretreatment [16]. While higher occupation of AChE sites would theoretically make the pretreatment more effective, it could also lead to increased anticholinesterase toxicity. It should be noted that the efficacy of PB prophylaxis is solely due to the protection of AChE in the peripheral nervous system, as PB does not readily cross the blood-brain-barrier due to the presence of a quaternary nitrogen in its structure. In military settings, PB is administered as 30 mg tablets taken every 8 hours to achieve

this outcome. The oral bioavailability of PB in humans is low (around 10-15%). The time to peak plasma concentrations of PB is about 2 hours (though this can be significantly increased if taken with food), and the elimination half-life of PB from plasma is 100-200 minutes [201, 202]. AChE levels return to normal activity 10 to 12 hours following the last dose of 30 mg PB tablets [203].

Soldiers taking PB have reported acute side effects including gastrointestinal distress (50%), urinary urgency (5-30%) and headache (<5%) [204]. Pyridostigmine was originally implicated in contributing to Gulf War Illnesses [205], however recent research suggests the pathogenesis is multifactorial, with PB only being a possible contributing factor [206]. Due to the incomplete efficacy, non-ideal pharmacokinetics, and potential side effects of PB administration, further research into prophylactic treatments based on PB is warranted.

In addition to PB, several other reversible AChE inhibitors have been investigated as prophylactics. As noted above, physostigmine is a centrally-acting carbamate which has been shown to provide increased protection against DFP, soman, and sarin in comparison to PB [197, 207, 208]. Despite this, the *in vivo* pharmacokinetics of physostigmine (half-life of 30 minutes) pose a significant barrier to practical use [209]. Several centrally-acting reversible AChE inhibitors used in treating dementia and Alzheimer's disease — rivastigmine, donepezil, huperzine A, and galantamine — have also been investigated for their prophylactic capability [210]. Rivastigmine was tested in human volunteers and determined to have limited use as a prophylactic due to non-linear pharmacokinetics, high inter-subject variability, and cognitive function decrements [211]. Galantamine provides marked protection against paraoxon, sarin, and soman treated

guinea pigs, particularly when combined with atropine post-treatment [212]. It has also been shown to prevent soman-induced brain damage in guinea pigs [213]. Centrally-acting cholinesterase inhibitors, however, are likely to induce behavioral side effects [214]. Physostigmine has been shown to alter behaviors such as startle reflexes and prepulse inhibition [215]. Furthermore, physostigmine, galantamine, huperzine, and donepezil significantly depress locomotor activity in rats [216]. While these investigational drugs may have improved efficacy compared to PB, issues with tolerability have not been definitively solved.

2.3.2 Bioscavengers

Bioscavengers are proteins which can bind to and inactivate toxicants in the circulation before they can distribute into target tissues. This approach was first attempted in 1987 by Wolfe and colleagues, who found that pre-administered AChE was able to prevent lethality in rodents exposed to 3.5 LD_{50}s of VX [217]. AChE acts as a stoichiometric scavenger, as a ratio of two moles of AChE to one mole of VX was necessary to maintain protection. In 1991, Broomfield and colleagues showed that BChE was an effective prophylactic in rhesus monkeys, blocking cholinergic signs of toxicity and behavioral changes following OP challenge [218]. These initial studies spurred further interest in the development of a suitable bioscavenger for protection against OP intoxication.

Both AChE and BChE bind stoichiometrically to OP anticholinesterases. The so-called "second-generation" bioscavengers catalytically hydrolyze OP molecules; therefore, they are theoretically capable of protecting individuals against higher OP exposure levels while requiring lower doses of the enzyme. The first *in vivo* study

utilizing a catalytic scavenger, a bacterial parathion hydrolase, was conducted by Ashani and colleagues [219]. Administration of a small amount of this bacterial enzyme was able to increase the LD_{50} of paraoxon 3-fold in rodents. Further studies on catalytic scavengers have focused on bacterial phosphotriesterases and human paraoxonase, among others [220].

Several characteristics have been set forth which describe an ideal enzyme-based prophylactic (i.e. bioscavenger) [221]. First, the molecule must react rapidly and efficiently against a broad spectrum of OP molecules. Preferably, a bioscavenger should inactivate enough OP molecules to render a non-toxic dose within one median circulation time (~ 1 minute) to prevent all effects of OP toxicity [222]. Second, the scavenger must be biologically compatible (i.e. no toxic effects and lack of immunoreactivity) with a long *in vivo* half-life. Lastly, the scavenger should be suitable for large-scale industrial production, being inexpensive to produce and possessing a long shelf-life.

2.3.2.1 Stoichiometric

While acetylcholinesterase was the first studied enzyme bioscavenger, it has not been the primary focus of further research. This could be due to the lack of a suitable source of purified human AChE [88]. Therefore, studies on this enzyme have utilized sources such as fetal bovine serum AChE or recombinant human AChE (rhAChE). While these enzymes are effective against several nerve agents (VX, soman, sarin), their non-native source poses potential immunogenicity issues and a short *in vivo* half-life (particularly with rhAChE) [217, 221, 223-225]. It is interesting to note, however, that AChE has better stereoselectivity for the more toxic OP enantiomers as compared to BChE [223].

Carboxylesterase (CarbE) is an enzyme found in plasma and other tissues which is highly sensitive to inhibition by a number of OP compounds [226]. Inhibition of endogenous plasma CarbE activity decreases the LD_{50} of soman, indicating that the sequestration of OP molecules by carboxylesterase is an endogenous scavenger for modulating toxicity [227]. This is supported by the notion that species with high levels of CarbE are more resistant to OP toxicity [228]. CarbE is generally considered a broad-spectrum enzyme; however, the rate at which it reacts with some OP compounds is poor. While CarbE reacts at a similar rate to AChE and BChE with paraoxon, sarin, soman and DFP, it exhibits significantly slower reactivity with echothiophate and VX [229]. This observation lessens CarbE's utility as a broad spectrum bioscavenger. At present, it is unknown how CarbE would perform as an exogenously injected bioscavenger.

Butyrylcholinesterase is the most well-studied of the potential enzyme-based prophylactics [88]. Prophylactic administration of BChE can provide protection against subcutaneous soman (5.5 x LD_{50}) and VX (8 x LD_{50}), without the standard antidotes [230, 231]. This strategy is also effective following dermal (VX) and inhalation exposures (soman and sarin) [232-234]. Pretreatment with BChE not only prevents lethality, but it prevents nonlethal neurological and behavioral deficits resulting from an OP exposure [235, 236]. Furthermore, several studies have demonstrated the safety of administration of large amounts of BChE. Animals receiving human BChE (60 mg/kg; im or ip) exhibit no clinical signs of toxicity, have physiologically normal serum chemistry and hematological profiles, and lack histopathological changes post-mortem [231]. BChE administration also does not alter behavioral endpoints such as acoustic

startle reflexes and prepulse inhibition [215], attention, short-term memory [237], avoidance learning, motor activity or schedule-controlled behavior [236, 238].

2.3.2.2 Catalytic

Since OP compounds are hemi-substrates of BChE, it is conceivable that an OP-hydrolyzing BChE mutant could be rationally designed. Over three decades ago it was hypothesized that introduction of another nucleophile near the active site may facilitate hydrolysis of OP compounds [239]. Subsequent evaluation of a series of single point mutations in the oxyanion hole of BChE to histidine found one mutant ($BChE_{G117H}$) with a marked increase in paraoxon, echothiophate, sarin, and VX hydrolysis [14, 240]. Despite these *in vitro* improvements, $BChE_{G117H}$ was decidedly less protective than recombinant BChE *in vivo* against sarin, soman, or VX [241]. Since the characterization of $BChE_{G117H}$, over 60 different BChE mutants have been used to test the effects of alternating histidine positions, changing amino acids at the 117 position, adding positive charges in $BChE_{G117H}$, and introducing negative charges to increase the nucleophilicity of histidine, among others [242]. To date, no other mutants have shown significant improvements in organophosphate hydrolysis compared to $BChE_{G117H}$.

Other human enzymes which possess catalytic activity towards OP compounds are of considerable interest. Paraoxonase-1 (PON1) is a plasma enzyme associated with high-density lipoproteins which has a variety of functions, including organophosphate hydrolysis [243]. PON1 efficiently hydrolyzes several OP compounds, including G-type nerve agents [244, 245]. While PON1 does not function at the ideal k_{cat}/K_M ($>10^7$ M^{-1} min^{-1}), it only needs to be improved by one to two orders of magnitude to reach this goal [246]. In mice, recombinant PON1 (10 mg/kg) was able to protect against 4 x LD_{50} of

chlorpyrifos oxon, but not 2 x LD_{50} of any G-type nerve agents [247]. In another study, however, 5U of human PON1 partially protected rodents against inhalation exposure to sarin and soman (1.2 x LCt_{50}) [248]. The incomplete protection afforded by wild-type PON1 may be due to its propensity to bind to the less toxic nerve agent enantiomers [249]. Directed evolution of human PON1 produced a mutant (IIG1) with 40- to 3,400-fold increased efficiency at hydrolyzing the toxic enantiomers of sarin, soman, and cyclosarin [250]. IIG1 also acquired the ability to slowly hydrolyze VX, though not efficiently enough to be useful *in vivo*. IIG1 was able to protect against 2 x LD_{50} of cyclosarin at low levels (1 mg/kg, iv) [251]. Large-scale implementation of PON1, however, faces production, stability and pharmacokinetic challenges [252]. Other human enzymes such as liver prolidase and senescence marker protein 30 have been suggested as potential candidates of interest, though data are sparse on their efficacy [253-255].

Bacterial phosphotriesterases (PTE) are the most active and broad-spectrum OP hydrolyzing enzymes; however, they face difficulties translating to human use due to issues with immunogenicity, making structural modifications necessary [256]. The PTE from *Brevundimonas diminuta* (formerly *Pseudomonas diminuta*), commonly called organophosphorus hydrolase (OPH), efficiently hydrolyzes both G-type and V-type nerve agents [257-259]. The wild-type enzyme was shown to protect rodents against multiple LD_{50}s of paraoxon, an analog of DFP, sarin, and tabun [207, 219, 260]. Furthermore, mutagenesis studies have been relatively successful in further increasing the catalytic efficiency of OPH [261, 262]. Evaluation of an evolved OPH mutant showed that a 5 mg/kg dose was able to protect against two-times the LD_{50} of VX, even when given post-exposure [263, 264]. Phosphotriesterases from other bacterial sources including

Sulfolobus solfataricus, *Agrobacterium radiobacter*, and *Pseudomonas pseudoalcaligenes* have also been tested with some success [265-267]. Overall, more research is necessary before use of a suitable catalytic scavenger can be implemented.

CHAPTER III

CHARACTERIZATION OF THE RELATIVE *IN VITRO* ENZYME ACTIVITY, INHIBITOR INTERACTION, OP BIOSCAVENGING CAPACITY, AND STABILITY OF FREE AND COPOLYMER-COMPLEXED BCHE

3.1 INTRODUCTION

Though BChE is an effective bioscavenger, large scale production of human serum BChE (huBChE) is not economically feasible. A dose of 200 mg of huBChE is predicted to protect a 70 kg individual from 2 x LD_{50} of VX, soman, and sarin [268]. Using this estimate it is predicted that the US could produce around 5,000 doses annually by dedicating the entire supply of outdated plasma for BChE purification [241]. In contrast, recombinant human BChE (rhBChE) can be produced in large amounts using systems including CHO cells [269], insect cells [270], in transgenic goat's milk [271], and tobacco leaves [241]. Recombinant enzymes, however, pose additional challenges including a reduced circulatory time and reduced stability resulting from altered oligomerization and glycosylation [51, 81]. In mice, human serum BChE has a

half-life of 18 hours in the circulation while tetrameric rhBChE has a half-life of only 6 hours [272]. Monomeric rhBChE has an even shorter circulatory time, with a half-life of 2 minutes [273]. A similar trend would be expected with administration in humans.

Structural modification of rhBChE may improve its pharmacokinetic characteristics. For example, poly(ethylene glycol) (PEG) is a long amphiphilic molecule which can be attached to therapeutic proteins and enzymes to limit their clearance from the circulation. PEG conjugation can improve solubility and stability, as well as extend *in vivo* half-life by protecting against proteolytic degradation, reducing renal clearance and masking antigenic epitopes [11]. This is due, in part, to the increased size of PEG-conjugated proteins. Each ethylene glycol molecule associates with 2-3 water molecules, increasing the molecular volume to weight ratio and creating a steric barrier to prevent proteolytic and immunogenic interactions [274]. Direct PEGylation has been previously shown to extend the half-life of rhBChE in mice [271, 272]

Gaydess and colleagues reported a poly-L-lysine (PLL) copolymer grafted with PEG (PLL-g-PEG), which is able to ionically associate and form a stable complex with BChE. These copolymer complexes aided in the delivery of tetrameric BChE into the brain [9]. The ability of a copolymer carrier to alter pharmacokinetic properties of BChE may make it potentially useful as a bioscavenger. Furthermore, this copolymer formulation readily allows for conjugation of targeting ligands. Ligands such as the small peptide ERY1 or the monoclonal antibody TER119 may allow selective binding of copolymer-complexed BChE to circulating erythrocytes, which could lead to pharmacokinetic improvements significantly beyond the effect of PEG alone [275].

Despite the potential pharmacokinetic improvements, the copolymers' effect on pharmacodynamics cannot be ignored. Bioscavengers must react rapidly with toxicants and be stable *in vitro* and *in vivo* [276], and enzyme modification *via* copolymer complexation may alter characteristics important for this goal (e.g., binding affinity, catalytic rate). While the effect of direct PEG conjugation of BChE on catalytic activity, proteolytic sensitivity, and thermostability has been previously investigated [272, 277], the effect BChE complex formation with a PLL-g-PEG copolymer on catalytic and scavenging properties has not been previously studied.

The major goal of Aim 1 was to evaluate enzyme characteristics in copolymer complexes related to catalytic activity and bioscavenging capacity. We hypothesized that PLL-g-PEG complexes with BChE would have little effect on esterase activity or binding to OPs, while enhancing stability. First, we estimated the kinetic parameters for substrate hydrolysis (V_{max}, K_M) for free (i.e., BChE treated in the same manner as enzyme undergoing copolymer complexation except that no copolymer is added) and the copolymer-complexed enzyme. We systematically characterized BChE-copolymer complexes using different sizes of copolymer (low [4-15 kDa], medium [15-30 kDa], high [30-70 kDa]) to study potential changes in interactions with substrates and inhibitors. We also evaluated the effect of copolymer complexation on enzyme-inhibitor kinetics with four selected OP inhibitors (paraoxon, DFP, echothiophate, and pyridostigmine) by comparing the bimolecular rate constant (k_i) obtained with each inhibitor. These studies provided insight into effects that the copolymer may have on the enzyme's catalytic capacity and potential to bind to and inactivate OP molecules. We also examined the effect of copolymer complexation on enzyme stability *in vitro* to both heat

and proteolytic enzymes (chymotrypsin, trypsin, and pronase). These studies provided insight into how the PLL-g-PEG copolymer may influence the stability of the complexed enzyme, both in the circulation and with storage.

3.2 MATERIALS AND METHODS

3.2.1 Chemicals

Recombinant human butyrylcholinesterase was produced by Dr. Liyi Geng (Mayo Clinic; Rochester, MN) as described in Pope and colleagues [10]. Paraoxon (O,O'-diethyl-*p*-nitrophenyl phosphate; PO) (98.6% purity by HPLC) was purchased from ChemService (West Chester, PA). A 10 mM stock solution of paraoxon was prepared in 100% dry ethanol and kept desiccated under nitrogen at -80°C until use. Diisopropylfluorophosphate (2-[fluoro(propan-2-yloxy)phosphoryl]oxypropane; DFP) (99% purity by NMR) was kindly provided by Dr. Derik Heiss at Battelle Memorial Institute (Columbus, OH) and stored as provided at -80°C [278]. Echothiophate iodide (2-diethoxyphosphorylsulfanylethyl(trimethyl)azanium; EthP) was originally obtained from Wyeth-Ayerst and was a kind gift from Dr. Oksana Lockridge (University of Nebraska, Omaha, NE). Pyridostigmine bromide (3-(dimethylaminocarbonyloxy)-1-methylpyridinium bromine; PB) (100% purity by HPLC) was purchased from Sigma-Aldrich (St. Louis, MO) and kept desiccated under nitrogen at room temperature until use. Chymotrypsin (Type II from bovine pancreas; ≥ 40 U/mg), trypsin (from bovine pancreas; 12,602 BAEE U/mg), and pronase (from *Streptomyces griseus*; ≥ 45 U/mg) were purchased from Sigma-Aldrich and diluted on day of assay. Carboxylesterase (from porcine liver; ≥ 15 U/mg) was purchased from Sigma-Aldrich and 40U/ml aliquots were prepared in buffer and stored at -20°C until use. Pre-cast non-denaturing gradient gels

(Mini-PROTEAN TGX Gel 4-20%) and native sample buffer (62.5 mM Tris-HCl, pH 6.8 containing 40% glycerol and 0.01% bromophenol blue) were purchased from Bio-Rad (Hercules, CA). Butyrylthiocholine iodide (BTChI), *p*-nitrophenyl acetate (p-NPA), ethopropazine, and remaining chemicals and reagents were purchased from Sigma-Aldrich.

3.2.2 Copolymer-Complexation of BChE

Copolymer-BChE complexes (C-BCs) were prepared by Dr. Nicholas Flynn (Chemical Engineering, Oklahoma State University). First, three different PLL-g-PEG copolymers were prepared using methoxypoly(ethylene glycol, mPEG) containing an amine-reactive, n-hydroxysuccinimide ester (NHS) and poly-L-lysine (PLL), of either high (30-70 kDa), medium (15-30 kDa), or low (4-15 kDa) molecular weight. A sufficient amount of a 50/50 mixture of 2 and 5 kDa mPEG-NHS in PBS (to obtain an average 10:1 PEG-PLL grafting ratio) was allowed to react with one of each of the three sizes of PLL at room temperature for two hours. A PEG:PLL grafting ratio of 10:1 was confirmed by ^{1}H NMR spectroscopy. The resulting copolymers were purified using a centrifugal concentrator (10 kDa cutoff), rinsed with ultrapure water, and then lyophilized and stored at -20°C until use.

Electrostatic complexes of the copolymer and rhBChE were prepared essentially as reported by Flynn and colleagues (2016) [279]. The copolymer was combined with PBS to make a 6 mg/ml solution. An aliquot (7.5 µl) is added drop-wise to 25 ml of rhBChE (0.27 mg/ml) at room temperature for one hour with constant mixing. Copolymer-to-protein mass ratio was kept at 7:1 in all reactions. After one hour, 5 µl of glutaraldehyde (0.025% v/v in PBS) was added drop-wise and the reaction proceeded for

another three hours at room temperature to cross-link amino groups and stabilize the copolymer-BChE complexes [9]. Free enzyme preparations are made by adding vehicle only (PBS) instead of either copolymer or glutaraldehyde, but with all other conditions being the same. The resulting free and copolymer-complexed enzyme preparations contain the same amount of BChE protein (0.18 mg/ml). All enzyme preparations were stored at 4°C until use.

3.2.3 Colorimetric BChE Assay

A modified Ellman method was used to measure enzyme activity [280, 281]. All enzyme preparations were serially diluted with PBS containing bovine serum albumin (BSA; 0.05% w/v) to stabilize enzyme activity [282, 283]. Twenty-five µl (about 11 ng protein) of a diluted enzyme preparation was added to wells in a flat bottom 96-well plate (Fisher Scientific; Hampton, NH). To initiate the reaction, a cocktail containing BTChI (1 mM final concentration) and DTNB (5,5'-dithio-bis-(2-nitrobenzoic acid)) (100 µM final concentration) in 10 mM Tris-HCl containing 1 mM EDTA, pH 7.2 was added to bring the volume of each well to 200 µl. Plates were incubated at 37°C and kinetic measurements are completed within five minutes using a Spectramax 340PC microplate reader (Molecular Devices; Sunnyvale, CA). Enzyme activity was estimated based on the rate of appearance of the reaction product, 2-nitro-5-thiobenzoate (ε = 14,150 M^{-1} cm^{-1}) at 412 nm, and was uniformly corrected for non-enzymatic substrate hydrolysis.

3.2.4 Choline Substrate Kinetics

Substrate kinetics of free and copolymer-complexed BChE were evaluated using a range of concentrations of BTChI (10 µM to 1 mM). Quadruplicate reactions were followed photometrically under the conditions described in section 3.2.3. V_{max} and K_M

were determined using non-linear regression using the Michaelis-Menten equation. Turnover number, k_{cat}, was calculated using the relationship $V_{max} = k_{cat}[E]$, where [E] represents the concentration of BChE active sites in the reaction.

3.2.5 Inhibitor Kinetics

Inhibitor kinetics with the free and copolymer-complexed enzymes were compared using the organophosphorus inhibitors paraoxon (PO), diisopropylfluorophosphate (DFP), and echothiophate (EthP) as well as the carbamate inhibitor pyridostigmine bromide (PB). All inhibitors were diluted on the day of assay with 10 mM Tris-HCl containing 1 mM EDTA, pH 7.2 and ethanol (final concentration, 0.06% v/v). First, 12.5 µl of enzyme (about 11 ng protein) was placed in wells of U-bottom 96-well plates (Corning; Corning, NY). At specified times (0-10 minutes), 12.5 µl of vehicle or one of a range of concentrations of one of the inhibitors was added in duplicate. The reactions were allowed to pre-incubate at 37°C with continuous shaking. Residual BChE activity was then measured by adding 175 µl of the cocktail containing substrate and color reagent (see section 3.2.3). After range finding studies, four concentrations of each inhibitor were selected to evaluate concentration- and time-dependent inhibition of BChE activity: paraoxon (50, 100, 250 and 500 nM), DFP (5, 10, 25 and 50 nM), echothiophate (100, 250, 500 and 750 nM), and pyridostigmine (10, 25, 50 and 100 µM). Results of the inhibitor kinetics were evaluated as described by Richardson and coworkers [284]. Briefly, primary plots were constructed using the natural log of residual BChE activity versus time with each of the different enzyme preparations with the four concentrations of each of the selected inhibitors. Secondary

plots of the negative slope of each primary plot versus the concentration of inhibitor yielded straight lines with a slope = k_i.

3.2.6 Sequestration (Bioscavenging *In Vitro*)

An indirect enzyme inhibition assay was used to evaluate *in vitro* bioscavenging potential of free enzyme and C-BCs using paraoxon as the inhibitor. Carboxylesterase (CarbE) was used as a marker enzyme and assayed essentially as described by Wei and colleagues [285]. First, *in vitro* sensitivity of CarbE to paraoxon was evaluated. CarbE (10 μl, 0.4 U/ml) was added to wells in a 96-well plate followed by addition of 10 μl of either vehicle (10 mM Tris–HCl containing 1 mM disodium EDTA and 4% ethanol, pH 7.2; Tris-E/4% EtOH) or paraoxon (0.3–1000 nM). Reactions were pre-incubated for 20 min at 37°C before adding substrate (*p*-nitrophenyl acetate, 3 mg/ml in acetonitrile). Absorbance change at 405 nm was monitored in kinetic mode at 37°C using a Spectramax 340PC microplate reader (Molecular Devices; Sunnyvale, CA). A concentration of paraoxon that elicited near complete inhibition of CarbE was chosen for further use in the *in vitro* bioscavenger assay.

Paraoxon inactivation *in vitro* (as a measure of bioscavenger potential) was evaluated essentially as described above, but with an additional pre-incubation step. In 1.5 ml Eppendorf tubes, 6 μl of either vehicle (PBS containing 0.05% w/v BSA) or one of a series of dilutions of either the free or the copolymer-complexed enzyme is added to 6 μl of either vehicle (Tris-E/4% EtOH) or paraoxon (40 nM), followed by incubation at 37°C for 20 minutes in a reciprocating water bath. Twelve μl of CarbE (0.4 U/ml in Tris-E) was then added to each tube and incubated for another 20 minutes under the same

conditions. The tubes were then transferred to ice to stop the reaction and aliquots (20 µl) were added to wells in a cold 96-well plate. Tris-E buffer (177 µl) was added to each well followed by addition of 3 µl of a mixture of p-nitrophenyl acetate (3 mg/ml) and ethopropazine (a specific inhibitor of BChE, 10 µM final) in acetonitrile. Ethopropazine was added to block any residual BChE from hydrolyzing the CarbE substrate. Absorbance change at 405 nm was recorded in kinetic mode as above. CarbE activity in the reactions that are pre-incubated with only vehicles (without BChE or PO) was defined as vehicle control.

3.2.7 Heat Inactivation

Heat inactivation was studied essentially as described by Gall and coworkers [286]. Fifty-five µl aliquots of free and copolymer-complexed enzymes (0.44 µg/ml in PBS containing 0.05% w/v BSA) were incubated at a range of temperatures (in 5° intervals from 30-75°C) for one hour, and then transferred to ice to stop the inactivation reaction. Aliquots were subsequently measured for residual BChE activity as described in section 3.2.3. The data were plotted as percent of control activity versus log-transformed temperatures, with 100% activity defined by BChE activity in respective samples incubated at 4°C. Time course studies were conducted similarly by incubating 55 µl aliquots of enzyme preparations at a constant temperature (55°C) and removing samples for activity analysis at selected times (1, 5, 10, 15, 30, 60, 120, 180, 300, 420, 600, and 900 minutes).

3.2.8 Protease Inactivation

Time-dependent proteolytic inactivation of the free rhBChE and C-BCs was evaluated using trypsin, chymotrypsin, and pronase in PBS. Concentrations of chymotrypsin (37.5 μg/ml), trypsin (187.5 μg/ml), and pronase (25 μg/ml) were selected based on relatively similar degrees of time-dependent inactivation. The free and copolymer-complexed enzymes (0.44 μg/ml in PBS containing 0.05% w/v BSA) was incubated with either trypsin, chymotrypsin, or pronase at 37°C. Aliquots (1.5 μl) were removed at 0, 1, 2, 4, 6 and 8 hours and diluted (1:1000) into ice cold buffer to stop the reaction. Diluted samples were assayed for residual BChE activity using the method described above (section 3.2.3).

3.2.9 Native BChE Activity Gels

Activity gels were performed using inactivated samples (heat and trypsin digested). Samples used for activity gels were prepared similarly to those described in described in section 3.2.7 and 3.2.8. In brief, BChE or MMW C-BCs (both 0.44 μg/ml) were incubated at 55°C and 5 μl aliquots were transferred to ice after one minute or eight hours of pre-incubation. For trypsin inactivation, enzymes were incubated with 187.5 μg/ml trypsin (final) and 5 μl aliquots were removed at the one hour and eight-hour time points. Control samples were prepared similarly, excepting the inactivation procedures. To run the gels, the 5 μl samples were mixed with 5 μl native sample buffer and the total mixture was loaded into the wells of a non-denaturing gradient gel (4-20%). The gel apparatus (Mini-PROTEAN Tetra Cell and PowerPac Universal Power Supply)(Bio-Rad; Hercules, CA) was filled with running buffer (25 mM Tris Base and 200 mM glycine in

water) and run at a constant 120V. Gels were run for two hours in a cold room before removal from apparatus.

Gels were stained for BChE activity using the method of Karnovsky and Roots [287]. The staining solution was composed of 5 mM sodium citrate, 3.15 mM copper sulfate, 0.5 mM potassium ferricyanide (added just before staining), and 2 mM BTChI in 200 mM maleate buffer (adjusted to pH 6.0 day of assay). Gels were placed in the staining solution covered from light and placed on a platform shaker for two hours. After removal from staining solution, gels were rinsed with deionized water and then photographed using an Amersham Imager 600 (GE Healthcare Bio-Sciences; Pittsburg, PA).

3.2.10 Statistical Methods

All data were derived using at least three independent enzyme preparations. Data for substrate and inhibitor kinetic parameters, and sequestration EC_{50} were analyzed by a one-way analysis of variance test (ANOVA) with enzyme type (i.e., free enzyme and three PLL-g-PEG-complexed enzymes) as the main factor. When concentration-dependent inactivation of an enzyme preparation was evaluated (i.e. IC_{50}, EC_{50}) the inhibitor concentrations (x-values) were log-transformed and the data fit to a nonlinear regression equation (using a variable slope model). The same method was used to calculate the T_{50} value of data resulting from one-hour heat inactivation studies. In time-dependent heat inactivation studies, the data were fit to a one-phase decay model and the resulting half-life values were compared using a one-way ANOVA with enzyme type as the main factor. In the protease-mediated inactivation studies, data were also fit to a one-phase decay model and the resulting curves were compared using an extra sum-of-

squares F test. Similar to above, the calculated half-life values were compared using one-way ANOVA. In both cases, the plateau value of the one-phase decay fit was constrained between 0-100 because data was reported as percent of residual activity. When *post hoc* tests were warranted, Tukey's multiple comparisons test was used (unless otherwise noted). Statistical significance was defined as a p-value < 0.05 in all cases, and p-values resulting from multiple comparisons analysis reported in-text are multiplicity adjusted. All statistical tests were conducted using GraphPad Prism software (La Jolla, CA), version 6.0.

3.3 RESULTS

3.3.1 Catalytic Activity of free rhBChE and C-BCs

Prior to experimental studies with C-BCs, the activity of recombinant human BChE was evaluated following a large dilution (1:200). We found that rhBChE lost significant activity following dilution with PBS, and this could be prevented by including BSA in the dilution buffer (Fig. 3-1). It has been previously reported that BSA may serve as a stabilizer for proteins during dilution [288]. These findings were used as the basis for inclusion of BSA in buffers used for subsequent studies with rhBChE and C-BCs.

In order to determine the effects of copolymer encapsulation on enzyme activity, we first compared the activity of free rhBChE and C-BCs. Figure 3-2 shows that activity of low, medium, and high molecular weight C-BCs was significantly decreased compared to free rhBChE. Because these results suggested that enzyme activity was indeed affected by the presence of the copolymer, we evaluated enzyme activity more completely using substrate kinetics (Fig. 3-3). Table 3-1 shows the substrate kinetics parameters determined using nonlinear regression fit to the Michaelis-Menton equation. The turnover

rate (k_{cat}) of all C-BCs was significantly decreased in comparison to the free enzyme ($F_{(3, 130)} = 19.05$, $p < 0.0001$ in all cases), however, further pairwise comparisons revealed no differences between the different PLL backbone lengths. The K_M of each was not significantly decreased, there was, however, a trend toward increasing K_Ms as the length of copolymer backbone increased (LMW<MMW<HMW). The combination of these effects resulted in a 40-56% decrease in the enzyme efficiency, represented by k_{cat}/K_M.

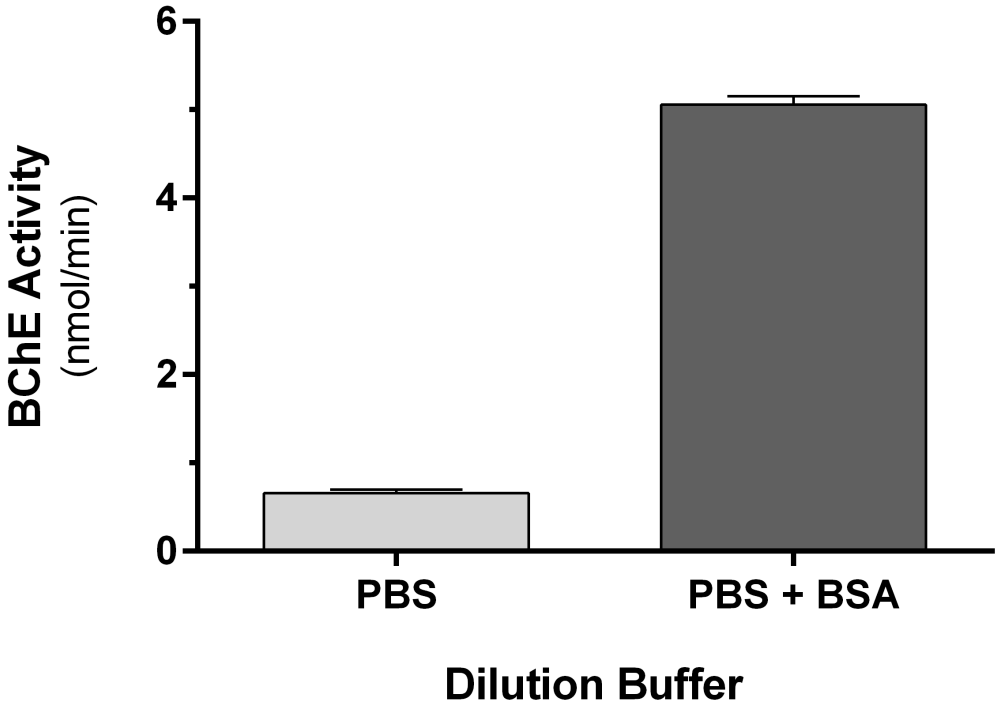

Figure 3-1. Activity of rhBChE after dilution with PBS or PBS + BSA. Free rhBChE (0.18 mg/ml) was diluted 1:200 using PBS or PBS containing 0.5 mg/ml BSA and then assayed as described in section 3.2.3. Data are reported as mean ± SD (n=4).

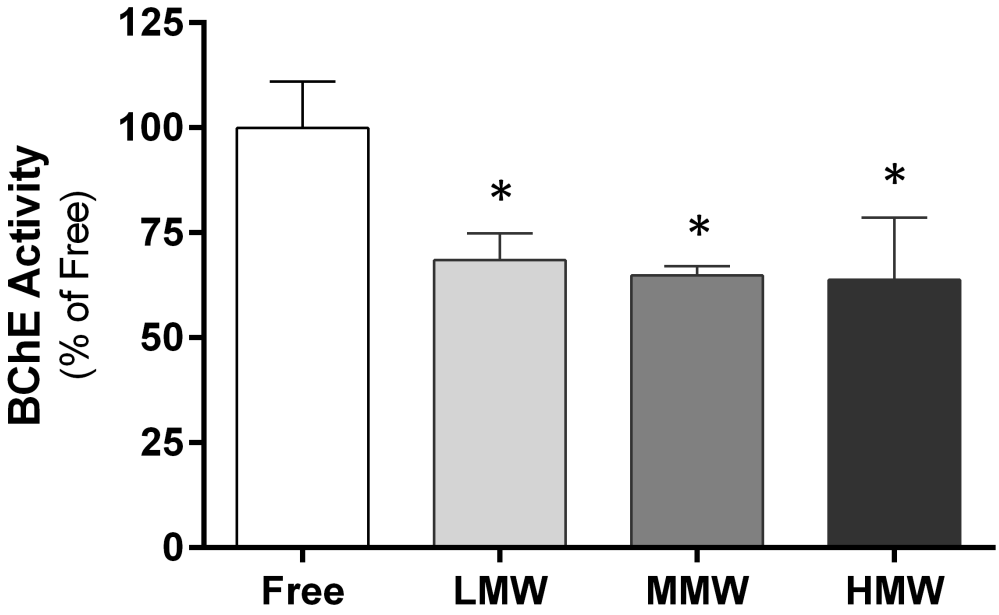

Figure 3-2. Activity of free rhBChE and C-BCs. Enzyme activity was determined as described in section 3.2.3, using 1 mM BTChI as the substrate. Data are reported as percent activity in relation to free rhBChE (mean ± SD; n=4). Asterisks indicate a significant difference from free rhBChE as determined by one-way ANOVA followed by a *post hoc* Tukey's test ($p < 0.05$).

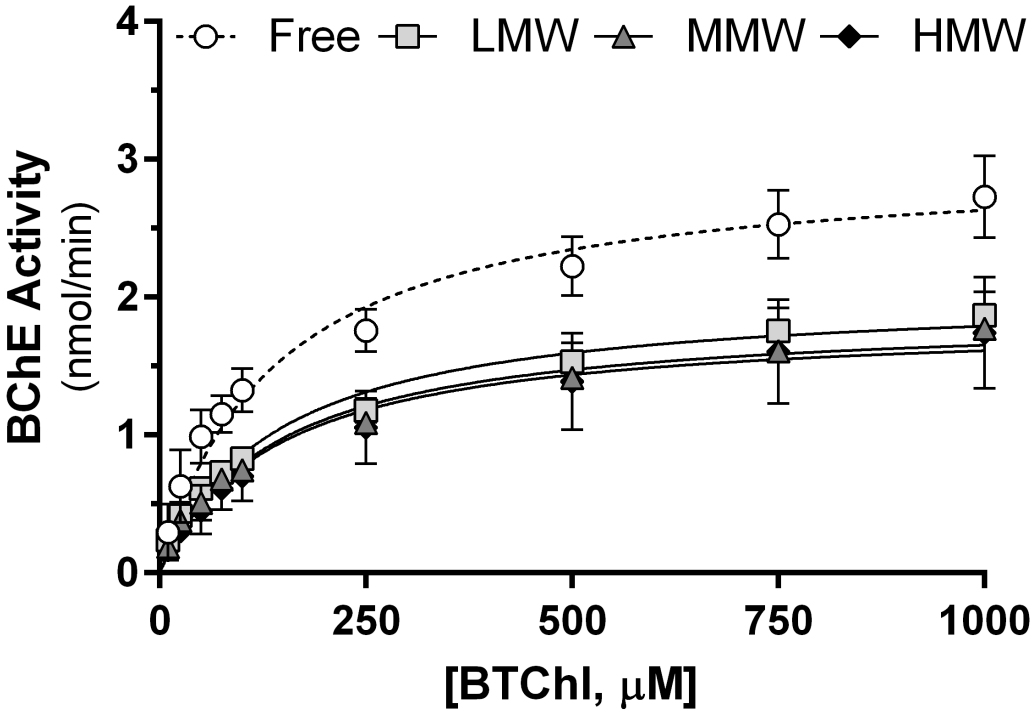

Figure 3-3. Concentration-dependent hydrolysis of BTChI by free rhBChE and C-BCs. Each enzyme preparation was incubated with BTChI (10-1000 μM) for 5 min at 37°C and activity was measured using a modified Ellman method. Data represent mean ± SD determined from four independent replicates.

Table 3-1. Substrate kinetic parameters (k_{cat}, K_M, and k_{cat}/K_M) for free rhBChE and C-BCs. Each enzyme preparation was incubated with butyrylthiocholine (10-1000 μM) for 5 min at 37°C and activity measured using the photometric method. Data represent mean values with 95% confidence intervals in parentheses (n=4).

	k_{cat} (min^{-1})	K_M (μM)	k_{cat}/K_M (min^{-1} M^{-1})
Free	22,125 (20,437 - 23,812)	116.8 (85.5 - 148.0)	1.89×10^8
LMW	15,601* (14,567 - 16,635)	136.5 (107.3 - 165.8)	1.14×10^8
MMW	14,922* (14,102 - 15,742)	156.9 (128.9 - 184.9)	0.95×10^8
HMW	15,225* (12,958 - 17,493)	183.3 (101.3 - 265.4)	0.83×10^8

* Indicates a significant difference compared to the free rhBChE.

3.3.2 Sensitivity of free rhBChE and C-BCs to Inhibition

While enzyme activity assays provide a means for determining the effect of the copolymer-complexation on catalytic function, the primary goal of this formulation is inhibitor binding (i.e. bioscavenging activity). Therefore, we evaluated the effect of copolymer-complexation on the enzyme's inhibitor binding capacity using the method developed by Aldridge and Reiner in 1972 and refined by Richardson and coworkers [283, 287]. Primary plots of inhibition show the natural log of residual enzyme activity versus pre-incubation time with varying concentrations of paraoxon, DFP, echothiophate, and pyridostigmine. Inhibitor concentrations were chosen to elicit similar free enzyme inhibition (as opposed to uniform inhibitor concentrations) due to the large difference in inhibitor potency. Figure 3-4 shows the primary plot results of free rhBChE with the four inhibitors. Primary plots for each of the remaining conditions yielded linear relationships (R^2 = 0.93 - 0.99) that extrapolated to zero (Figs. 3-5, 3-6, and 3-7). Negative slopes of the primary plots (-*k*') were then plotted against inhibitor concentrations to yield secondary plots (Fig. 3-8). The secondary plots all had linear relationships (R^2 = 0.82 - 0.98) with slopes equaling k_i (summarized in Table 3-2).

In the case of each inhibitor, there was a statistically significant difference detected in the slopes of the secondary plots (paraoxon: $F_{(3,240)} = 3.9$, $p = 0.009$; DFP: $F_{(3,288)} = 24.87$, $p < 00001$; PB: $F_{(3,277)} = 24.78$, $p < 0.0001$; EthP: $F_{(3,270)} = 194.4$, $p < 0.0001$). *Post hoc* analysis with paraoxon revealed a difference between free rhBChE and the HMW copolymer preparation only ($p = 0.004$). In contrast, *post hoc* analyses with the three remaining inhibitors revealed a statistically significant difference between free rhBChE and each of the copolymer preparations (LMW, MMW, and HMW) ($p < 0.0001$ in all

cases). Further pairwise comparisons revealed additional significant differences between the low molecular weight copolymer versus the high molecular weight copolymer ($p < 0.0001$) and the medium molecular weight copolymer versus the high molecular weight copolymer ($p < 0.0001$) only when echothiophate was used as the inhibitor. While significant differences were noted with each inhibitor, the extent of the reduction was notably different. For example, the inhibitory potency of paraoxon against the BChE complexed using the HMW PLL-based copolymer was reduced by 12%, while the potency of DFP was reduced by 16-23%, PB by 31-41%, and EthP by 41-60%. Thus, kinetic studies suggested that inhibitory potency was reduced with the inhibition of copolymer-complexed enzymes in an inhibitor-dependent manner, i.e., minimal changes were noted with paraoxon as the inhibitor while differing degrees of reduction in inhibitory potency were shown with the other three inhibitors. Note that overall inhibitory potency of the four inhibitors against the four enzyme preparations was DFP > paraoxon > echothiophate>>>pyridostigmine.

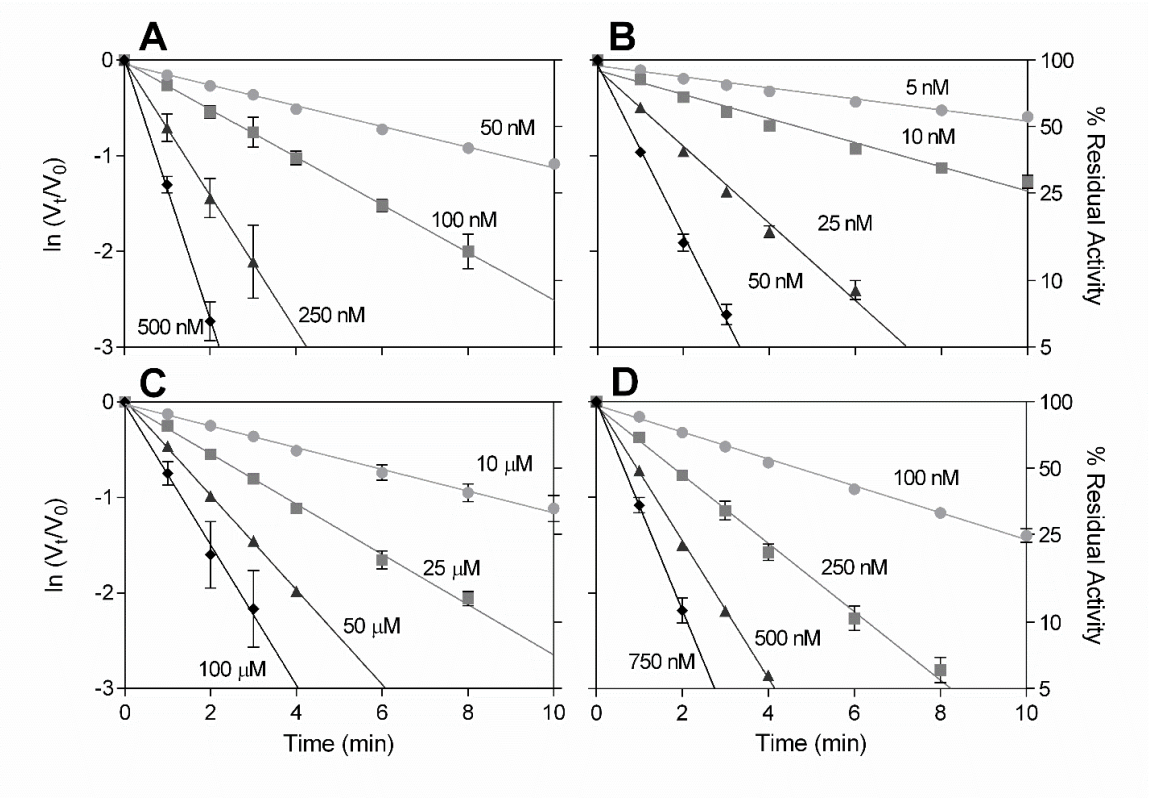

Figure 3-4. Concentration- and time-dependent inhibition of free rhBChE by PO (A), DFP (B), PB (C), and EthP (D). Primary plots show the natural log of residual free enzyme activity (V_t/V_0) versus time of pre-incubation with selected inhibitor concentrations. Data are reported as mean ±SD (n=3).

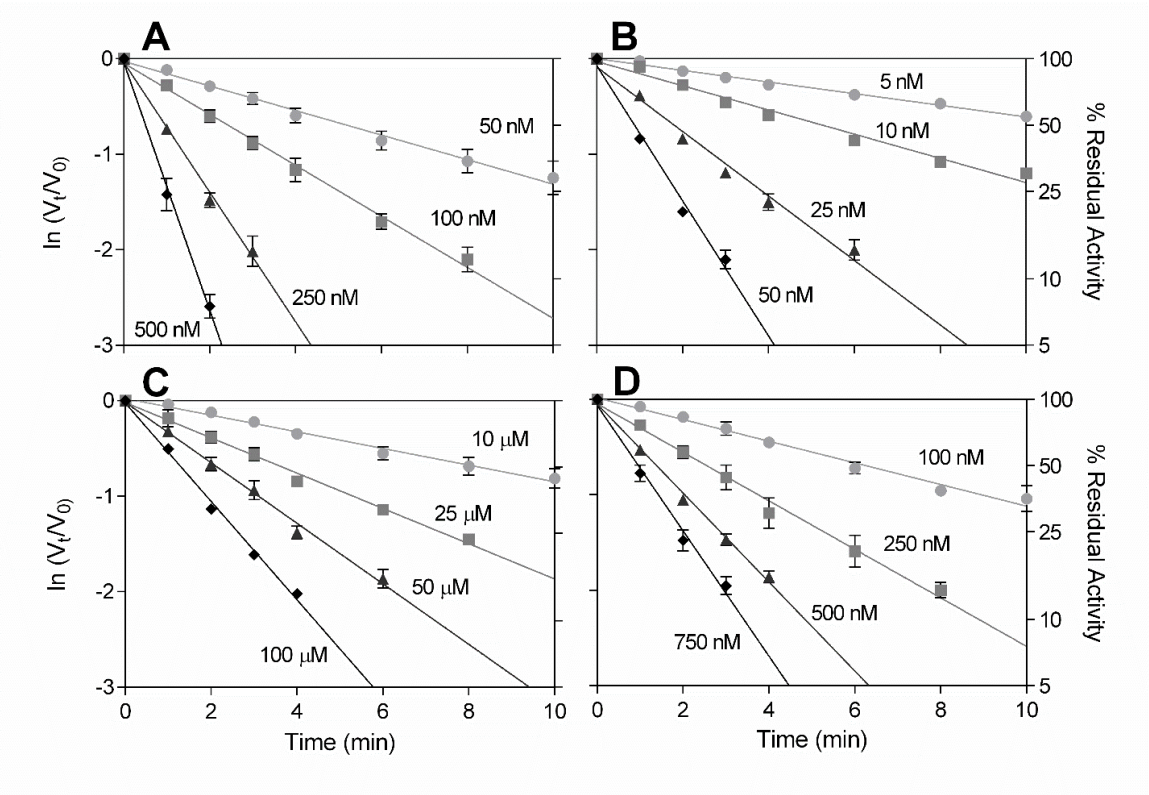

Figure 3-5. Concentration- and time-dependent inhibition of LMW C-BCs by PO (A), DFP (B), PB (C), and EthP (D). Primary plots show the natural log of residual free enzyme activity (V_t/V_0) versus time of pre-incubation with selected inhibitor concentrations. Data are reported as mean ±SD (n=3).

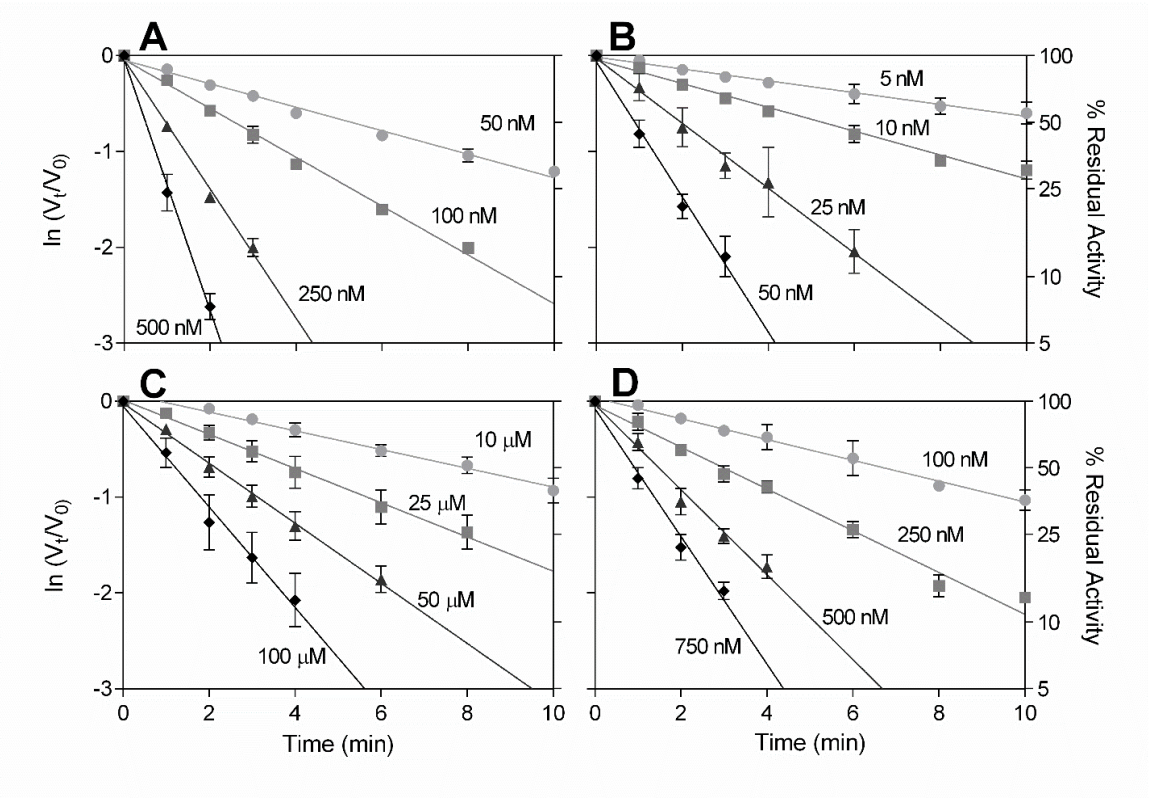

Figure 3-6. Concentration- and time-dependent inhibition of MMW C-BCs by PO (A), DFP (B), PB (C), and EthP (D). Primary plots show the natural log of residual free enzyme activity (V_t/V_0) versus time of pre-incubation with selected inhibitor concentrations. Data are reported as mean ±SD (n=3).

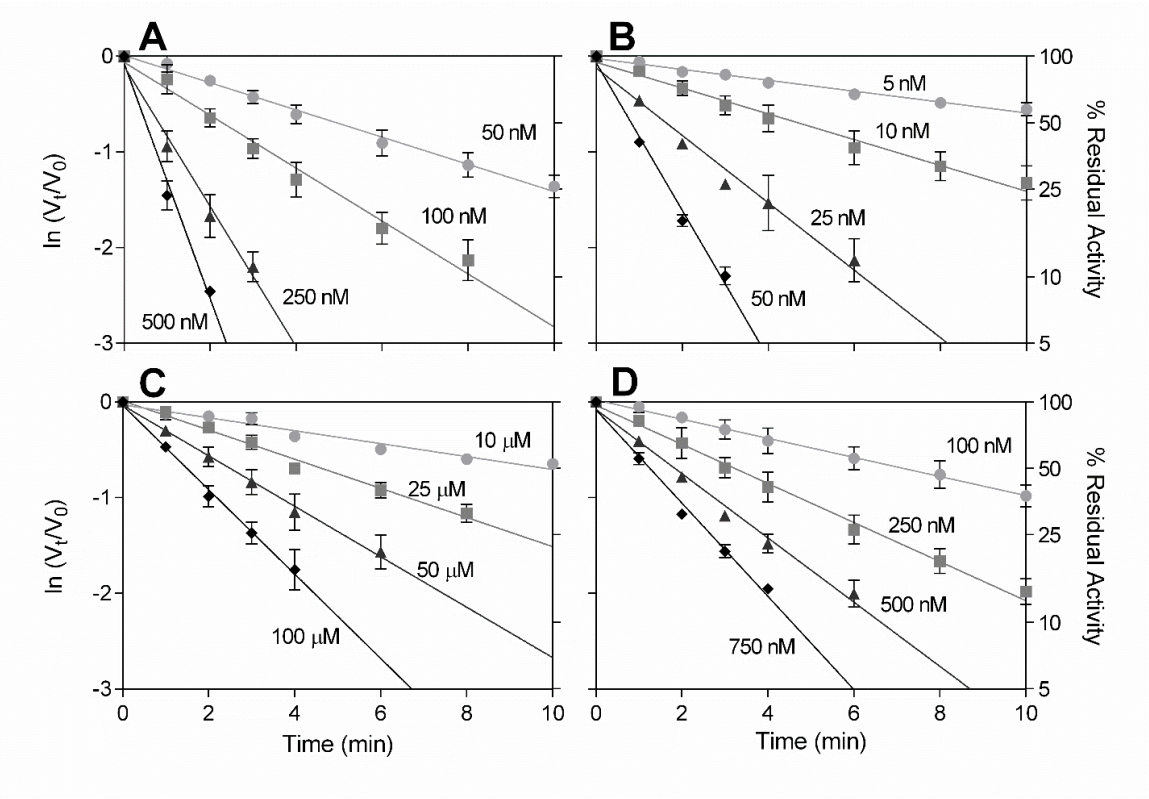

Figure 3-7. Concentration- and time-dependent inhibition of HMW C-BCs by PO (A), DFP (B), PB (C), and EthP (D). Primary plots show the natural log of residual free enzyme activity (V_t/V_0) versus time of pre-incubation with selected inhibitor concentrations. Data are reported as mean ±SD (n=3).

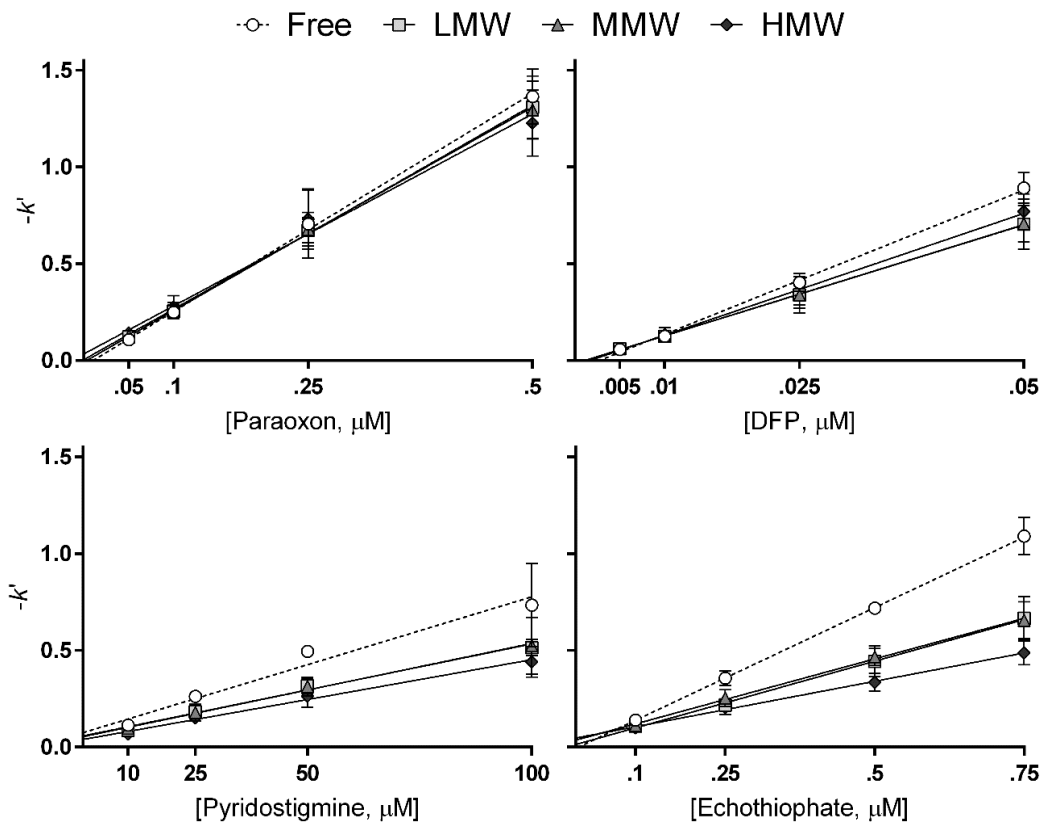

Figure 3-8. Secondary plots for bimolecular rate constant (k_i) determination. Plots represent -*k*' values (determined from primary plots in Figs. 3-4 to 3-7) versus inhibitor concentrations. The slope of these secondary plots determines k_i. Data are reported as mean ± SD (n=3).

Table 3-2. Bimolecular rate constants (k_i) of free rhBChE and C-BCs. Enzymes were exposed to either paraoxon (PO), diisopropylfluorophosphate (DFP), pyridostigmine bromide (PB) or echothiophate (EthP) at different inhibitor concentrations for different times, and then residual enzyme activity was measured as in section 3.2.3. Data represent mean values with 95% confidence intervals in parentheses (n=3).

	Enzyme Formulation	k_i (μM^{-1} min^{-1})	% Reduction
PO	Free	2.82 (2.7 - 3.0)	
	LMW	2.61 (2.5 - 2.7)	7.5
	MMW	2.65 (2.5 - 2.8)	5.9
	HMW	2.48 * (2.3 - 2.6)	12.1
DFP	Free	18.61 (18.0 - 19.2)	
	LMW	14.35 * (13.7 - 15.0)	22.9
	MMW	14.32 * (13.3 - 15.4)	23.1
	HMW	15.72 * (14.9 - 16.6)	15.5

	Enzyme Formulation	k_i (μM^{-1} min^{-1})	% Reduction
PB	Free	7.02×10^{-3} ($6.3 - 7.8 \times 10^{-3}$)	
	LMW	4.82×10^{-3} * ($4.5 - 5.1 \times 10^{-3}$)	31.4
	MMW	4.76×10^{-3} * ($4.2 - 5.3 \times 10^{-3}$)	32.2
	HMW	4.12×10^{-3} * ($3.8 - 4.5 \times 10^{-3}$)	41.3
EthP	Free	1.46 (1.4 - 1.5)	
	LMW	0.84 *# (0.8 - 0.9)	42.3
	MMW	0.86 *# (0.8 - 0.9)	40.9
	HMW	0.59 * (0.5 - 0.6)	59.7

* Indicates a significant difference compared to free rhBChE.
# Indicates a significant difference compared to HMW C-BCs.

3.3.3 *In Vitro* Scavenging Capacity of C-BCs Against Paraoxon

To further evaluate the effect of copolymer-complexation on bioscavenging capacity, we conducted an *in vitro* scavenging assay using a marker enzyme, carboxylesterase (CarbE), and paraoxon as a model OP compound. During a pre-incubation step, free rhBChE and C-BCs were separately incubated with PO, followed by addition of CarbE. If unbound paraoxon was remaining following the pre-incubation step, it would inhibit the added CarbE. Prior to this assay, the sensitivity of CarbE to PO was determined (Fig. 3-9), and a PO concentration was selected that elicited near 100% CarbE inhibition (20 nM). The BChE-specific inhibitor ethopropazine was included during the final CarbE activity quantitation to prevent excess (i.e. unbound) BChE from hydrolyzing the CarbE substrate. A preliminary assay was also conducted with ethopropazine to select a concentration which inhibited BChE but not CarbE (Fig. 3-10).

Figure 3-11 shows there was essentially complete CarbE inhibition when paraoxon was pre-incubated with only PBS before adding the marker enzyme. In contrast, pre-incubation of paraoxon with free rhBChE (Fig. 11A; $F_{(7,32)}= 90.27$, $p < 0.0001$) or C-BCs made with low molecular weight PLL- (Fig. 11B; $_{(7,14)} = 8.75$, $p = 0.0003$), medium molecular weight PLL-(Fig. 11C; $F_{(7,16)} = 55.82$, $p < 0.0001$) and high molecular weight PLL- (Fig. 11D; $F_{(7,24)} = 49.20$, $p < 0.0001$) based copolymers protected against CarbE inhibition in a relatively similar, concentration-dependent manner. Percent of residual CarbE activity is proportional to the amount of PO sequestered (i.e. if 100% CarbE activity remains, then 100% of PO molecules were sequestered in the first pre-incubation step). Therefore, a plot of percent sequestration versus log of the protein concentration allowed for estimation of relative *in vitro* scavenging capacity (Fig. 3-12). The EC_{50} (i.e.

amount of rhBChE necessary to protect 50% of CarbE activity) for the free enzyme was 48.8 nM (95% confidence interval [CI] = 45.6 - 52.3). The EC_{50} for the C-BCs were 53.6 nM (CI = 43.2 - 66.4), 46.3 nM (CI = 42.5 - 50.4), and 59.3 nM (CI = 54.0 - 65.2) for LMW, MMW, and HMW C-BCs, respectively. *Post hoc* analyses determined that the HMW PLL copolymer was significantly different than both free rhBChE ($p = 0.02$) and the MMW C-BC preparation ($p = 0.008$).

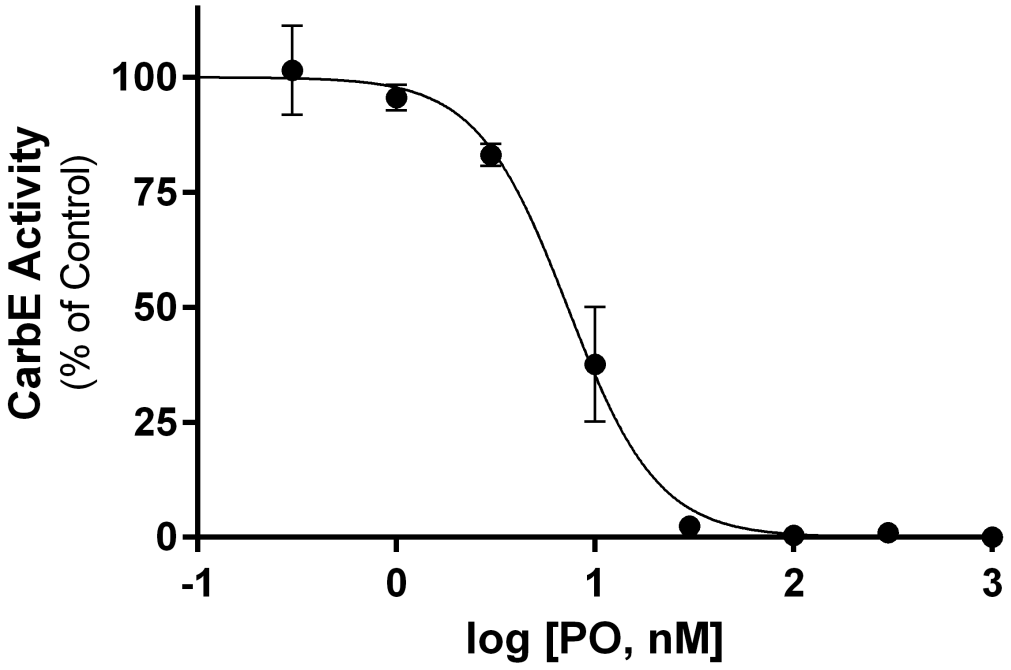

Figure 3-9. CarbE sensitivity to inhibition by paraoxon. CarbE (4 mU) was pre-incubated with paraoxon (0.3 - 1000 nM) for 20 minutes at 37°C, prior to addition of the substrate (p-nitrophenyl acetate, 50 μM) and measuring residual activity. Data are mean values ± SD (n=3). The determined IC_{50} value was 7.3 nM (95% confidence interval = 6.5 - 8.1).

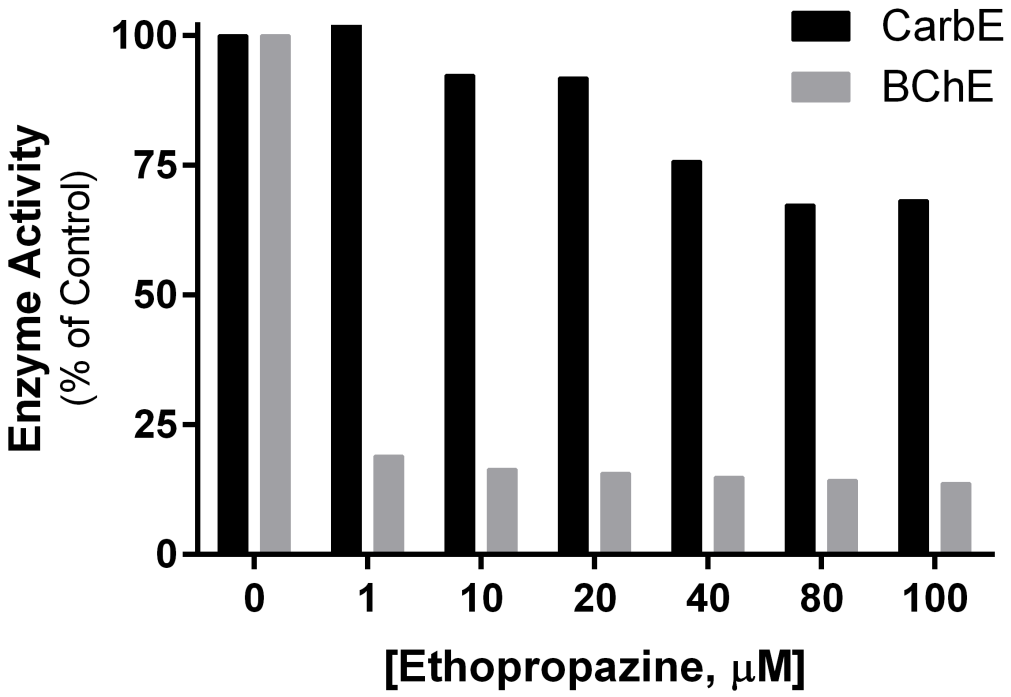

Figure 3-10. Sensitivity of CarbE and BChE to ethopropazine. CarbE (4 mU) or BChE (73.7 ng) was assayed using p-nitrophenyl acetate (50 μM final) containing ethopropazine (1-100 μM, final). Data are presented as percent of activity when no ethopropazine was added (mean values; n=1). Based on these data, a 10 μM final concentration of ethopropazine was added in the sequestration assay (described in section 3.2.6).

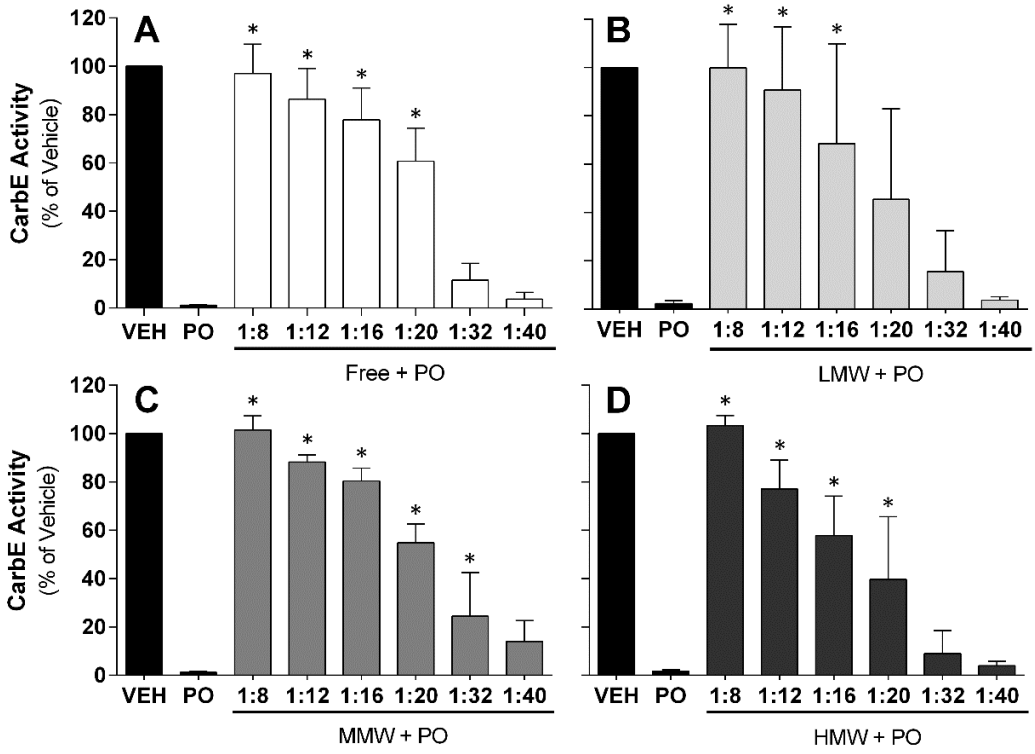

Figure 3-11. *In vitro* inactivation of paraoxon by free rhBChE and C-BCs. Dilutions (1:8 to 1:40) of free enzyme (A) and C-BCs using either the (B) low MW-, (C) medium MW- or (D) high MW PLL-based copolymer were first pre-incubated with either vehicle or PO (20 nM) for 20 min at 37°C. A marker enzyme, CarbE, was then added and the mixture incubated for another 20 min at 37°C. Remaining CarbE activity was measured by addition of substrate (p-nitrophenyl acetate) with ethopropazine (BChE-specific inhibitor). Activity in reactions pre-incubated without paraoxon and BChE were used as vehicle controls (VEH). Data are plotted as percent of control (mean ± SD) from 3 to 4 independent preparations. Asterisks indicate significant differences as compared to the paraoxon-only condition.

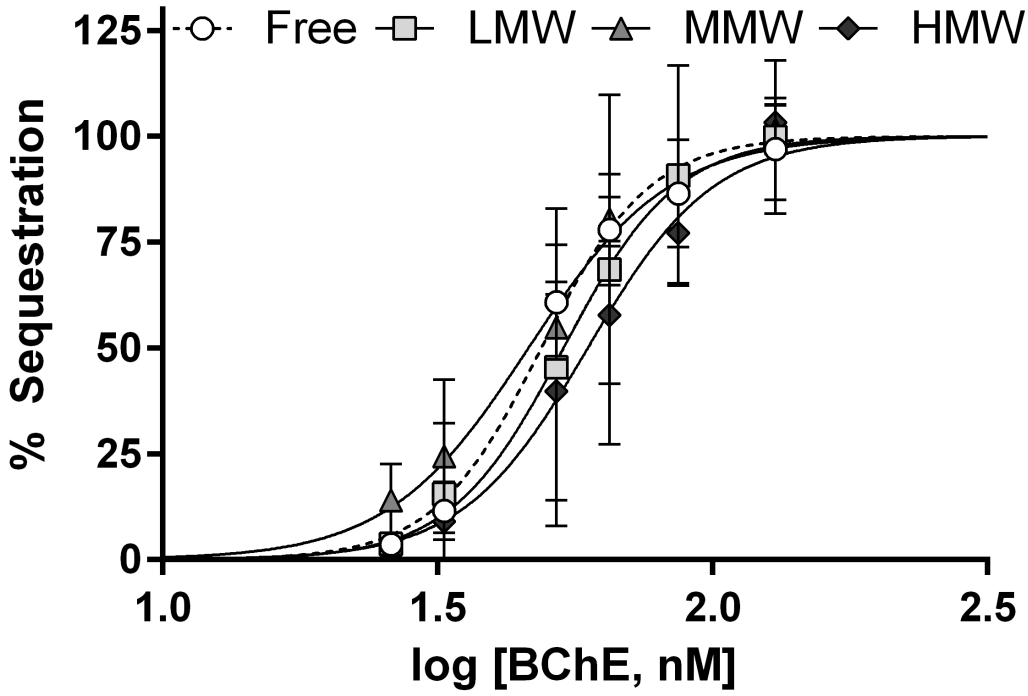

Figure 3-12. *In vitro* sequestration capacity of free rhBChE and C-BCs. Several concentrations of free rhBChE and low-, medium- and high molecular weight PLL C-BCs were first pre-incubated with either vehicle or paraoxon (20 nM) for 20 min at 37°C. CarbE was then added and the mixture incubated for another 20 min at 37°C. Remaining CarbE activity was measured by addition of substrate (p-nitrophenyl acetate) with ethopropazine (BChE-specific inhibitor). Data were plotted as percent sequestration (i.e. percent CarbE activity compared to inhibitor-free controls) (mean ± SD) from 3 to 4 independent preparations. Data were fit with nonlinear regression to determine EC_{50} values.

3.3.4 Sensitivity to Inactivation by Proteases and Heat

While the previous assays characterized the effect of copolymer-complexation on enzyme inhibition and catalytic activity, we also characterized the effect of copolymer-complexation on enzyme stability. Changes in *in vitro* heat sensitivity may affect shelf stability and storage conditions. Figure 3-13 shows comparative effects of a one-hour exposure to increasing temperatures on enzyme activity in the free rhBChE and C-BCs. The mean temperature at which 50% of the esterase activity was inactivated (T_{50}) with the free enzyme was 45.6°C (CI = 45.0 - 46.3). The T_{50} for the low, medium, and high molecular weight C-BCs were 57.7°C (CI = 56.9 - 58.6), 56.5°C (CI = 56.2 - 58.6), and 51.2°C (CI = 50.2 - 52.3), respectively. The difference in the T_{50} between the free enzyme and C-BCs was statistically significant in all cases ($p < 0.0001$). Further pairwise comparisons showed that LMW and MMW C-BCs were significantly different from the HMW C-BCs ($p < 0.0001$) . Next, a temperature near the T_{50} (55°C) was selected to perform an extended time course of inactivation of enzymatic activity in all preparations (Fig. 3-14). In agreement with the above results, nearly all free enzyme activity is lost after one hour at 55°C. The C-BCs retained partial activity (17 - 42%) up to 15 hours. The inactivation of all enzyme preparations fit well with a one-phase decay model (R^2 = 0.94 - 0.97), and the calculated half-lives were significantly different ($F_{(3, 192)} = 69.41$; $p < 0.0001$). *Post hoc* tests determined that the half-lives for the low- (70.0 min; CI = 56.8 - 91.2), medium- (51.5 min; CI = 42.2 - 66.0), and high- (24.8 min; CI = 21.2 - 29.9) molecular weight PLL C-BCs were all significantly different from the free enzyme (1.2 min; CI = 1.0 - 1.6) ($p < 0.0001$ in all cases). Pairwise comparisons between different copolymer weights did not reveal any further differences.

We also performed an assay with proteolytic enzymes, aiming to gain information on *in vivo* enzyme stability. Figure 3-15 compares the inactivation of BChE activity in the free and C-BCs following exposure to chymotrypsin, trypsin, and pronase. Pronase is a protease mixture from *Streptomyces griseus* which digests proteins into single amino acids [289]. Modeling these inactivation data with a one-phase decay model led to relatively high R^2 values for free rhBChE and C-BCs (R^2 = 0.75– 0.99). With each protease, an extra sum-of-squares F test determined that the best-fit curves for the free enzyme and C-BCs were statistically different from each other (chymotrypsin: $F_{(9,72)}$ = 16.52; trypsin: $F_{(9,60)}$ = 45.01; pronase: $F_{(9,60)}$ = 10.02, all $p < 0.0001$). Approximately 28% of free rhBChE activity was lost after one hour of incubation with chymotrypsin, with over 90% inactivation by eight hours. This same concentration of chymotrypsin reduced BChE activity by 17-22% in the C-BCs at one hour, and by eight hours between 53-75% loss of activity was noted. When trypsin was used, free enzyme activity was reduced by 44% at one hour while C-BCs lost between 21-22% activity. The separation between free enzyme and C-BC inactivation becomes greater after eight hours of incubation; free enzyme was 85% inactivated, and the inactivation of C-BCs was between 35-57%. When pronase was used, the free enzyme again appeared more sensitive than the copolymer-complexed enzymes (e.g., at 8 h, >95% inactivation was noted with free enzyme but 69-84% with the three copolymer-complexed enzymes). Interestingly, there were no significant differences detected in the inactivation half-life between the free enzyme and C-BCs with any of the tested proteases. Overall, these data suggest that a proportion of the BChE molecules in the C-BCs may be effectively shielded from the selected proteases and therefore could be more stable *in vivo*.

Enzyme activity following physical (i.e. heat) or biological (i.e. protease) inactivation was also visualized using native activity gels (Fig. 3-16). Free rhBChE control samples (lanes 2A and 2B) were composed primarily of monomers, with dimers and tetramers also present. Following one minute of heat treatment, monomeric activity was decreased, while activity in the tetramers and dimers appeared to remain relatively consistent. After eight hours of heat treatment, there was no remaining activity visible in the gel. This observation is supported by the colorimetric assay data. Trypsin inactivation of free rhBChE (one-hour incubation) resulted in active enzyme fragments with a molecular weight between that of the dimers and tetramers. While the dimeric activity band was greatly decreased, the overall amount of activity resulting from BChE monomers was minimally decreased. It is likely that disassociated tetramers and dimers contribute to the seemingly resistant monomeric activity. Following eight hours of trypsin inactivation, most of the free enzyme activity was inactivated, with the remaining activity arising primarily from BChE monomers. The majority of the MMW C-BCs did not migrate into the gel, possibly due to the large size of copolymer particles. The visible smearing underneath the main bands could be a result of smaller sized copolymers, as previous studies have suggested that the diameter of the C-BCs range from ~15-65 nm (median = 35 nm) [290]. After eight hours of inactivation, visible staining of MMW C-BC lanes appeared to be minimally decreased.

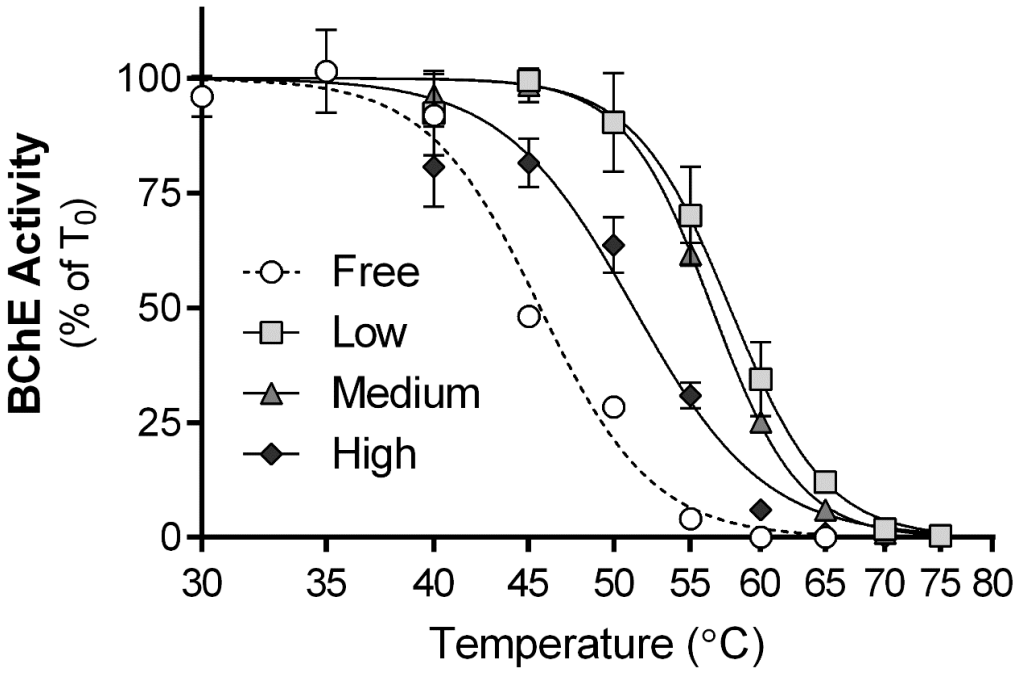

Figure 3-13. Heat inactivation of free rhBChE and C-BCs. Samples of the different enzyme preparations were incubated at 30-75°C for one hour, and then transferred to ice before being assayed for residual BChE activity using the colorimetric method described in section 3.2.3. Data are reported as percent of activity at time 0 (mean ± SD) from three independent replicates.

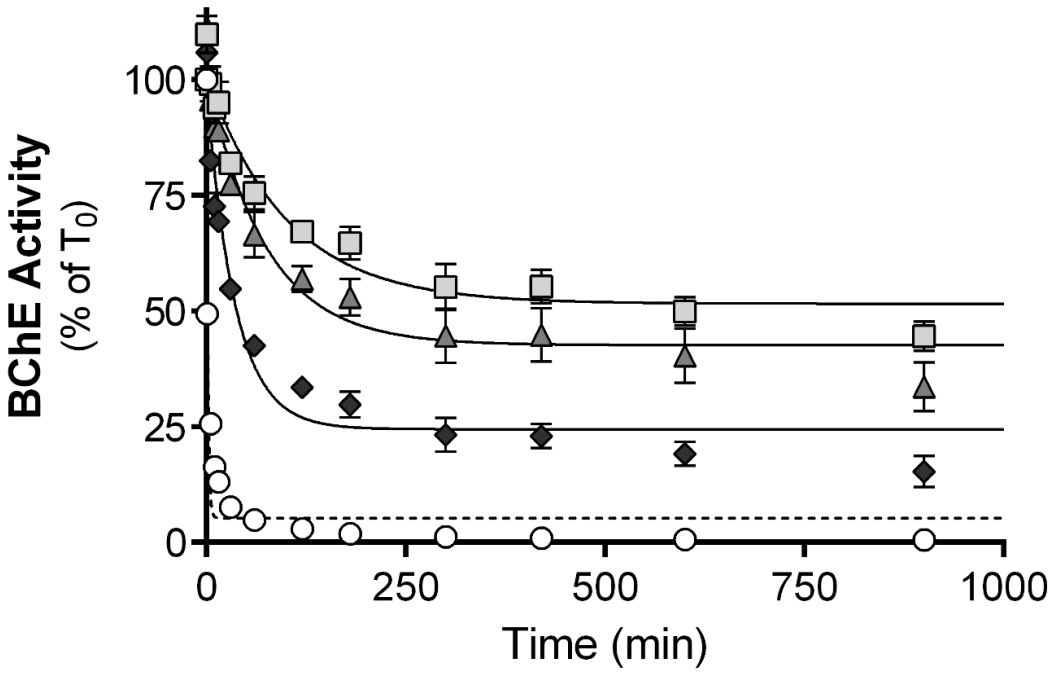

Figure 3-14. Time course of heat inactivation of free rhBChE and C-BCs. The different enzyme preparations were pre-incubated at 55°C, with samples being removed at intervals up to 900 minutes and assayed for residual BChE activity using the colorimetric method described in section 3.2.3. Data are reported as percent of activity at time 0 (mean ± SD) and have been fit using a one-phase decay model (n=3).

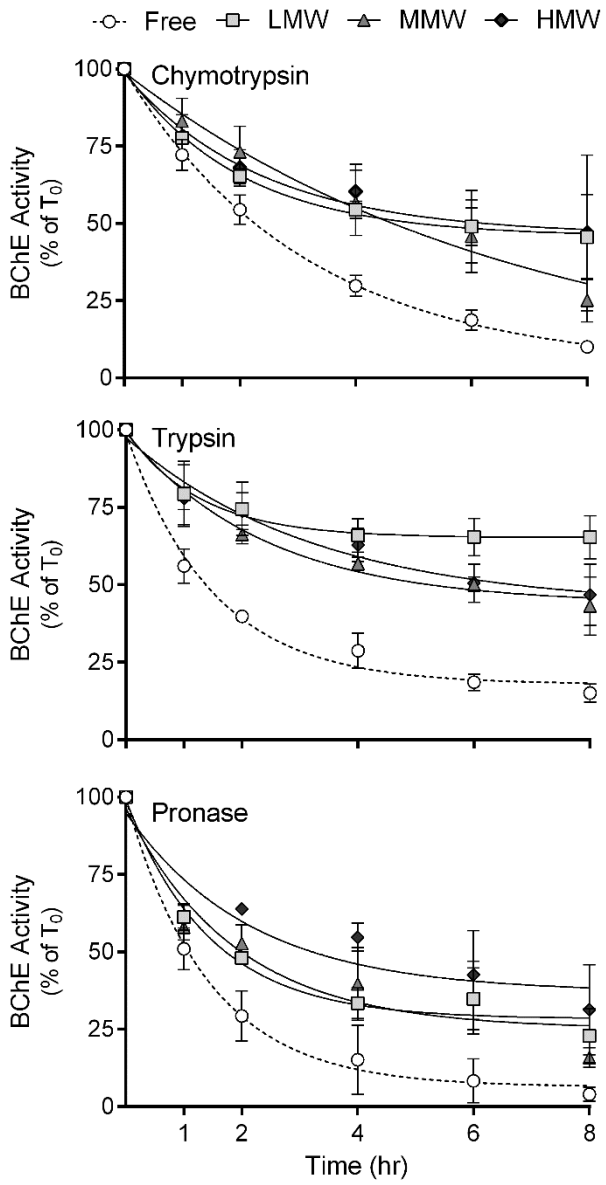

Figure 3-15. Protease-mediated inactivation of free rhBChE and C-BCs. The different enzyme preparations (low-, medium-, and high- molecular weight PLL) were incubated with either chymotrypsin, trypsin or pronase at 37°C and residual BChE activity was measured colorimetrically for up to eight hours. Data are reported as percent of activity at time 0 and fit with a one-phase decay model (mean ± SD; n = 3–4 independent replicates for each preparation).

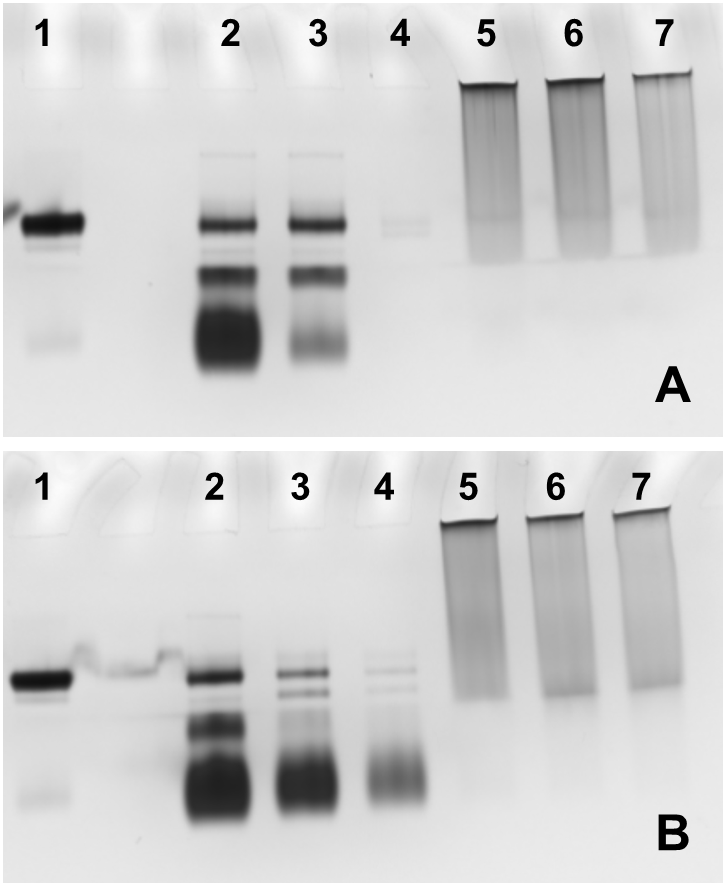

Figure 3-16. Native activity gels of free rhBChE and MMW C-BCs following physical and biochemical inactivation. Enzymes were either pre-incubated at a high temperature (55°C) (Panel A) or with trypsin (187.5 μg/ml at 37°C)(Panel B), and 5 μl samples were withdrawn at one minute (heat-inactivation), one hour (trypsin inactivation), and eight hours (both). Samples were run on non-denaturing gradient gels, followed by staining for BChE activity using the method of Karnovsky and Roots [287]. A sample of purified tetrameric human serum BChE (lane 1, both panels) was used as a marker enzyme. In both panels, lane 2 contains control (no inactivation) free rhBChE samples, and lanes 3 and 4 contain inactivated free enzyme samples (either 1 min and 8 h [A] or 1 h and 8 h [B]). MMW C-BC samples are loaded in lanes 5-7 (both panels) in the same order as free enzyme samples.

3.4 DISCUSSION

Poly(ethylene glycol) modification of proteins has been used to improve pharmacokinetic and pharmacodynamic properties of protein therapeutics [291]. BChE is an effective prophylactic against OP intoxication, though its circulatory half-life, among other things, make widespread implementation difficult. Therefore, the effect of PEGylation on BChE pharmacokinetics has become an area of interest [272, 292]. Gaydess and colleagues developed a PEG grafted poly-l-lysine copolymer which electrostatically assembled into a complex with BChE, and found that these complexes slightly increased the delivery of BChE across the blood brain barrier [9]. Previous studies in our lab further characterized the effects of copolymer:protein and PEG grafting ratios on these complexes [10]. This study aimed to further understand the influence of these polymeric constituents (made with either a low, medium, or high molecular weight PLL) on enzyme characteristics including substrate and inhibitor kinetics, *in vitro* scavenging capacity, and sensitivity to inactivation by heat and proteases.

As initial assays noted a marked reduction in catalysis in C-BCs using a single substrate concentration, we compared the kinetics of butyrylthiocholine hydrolysis between free and copolymer-complexed enzymes. The results generally agreed with our initial findings using a single substrate concentration. The turnover rate, k_{cat}, was significantly reduced with all three copolymer-complexed enzymes (Table 3-1). PEGylation has been found to decrease catalytic activity in other enzymes as well [12, 293, 294], though in some cases PEGylation has little or no effect on enzyme activity [13, 272]. It is also common for PEGylation to decrease binding affinity [12], though under our conditions K_M was not significantly increased. As there did appear to be a trend

towards increasing K_M values in our study, however, it is possible that further replicates could detect significant findings with the C-BCs as well. These data suggested that some BChE molecules within the C-BCs may interact with substrate in a relatively similar manner as the free enzyme, while others have lesser access to the substrate, leading to a reduction in substrate hydrolysis and catalytic efficiency. We postulated that charge repulsion may result from interaction of the quaternary nitrogen on the substrate with any free cationic residues of PLL, leading to hindered access of substrate to the BChE active site.

BChE exhibits complex substrate kinetics, based on location of the active site deep within a "gorge" in the enzyme quaternary structure, the possibility of additional substrate molecules binding to residues at the entrance to the gorge, and related conformational changes between two forms of the enzyme with differing catalytic activities [295, 296]. The end result is that classical Michaelis-Menten kinetics are typically not observed with charged substrates of BChE across a wide range of substrate concentrations. We selected substrate concentrations (10-1000 mM) to minimize the possibility of substrate inhibition, and our data fit relatively well with the Michaelis-Menten model. While our substrate kinetics evaluations do not fully describe the complexity of BChE-substrate interactions in the catalysis of butyrylthiocholine, they do support our original observation that the copolymer-complexed enzymes have an overall reduction in catalytic efficiency compared to the free enzyme.

We then characterized the kinetic interactions between BChE (as free or copolymer-complexed enzyme) and four different anticholinesterases. As we hypothesized that charge repulsion could potentially play a role in the apparent loss of

enzyme activity in the copolymer-BChE complexes, we evaluated kinetics of inhibition using both neutral (paraoxon and DFP) and positively charged (pyridostigmine and echothiophate) inhibitors. While the inhibitory potency of paraoxon was slightly decreased in the HMW C-BCs only (12% reduction), k_i values with DFP were significantly reduced (16-23%) with all three copolymer-complexed enzymes, suggesting that charge repulsion could not completely explain differential changes in catalysis and inhibition between charged and neutral ligands. With the positively charged inhibitors, however, inhibitory potency (k_i) was indeed reduced to a greater extent (pyridostigmine, 32-41% and echothiophate, 41-60% reduction; Table 3-2). Together, these findings suggest that a positive charge on an inhibitor (or substrate) could impair its access to the copolymer-complexed enzyme because of the polycationic nature of the PLL backbone, but that other factors, e.g., lipophilicity, might also influence ligand binding to copolymer-complexed enzymes. The extent of reduction in k_i with the four inhibitors studied generally agrees with observed or predicted $\log K_{OW}$ values (paraoxon, 1.98; DFP, 1.17; pyridostigmine, 0.94; echothiophate, -2.25) [297]. Further studies using a larger set of substrates and inhibitors with a wider range of physicochemical properties as well as copolymers with differing properties (e.g., varying sizes, residual cation density) could provide more insight into the molecular basis for selective interactions between ligands and copolymer-complexed enzymes.

Regardless of the molecular basis for differential binding of inhibitors to copolymer-complexed enzymes, reduced inhibitory potency with the copolymer-complexed enzymes could have practical implications in their use as bioscavengers. It is estimated that ideal bioscavengers should be able to completely detoxify an OP exposure

within one circulation time [298]. Thus, significant changes in the *rate* of inhibitor binding are an important parameter to consider in addition to the upper limit of inhibitor binding. For example, the apparent similar interactions between paraoxon and all enzyme preparations (reflected as similar k_i values) suggest that the copolymer-complexed enzymes would be equally effective as bioscavengers compared to the free enzyme. The results from the *in vitro* scavenging assay with paraoxon (Fig. 3-12) generally agreed with those from the inhibition kinetics assays (i.e. LMW and MMW C-BCs had the same ability to sequester paraoxon while the HMW C-BCs were slightly but significantly decreased). These results suggest that inhibitor kinetics are a better measure of bioscavenging potential than catalytic activity, though further *in vitro* scavenging assays (using different inhibitors) would be necessary to confirm this. Moreover, the lower k_i for pyridostigmine with a complexed enzyme suggests this inhibitor may have more difficulty binding to the active site region and therefore could be scavenged less effectively than by the free enzyme. Since pyridostigmine can be used as a prophylactic agent against OP toxicants by inhibiting acetylcholinesterase in the peripheral nervous system, lesser interaction with a copolymer-complexed enzyme could be an advantage if both pyridostigmine and an OP toxicant were present. These considerations are tempered however by the relatively small degree of change in inhibitory potency noted with all of the copolymer-complexed enzymes.

Each of the C-BC preparations tested was also more thermostable than free rhBChE (Figs. 3-13 and 3-14). Thermal stability of enzymes has been used for over a century to characterize protein function [299]. Enzymes undergo an irreversible conformational change at higher temperatures, leading to a dramatic loss of activity

above a certain temperature. Prepared enzyme prophylactics may be exposed to high temperatures during storage or use in battlefield scenarios, which may lead to enzyme aggregation and activity loss. While PEGylation has been found to increase temperature resistance in some systems [12, 13], PEGylation of the catalytic bioscavenger OPH slightly decreased the thermal stability of the enzyme [277]. The noted increase in thermostability of our copolymer-complexed BChE could be indicative of a higher *in vivo* and "shelf" stable preparation, which could be an advantage of copolymer-complexed enzymes in further bioscavenger development and application.

The current study has also demonstrated that our C-BCs were more resistant to the proteases chymotrypsin, trypsin, and pronase (Fig. 3-15). With each protease, the free, uncomplexed enzyme lost activity to a greater extent over the eight-hour incubation period compared to copolymer-complexed enzymes. These results support previous findings that PEGylated BChE, among other enzymes, are generally more resistant to protease degradation [13, 272, 300]. The higher plateau of inactivation noted with the copolymer-BChE complexes could be an indicator that some BChE molecules within the polyionic complexes are shielded from interaction with proteases. This was further supported by the native activity gels (Fig. 3-16, panel B). At each time point, the overall staining density decreased slightly but the distribution did not, suggesting that enzyme activity which remains inside the copolymer is somewhat shielded from inactivation. Regardless, these findings suggest that the copolymer-complexed enzymes could be more resistant than the free enzyme *in vivo* to degradation by endogenous proteases.

In general, the copolymer-complexed enzymes appeared to have different sensitivity to inactivation by inhibitors, proteases and heat. There were however, some

instances where the type of complex (i.e., based on the size of the PLL used in the copolymer) influenced sensitivity. When inhibition kinetics were compared using echothiophate as the inhibitor, k_i was significantly different with all three copolymer-complexed enzymes compared to the free enzyme, but complexes made with copolymer having the high molecular weight PLL was reduced further than in the other two types of complexed enzyme. *In vitro* scavenging assays demonstrated that the HMW copolymer was significantly different from free rhBChE and the MMW C-BCs, but no other differences were detected. Moreover, heat inactivation of the complexed enzymes appeared copolymer-dependent, i.e., the free enzyme was inactivated at lower temperatures than complexes with the high molecular weight PLL, but complexes made with the low and medium molecular weight PLL were even more resistant. Thermal stability resulting from PEGylation has been previously shown to be dependent on PEG molecular weight [12], though interestingly our findings seemed to suggest a negative correlation (i.e. the high molecular weight CBCs were the least stable). Other studies have also suggested factors such as PEG type (branched versus linear), PEG molecular weight, and grafting ratio affect the pharmacokinetics and pharmacodynamics of PEGylated enzymes [274, 301, 302]. Our results support the notion that PEG molecular weight differentially affects the properties of PEGylated enzymes. Furthermore, these findings suggest that tuning of copolymer properties could lead to further optimization for ligand binding and bioscavenger efficacy/selectivity as well as stability.

In conclusion, complexes of recombinant human BChE with PLL- g-PEG copolymers lose partial catalytic activity but differentially retain the ability to interact with inhibitors in a structure-dependent manner. While increased resistance to heat and

protease inactivation was noted, any potential benefits of increased stability could be countered, however, if the enzyme's ability to interact with toxicants was reduced. Kinetic analyses suggest that the copolymer, via electrostatic, hydrophobic or possibly other interactions, may influence how a chemical ligand interacts with the enzyme active site. Understanding how proteins and polymers interact within these complexes may aid in the design of more effective bioscavengers as well as other polymer-based protein therapeutics.

CHAPTER IV

EVALUATION OF SURFACE PEPTIDE NETWORKS ASSOCIATED WITH CATALYSIS IN A VARIANT ($BCHE_{G117H}$) FOR RE-ENGINEERING

4.1 INTRODUCTION

While the safety and efficacy of BChE is well-demonstrated in animal models, translation to widespread clinical use is difficult. Pharmacokinetic improvements using PEG and cell carriers may provide an improved dosing schedule; however, the stoichiometric nature of BChE results in an inherent pharmacodynamic drawback. Although a 200 mg dose of BChE is considered effective, a high OP exposure may overcome BChE's scavenging ability. In contrast to the stoichiometric nature of the native enzyme, the G117H mutant of BChE has catalytic activity against some OPs; however, its low hydrolytic rate makes further development necessary to function as a biologically relevant catalytic scavenger.

An emerging concept in enzyme function is that dynamic motions of peptide sequences on an enzyme's surface, distant from the active site region, can influence the

rate of a catalytic reaction. It has been proposed that catalytic rate is affected by thermodynamical coupling of the hydration-shell, the bulk solvent, and the catalyzed reaction [303]. For a number of enzyme systems, networks of conserved residues have been discovered that span from the surface of the protein to the active-site region, effectively coupling with the catalytic reaction mechanism [304]. In fact, enhancing energy flow through these networks may be a general approach for increasing enzyme-mediated catalysis. Conformational fluctuations in such peptide networks were shown to coincide with catalysis in the serine hydrolase lipase B from *Candida antarctica*, which utilizes the same catalytic triad as BChE and other serine hydrolases [15]. Importantly, insertion of a photosensitive azobenzene bridge joining the flexible surface loops on *C. antarctica* lipase B allowed enhanced photostimulation of catalysis. It is proposed that energy transfer from the surface loop to the catalytic site is influenced by the position, number, and the physicochemical nature of the peptides within the sequence. Thus, increasing the length of this loop and facilitating its interaction with the solvent may increase catalytic activity *via* increased energy transfer.

The major goal of Aim 2 was to characterize the catalytic activity of mutants of $BChE_{G117H}$ with systematically modified surface loops. We hypothesized that applying these principles to $BChE_{G117H}$ would aid in the development of a rationally-designed mutant with increased catalytic activity towards OP compounds. Based on BLAST analyses, a similar enzyme (serine carboxypeptidase) was found with a surface network having similar residues as noted in BChE, but with a higher number of peptides. Molecular dynamics simulations suggested that increasing the number of peptides in the loop may increase fluctuation of the loop and consequently increase energy transfer to the

active site. Using these data, a set of six loop mutants was expressed containing three additional residues. We estimated the kinetic parameters for substrate hydrolysis using a choline ester (butyrylthiocholine) and OP (paraoxon) substrate. To further characterize the ability of these mutants to reactivate following OP binding, resistance to inhibition and enzyme reactivation (k_3) assays were conducted using the OP inhibitors paraoxon, DFP and echothiophate. The set of six loop-mutant enzymes and four substrates (butyrylcholine, paraoxon, DFP, echothiophate) were also evaluated computationally to determine the dynamics of each mutant.

4.2 MATERIALS AND METHODS

4.2.1 Chemicals

Paraoxon (O,O'-diethyl-*p*-nitrophenyl phosphate; PO) (98.6% purity by HPLC) was purchased from ChemService (West Chester, PA). A 10 mM stock solution of paraoxon was prepared in 100% dry ethanol and kept desiccated under nitrogen at -80°C until use. Diisopropylfluorophosphate (2-[fluoro(propan-2-yloxy)phosphoryl]oxypropane; DFP) (99% purity by NMR) was kindly provided by Dr. Derik Heiss at Battelle Memorial Institute (Columbus, OH) and stored as provided at _-80°C [278]. Echothiophate iodide (2-diethoxyphosphorylsulfanylethyl(trimethyl)azanium; EthP) was originally obtained from Wyeth-Ayerst and was a kind gift from Dr. Oksana Lockridge (University of Nebraska, Omaha, NE). Butyrylthiocholine iodide (BTChI), 5,5'-dithio-bis-(2-nitrobenzoic acid)(DTNB), and remaining chemicals and reagents were purchased from Sigma-Aldrich.

4.2.2 Molecular Simulations of $BChE_{G117H}$

Molecular dynamics (MD) simulations were performed in collaboration with Dr. Pratul Agarwal (Oklahoma State University). MD simulations were performed to evaluate $BChE_{G117H}$ and $BChE_{G117H}$-derived loop mutants interacting with four substrates (butyrylcholine, paraoxon, echothiophate, and DFP) using AMBER v14 [305]. In all cases, simulations were performed using NVIDIA GPUs and AMBER's *pmemd.cuda* simulation engine using the *ff14SB* force field, as described previously[306-308]. Coordinates for BChE (4BDS) and acetylcholine (4BDS) are available in the protein data bank [309, 310], and served as templates to build the desired enzyme/substrate complex in AMBER's LEaP program. During the preparation step, each complex was neutralized using counter-ions and solvated using explicit SPC/E water molecules with a 10 Å minimum distance between the protein and the edge of the periodic box. After preparation, the system was equilibrated as described previously [311]. Production simulations were run under constant energy conditions (NVE ensemble) with an initial temperature of 300 K. These simulations ran for 200 nanoseconds (ns) with a time-step of 2 femtoseconds (with SHAKE applied to bonds and angles involving hydrogens). Computational snapshots were stored every 20 picoseconds, resulting in 10,000 coordinates for further analysis.

Protein flexibility was calculated using the aggregated root-mean-square-fluctuations for top 10 quasi-harmonic modes ($RMSF_{10}$). This analysis was done using AMBER's *ptraj* analysis program. The $RMSF_{10}$ method captures the slow intrinsic "breathing" which occurs during enzyme catalysis, as opposed to random fast motions [312]. Prior to this analysis, the trajectory coordinates were aligned to remove any

influence of molecular rotation on the results. The energy from the enzyme-substrate interactions were calculated based on a previously developed protocol [311, 313]. All enzyme-substrate atom pairs were evaluated to calculate the total electrostatic and van der Waals energy between them. The results reflect the average energy sum of the 10,000 snapshots collected over 200 ns.

4.2.3 Expression of Selected Recombinant Loop Mutants

Production of loop-mutant BChE was conducted by Krishna Bhattarai and Dr. Haobo Jiang (Entomology & Plant Pathology, Oklahoma State University). We constructed a monomeric $BChE_{G117H}$ mutant (control with no insertions) and six monomeric $BChE_{G117H}$ loop mutants with three amino acid insertions into the protein sequence (between residues 278-285) with an identity of ENX, keeping the glutamate and asparagine insertions constant but varying "X" with one of six different amino acids (A, G, I, P, R, and T). The constructs of all seven were cloned into the pMFH6 vector to express the mutants with a hexahistidine tag at the C-terminus. *In vivo* transposition of the expression cassette into a bacmid in DH10Bac cells, isolation of recombinant bacmid DNA, and transfection of the recombinant bacmid DNA into *Spodoptera frugiperda* Sf9 cells to generate recombinant baculovirus were performed according to the Bac-to-Bac Baculovirus Expression System (Invitrogen Life Technologies), The baculovirus stock was then amplified and tittered to infect Sf9 cells for large-scale expression of mutants. The expressed proteins, secreted in the medium, were purified using a Q Sepharose Fast Flow column followed by a Ni^{2+}-NTA agarose column. Protein concentrations were determined on a NanoDrop Spectrophotometer (Thermo Scientific ND1000).

4.2.4 Choline Substrate Kinetics

Substrate kinetics of $BChE_{G117H}$ and loop mutants were conducted similarly to the method described in section 3.2.4. Briefly, 17.5 ng of enzyme (diluted in PBS) was added to a 96-well place and combined with the substrate cocktail (100 µM DTNB in Tris-E buffer, pH 7.4) containing a range of BTChI concentrations (10, 25, 50, 75, 100, 250, 500, 750, 1000, 2000 µM). Enzyme activity was estimated based on the rate of appearance of the reaction product, 2-nitro-5-thiobenzoate (ε = 14,150 M^{-1} cm^{-1}) at 412 nm in quadruplicate reactions, and was uniformly corrected for non-enzymatic substrate hydrolysis. V_{max} and K_M were determined using non-linear regression using the Michaelis-Menten equation. Turnover number, k_{cat}, was calculated using the relationship $V_{max} = k_{cat}[E]$, where [E] represents the concentration of BChE active sites in the reaction.

4.2.5 Paraoxon Hydrolysis Assay

Enzyme activity against the OP substrate paraoxon was determined using a direct hydrolysis assay, similar to that used by Lockridge and coworkers [14]. $BChE_{G117H}$ and loop mutant enzymes were diluted to 0.06 mg/ml using PBS. Stock paraoxon (10 mM in 100% ethanol) was diluted on the day of assay to achieve final concentrations between 10-500 µM containing 5% ethanol. The final reaction volume was 100 µl containing 7.5 µl diluted enzyme, 72.5 µl 100 mM potassium phosphate buffer (pH 7.0), with the reaction being started by the addition of 20 µl of paraoxon. The product of paraoxon hydrolysis, *p*-nitrophenol, is monitored at 405 nm for one hour using a Spectramax M2 microplate reader (Molecular Devices; Sunnyvale, CA) pre-heated to 37°C. The extinction coefficient of p-nitrophenol (ε = 18,500 M^{-1} cm^{-1}) was used to determine enzyme activity which was corrected for non-enzymatic hydrolysis.

4.2.6 Resistance to Inhibition Assay

Prior to the reactivation assay, the sensitivity of wild-type enzyme to inhibition by the selected OP compounds was determined. BChE (20 ng) was pre-incubated with PO, DFP, or EthP (0.5 - 500 nM for all) for 20 minutes at 37°C, prior to addition of substrate (1 mM BTChI) for the measurement of activity as described in section 3.2.3. Enzyme activity was reported as percent residual activity as compared to control (no inhibitor) values.

The loop-mutant enzymes' ability to resist inhibition by OPs was conducted using a method derived from Wang and colleagues [314]. Based on previously determined protein content, working enzyme solutions were prepared prior to assay (2 μg/ml in 100 mM potassium phosphate buffer, pH 7.0). Twenty ng of enzyme and either paraoxon (50 μM final), diisopropylfluorophosphate (5 μM final), echothiophate (100 μM final), or buffer (to evaluate control enzyme activity) was pre-incubated for 10 minutes in a 96-well plate containing buffer (100 mM potassium phosphate, pH 7.0) and DTNB (0.5 mM final). Following pre-incubation, 20 μl of BTChI (1 mM final) was added to begin the reaction. The reaction was monitored as described in section 3.2.3, and results are reported as percent of non-inhibited control.

4.2.7 OP Reactivation Assay

The rate of dephosphylation (k_3) is a measure of an enzyme's ability to reactivate following OP exposure and thus can be a good measure of progress in catalytic bioscavenger development. The k_3 of $BChE_{G117H}$ and loop-mutants was determined exactly as described in Lockridge and colleagues [14]. In brief, enzyme (20 μg/ml) and OP (10 mM paraoxon, echothiophate, or DFP) were pre-incubated for one minute to

allow for complete saturation of enzyme active sites. Following incubation, a 5 µl sample was removed, diluted 400-fold into a cuvette containing necessary reaction elements (0.5 mM DTNB, 1 mM BTChI, 100 mM potassium phosphate buffer, pH 7.0) and gently mixed. The large dilution reduces the final OP concentration to below its K_M, resulting in rapid dissociation of non-covalently bound enzyme-OP Michaelis complexes. Reactivation of covalently bound enzyme was then followed at 412 nm at 37°C using a Spectramax M2 microplate reader (Molecular Devices; Sunnyvale, CA). As this assay is very time sensitive, the time between sample transfer and initiation of cuvette reading was kept constant (5 sec).

4.2.8 Statistical Methods

Differences in enzyme activity and substrate kinetics parameters with both BTChI and paraoxon, were evaluated using one-way ANOVA with enzyme type (i.e. $BChE_{G117H}$ or loop mutants [ENI, ENI, ENG, ENR, ENT]) as the main factor. When the concentration-dependent inactivation of wild-type rhBChE was evaluated (i.e. IC_{50}) the inhibitor concentrations (x-values) were log-transformed and the data fit to a nonlinear regression equation (using a variable slope model). Initial plots of enzyme reactivation were fitted using linear regression, constrained between 2 and 7 minutes. The difference between the actual versus extrapolated values between 0 and 2 minutes were then plotted on a log10 x-axis versus time. These secondary plots were fit using a one-phase decay model for determination of the rate constant (under these conditions, the rate constant represents k_3). For the resistance to inhibition and reactivation rate (k_3) assays, statistical differences were determined using two-way ANOVA with enzyme and OP type as the main effect variables. In all cases, a *post hoc* Dunnett's multiple comparisons test was performed to

determine differences among $BChE_{G117H}$ and the loop mutants. Statistical significance was defined as a p-value < 0.05 in all cases, and p-values resulting from multiple comparisons analysis reported in-text are multiplicity adjusted. All statistical tests were conducted using GraphPad Prism software (La Jolla, CA), version 6.0.

4.3 RESULTS

4.3.1 Molecular Dynamics Studies

Simulations of enzyme-substrate interactions over 200 nanoseconds were performed with five of the loop mutant enzymes and four OP compounds. Simulations were not performed with the ENP mutant due to low esteratic activity (described in section 4.3.2). Movies of the MD simulations have been deposited online and are available at: https://doi.org/10.17026/dans-xym-nu36. Figure 4-1 shows the average position of butyrylcholine (BCh), PO, DFP, and EthP in the active site pocket during the MD simulation with $BChE_{G117H}$. While the choline ester substrate retained contact with active site residues of $BChE_{G117H}$ (3-4 Å), the OP compounds generally did not keep stable contact with active site residues. Of the OP compounds, EthP had the strongest interactions with the enzymes' active site overall. In the case of PO, the ENI mutant had stronger interactions with the active site compared to $BChE_{G117H}$. Observed interactions with DFP were the most unstable overall, even leaving the protein completely when modeled with $BChE_{G117H}$ and ENG, though slightly improved interactions were noted with the other loop mutants (ENA, ENG, ENI, ENR, ENT).

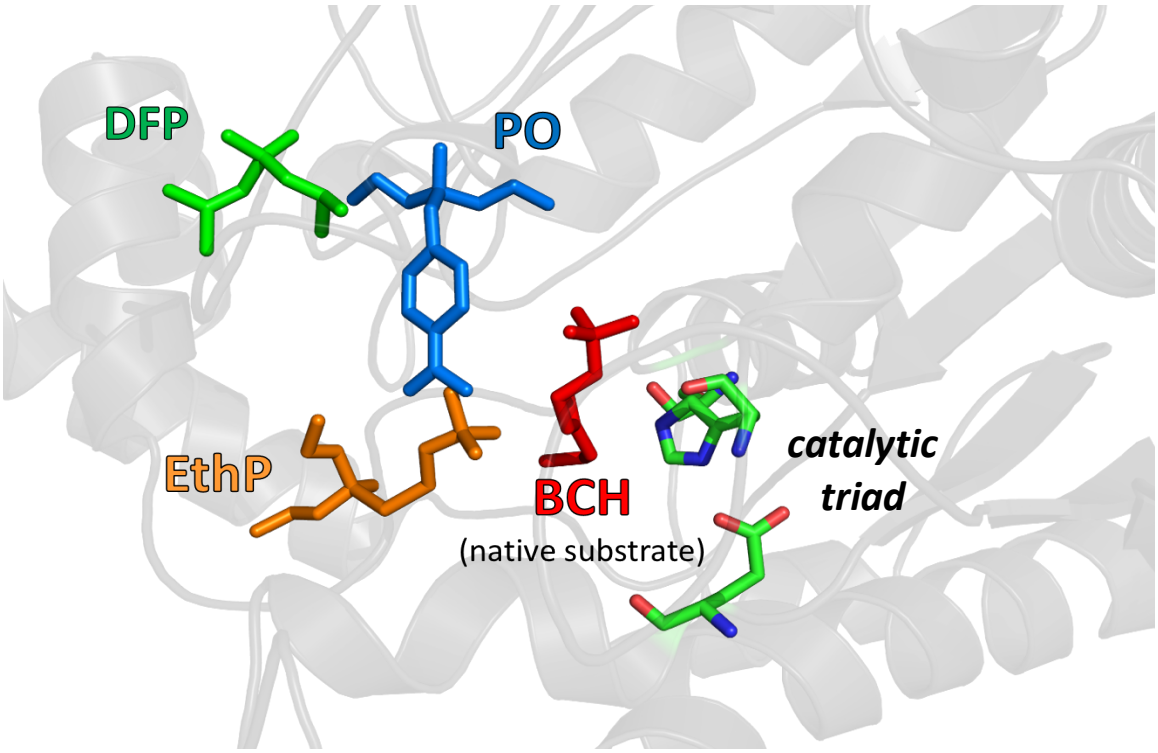

Figure 4-1. Average distance of substrate molecules to the active site of $BChE_{G117H}$. Molecular dynamics studies were performed to model the interaction of butyrylcholine, PO, DFP, and EthP with the active site triad of $BChE_{G117H}$. The positions of the molecules reflect their average position during the 200 ns simulation.

4.3.2 Activity of Loop Mutants with BTChI as Substrate

The activity of $BChE_{G117H}$ and the $BChE_{G117H}$-derived loop mutants were evaluated first using the choline substrate, BTChI. Figure 4-2 shows that all loop mutants had significantly reduced activity (62-95%) compared to $BChE_{G117H}$ ($F_{(6,28)} = 606.8$, $p < 0.0001$). The rank order of activity of the loop mutants can be separated into three tiers, based on the determined 95% confidence intervals (ENP < ENI, ENA, ENR < ENG, ENT). Due to its low activity, ENP was not included in further evaluations. The activity of the loop mutants using BTChI was further characterized using a substrate kinetics assay described in section 4.2.4 (Fig 4-3). Table 4-1 shows the kinetics parameters (k_{cat}, K_M, and k_{cat}/K_M) determined using nonlinear regression fit to the Michaelis-Menton equation. The turnover rate with BTChI was significantly reduced (40−84%) in all enzymes with loop insertions compared to $BChE_{G117H}$ ($F_{5,156} = 58.06$, $p < 0.001$). A significant effect was also found in K_M values ($F_{5,156} = 5.25$, $p = 0.0002$). *Post hoc* analysis indicated that ENG ($p = 0.04$) and ENR ($p < 0.0001$) mutants had a significantly higher K_M in comparison to $BChE_{G117H}$. These parameters together as the ratio k_{cat}/K_M suggest that the catalytic efficiency of the loop mutants was reduced compared to $BChE_{G117H}$. Note that the mutants were designed based on computational identification of increased dynamics of the loop region during modeling of paraoxon hydrolysis.

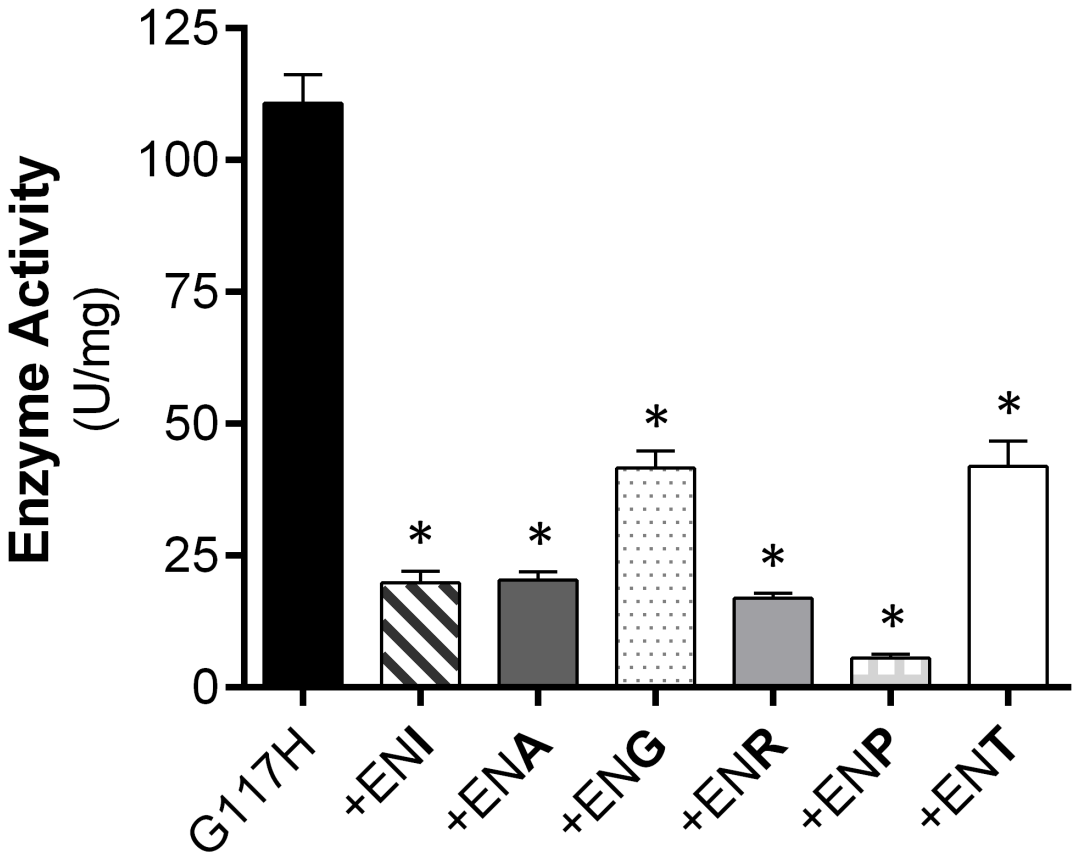

Figure 4-2. Activity of $BChE_{G117H}$ and loop mutants with BTChI as substrate. Enzyme activity was determined as described in section X, using 20 ng of enzyme and 1 mM BTChI as the substrate. Data are reported as units of enzyme activity (defined as μmol/min) per milligram of enzyme (mean ± SD; n=5). Asterisks indicate a significant difference from $BChE_{G117H}$.

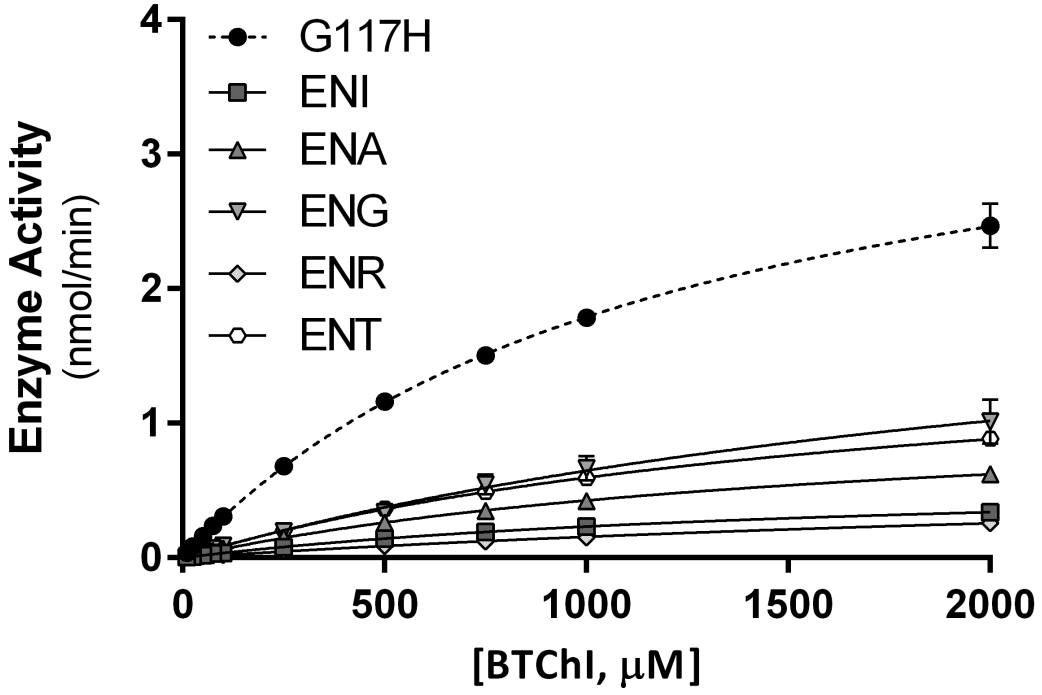

Figure 4-3. Concentration-dependent hydrolysis of BTChI by $BChE_{G117H}$ and loop mutants. Each enzyme preparation was incubated with butyrylthiocholine (10 μM - 2000 μM) for 5 min at 37°C and activity measured using a modified Ellman method. Data represent mean ± SD determined from three independent replicates.

Table 4-1. Substrate kinetic parameters (k_{cat}, K_M, and k_{cat}/K_M) for $BChE_{G117H}$ and loop mutants. Each enzyme was incubated with BTChI (10-2000 μM) for 5 min at 37°C and activity measured using the photometric method. Data were analyzed using the Michaelis-Menten equation and represent mean values with 95% confidence intervals in parentheses (n=3).

	k_{cat} (min^{-1})	K_M (mM)	k_{cat}/K_M ($min^{-1}M^{-1}$)
G117H	13,884 (13,117 - 14,651)	1.21 (1.08 - 1.33)	11.5 x 10^6
+ENI	2,207 * (2,051 - 2,362)	1.70 (1.49 - 1.90)	1.3 x 10^6
+ENA	4,024 * (3,607 - 4,441)	1.68 (1.38 - 1.97)	2.4 x 10^6
+ENG	8,363 * (5,741 - 10,986)	2.66 * (1.42 - 3.90)	3.1 x 10^6
+ENR	2,568 * (1,832 - 3,304)	3.68 * (2.23 - 5.12)	0.7 x 10^6
+ENT	5,976 * (5,462 - 6,490)	1.84 (1.58 - 2.10)	3.2 x 10^6

* indicates a significant difference compared to $BChE_{G117H}$

4.3.3 Resistance to Inhibition

Prior to the evaluation of loop mutant enzymes against OP inhibitors, we first measured the inhibitory potency of the selected inhibitors (PO, DFP, EthP) using wild-type rhBChE to select a starting point for values for use in subsequent assays (Fig. 4-4). The determined IC_{50} values were 23.3 (95% confidence interval [CI] = 15.2 - 35.5), 9.4 (CI = 1.2 - 71.8), and 55.4 (CI = 45.0 - 68.2) for PO, DFP, and EthP, respectively. An enzyme's ability to resist inhibition by a high OP concentration can be used as a preliminary screening assay for OP hydrolyzing ability [314]. We initially defined a high concentration as one which can inhibit >99% of the wild-type enzyme (PO and EthP = 500 nM, DFP = 50 nM), and tested this against $BChE_{G117H}$ and the loop mutant enzymes (Fig. 4-5A). The results showed that the $BChE_{G117H}$ retained 100% of the control activity (mean[CI] = 105 [96 - 114]), and the loop mutant enzymes were inhibited by no more than 10%. In order to detect differences between the enzyme types, it was necessary to find OP concentrations which are able to partially inhibit $BChE_{G117H}$. Therefore, we repeated the resistance to inhibition assay with inhibitor concentrations increased 10-fold, though $BChE_{G117H}$ remained mostly resistant to inhibition (mean[CI] = 97.8 [84.1 - 111.4]) (Fig. 4-5B). Interestingly, the loop mutants retained complete activity as well. The final selected OP concentrations (PO = 50 μM, DFP = 5 μM, EthP = 100 μM) resulted in inhibition of $BChE_{G117H}$ between 10-40%.

Figure 4-6 shows the ability of $BChE_{G117H}$ and loop mutants to resist inhibition by a high concentration of OP following a 10-minute incubation period. Under these conditions, there was a significant main effect of inhibitor-type ($F_{(2, 36)} = 594.7$, $p < 0.0001$) and enzyme type ($F_{(5, 36)} = 2.537$, $p = 0.046$), as well as a significant interaction

($F_{(10, 36)} = 7.401$, $p < 0.0001$). With paraoxon, $BChE_{G117H}$ was somewhat more resistant to inhibition compared to all five loop mutants studied, i.e., it retained 57% of its activity following paraoxon exposure while loop-mutants retained only 31−44% of pre-exposure activity. In contrast, when DFP was used as the inhibitor the loop mutants were generally more resistant to inhibition. Specifically, ENI, ENA, ENG, and ENR mutants retained nearly full activity (96−100%) following DFP exposure, which was statistically significant ($p < 0.05$) compared to the activity retained with $BChE_{G117H}$ (82%). A similar finding was noted following exposure to EthP, with two loop mutants (ENA and ENR) being more resistant to inhibition than $BChE_{G117H}$ ($p = 0.03$ and 0.0007, respectively). A trend was also noted with ENI ($p = 0.06$) and ENG ($p = 0.09$)

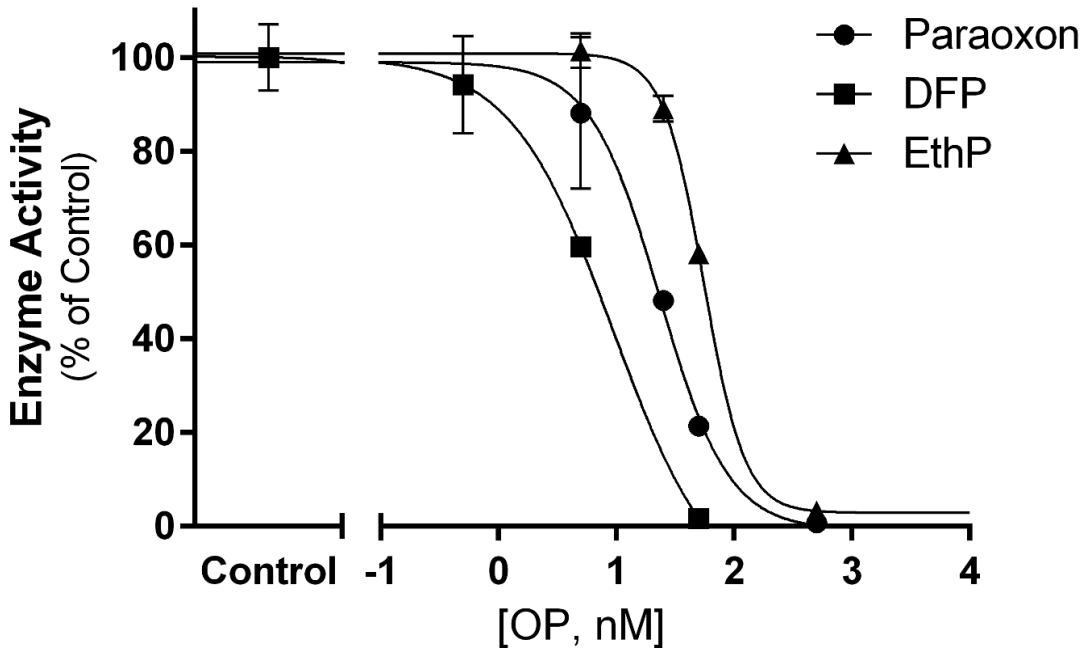

Figure 4-4. BChE sensitivity to inhibition by PO, DFP, and EthP. BChE (20 ng) was pre-incubated with PO, DFP, or EthP (0.5 - 500 nM for all) for 20 minutes at 37°C, prior to addition of substrate (1 mM BTChI) and measuring residual activity. Data represent mean values ± SD (n=2). The determined IC_{50} values were 23.2 nM, 9.4 nM, and 55.4 nM for PO, DFP, and EthP, respectively.

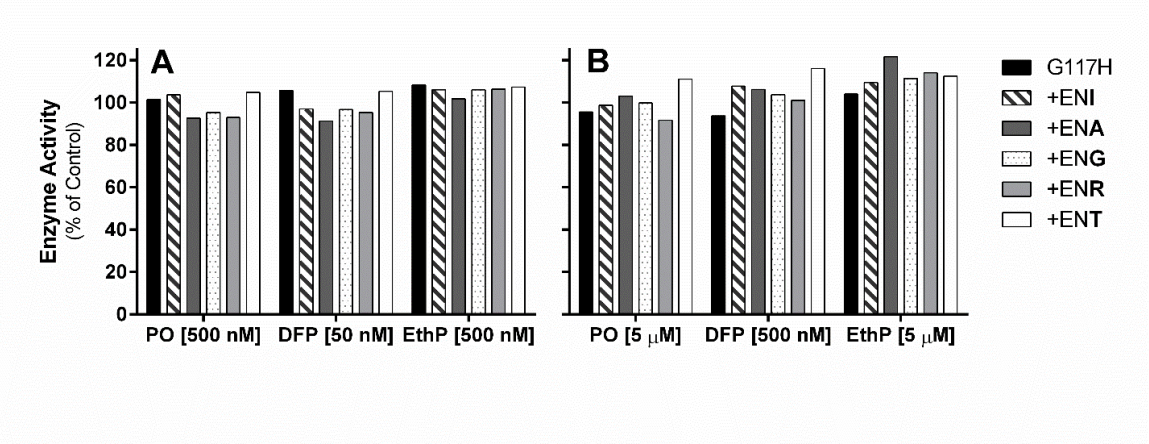

Figure 4-5. Preliminary range finding assays for resistance to inhibition of $BChE_{G117H}$ and loop mutants. All enzymes were exposed to paraoxon, DFP, or EthP for 10 minutes followed by colorimetric BChE activity determination using BTChI as substrate (1 mM final). Inhibitor concentrations in Panel A (PO = 500 nM, DFP = 50 nM, EthP = 500 nM) represent determined IC_{99} values, while concentrations in Panel B have been increased by a factor of 10. Data represent the percent of control (no inhibitor) values (n=1).

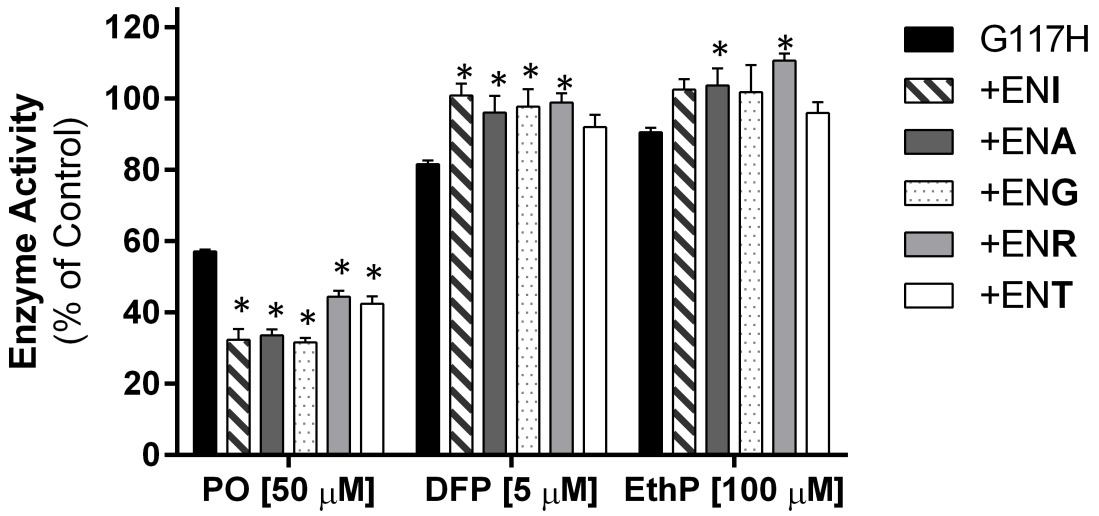

Figure 4-6. Comparative resistance to inhibition of $BChE_{G117H}$ and loop-mutants following a 10-min exposure to paraoxon (50 μM final), DFP (5 μM final) or EthP (100 μM final). Data are reported as percent of control (no inhibitor) values (mean ± SD of three independent replicates). An asterisk indicates a significant difference compared to $BChE_{G117H}$.

4.3.4 Reactivation of Loop Mutants

While the resistance to inhibition screening assay suggested that the loop insertions may alter the interaction of the mutant enzymes and inhibitors, it cannot determine the mechanism of resistance. Possible interpretations include changes in binding affinity for the inhibitor and/or increased reactivation rate following binding. Therefore, we next conducted an assay to determine the reactivation rate of $BChE_{G117H}$ and loop mutants against OP compounds in isolation. The rationale for this assay includes an initial incubation step with an excess of an OP compound in order to putatively occupy all active sites of the enzyme being tested followed by a marked (400-fold) dilution to dissociate any reversible enzyme-OP Michaelis complexes. Thus, measuring the rate of recovery of enzyme activity under these conditions reflects the rate of dephosphylation. The reactivation rate (k_3) was calculated by plotting the difference between observed and estimated values versus time during the recovery period, as described previously by Lockridge and coworkers [14]. Note that the reported k_3 values in cases where recovery did not achieve 100% of baseline were corrected using the approach of Hovanec and colleagues [315].

Figures 4-7, 4-8, and 4-9 show the raw reactivation data for each enzyme against paraoxon, DFP, and echothiophate, respectively. Baseline (100%) activity for each enzyme was estimated using enzyme without inhibitor, and while enzymes which were incubated with PO and EthP reached the baseline activity during the 7-minute measurement window, the DFP exposed enzymes did not. When $BChE_{G117H}$ was incubated with DFP, the maximum hydrolysis rate achieved was only 67% compared to baseline (Table 4-2). The reactivation achieved by the loop mutant enzymes was

proportionally more (between 72-90%), particularly with the ENR loop mutant which reactivated completely (as determined by an overlapping 95% confidence interval with the baseline activity). The k_3 values of $BChE_{G117H}$ with echothiophate (mean[CI] = 1.28 min^{-1} [1.21 - 1.35]) and paraoxon (mean[CI] = 1.27 min^{-1} [1.06 - 1.49]) were relatively similar to those reported previously [14]. To our knowledge, the reactivation rate of $BChE_{G117H}$ with DFP has not been previously reported. Two-way ANOVA determined that there was a significant main effect of enzyme type ($F_{(5, 807)} = 8.335$, $p < 0.0001$) as well as a significant interaction ($F_{(10, 807)} = 3.619$, $p < 0.0001$). *Post hoc* multiple comparisons determined that when paraoxon was used, the ENA loop mutant showed a slight but significant *increase* in k_3 ($p = 0.01$) as compared to $BChE_{G117H}$ (Figure 25). In contrast, when DFP was used, the k_3 of the ENI ($p = 0.0006$) and ENR ($p = 0.006$) loop mutants was significantly *decreased* as compared to $BChE_{G117H}$. There were no differences noted between any enzymes when EthP was used.

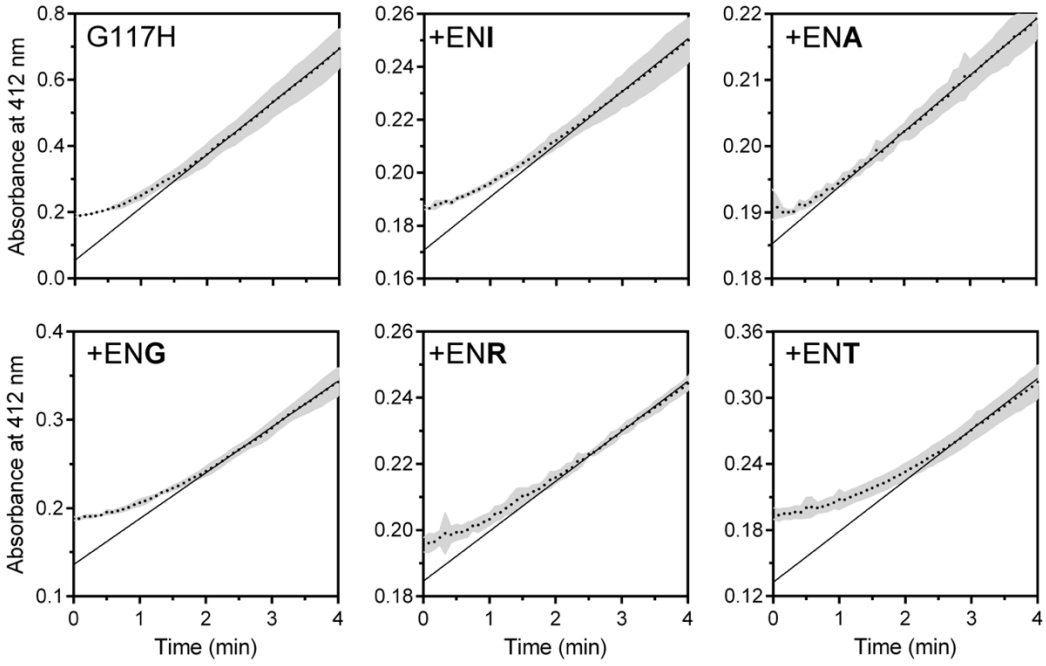

Figure 4-7. Recovery of $BChE_{G117H}$ and loop mutant activity following exposure to PO. Enzymes were incubated with 10 mM PO for 1 minute prior to a 400-fold dilution into the substrate cocktail (containing 1 mM BTChI substrate, final) as described in section 4.2.7. The dotted line represents the mean value of the raw data points (n=3), while the solid line is the linear regression fit (between 2-7 minutes). The standard deviation of the raw data points is represented as the shaded grey area. Note that while the x-axes are on the same scale for each panel, the y-axes are different for each panel.

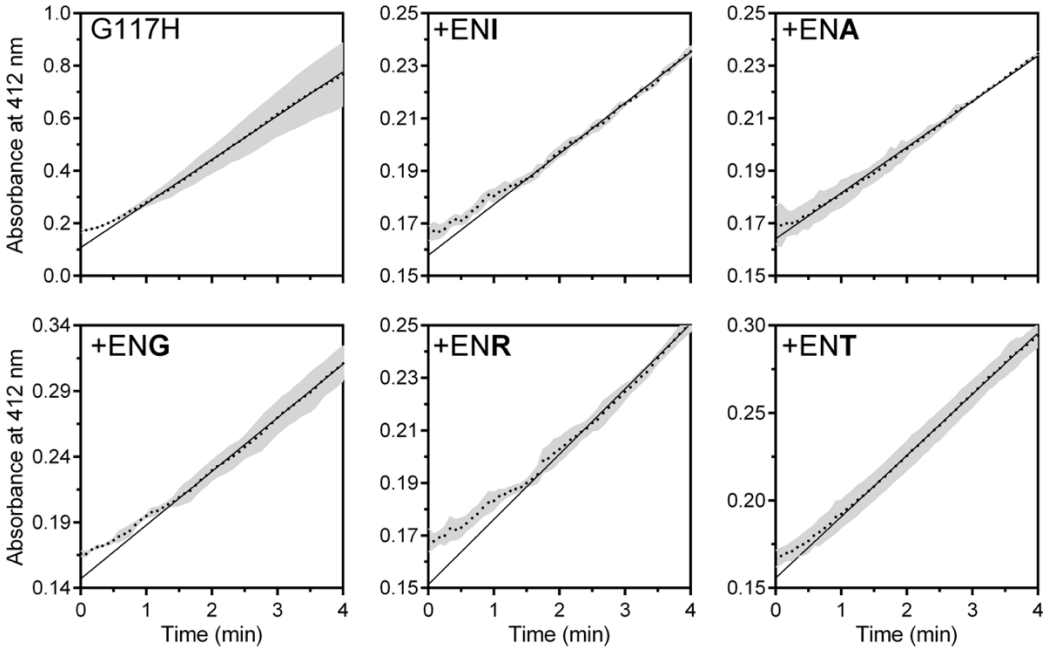

Figure 4-8. Recovery of $BChE_{G117H}$ and loop mutant activity following exposure to DFP. Enzymes were incubated with 10 mM DFP for 1 minute prior to a 400-fold dilution into the substrate cocktail (containing 1 mM BTChI substrate, final) as described in section 4.2.7. The dotted line represents the mean value of the raw data points (n=3), while the solid line is the linear regression fit (between 2-7 minutes). The standard deviation of the raw data points is represented as the shaded grey area. Note that while the x-axes are on the same scale for each panel, the y-axes are different for each panel.

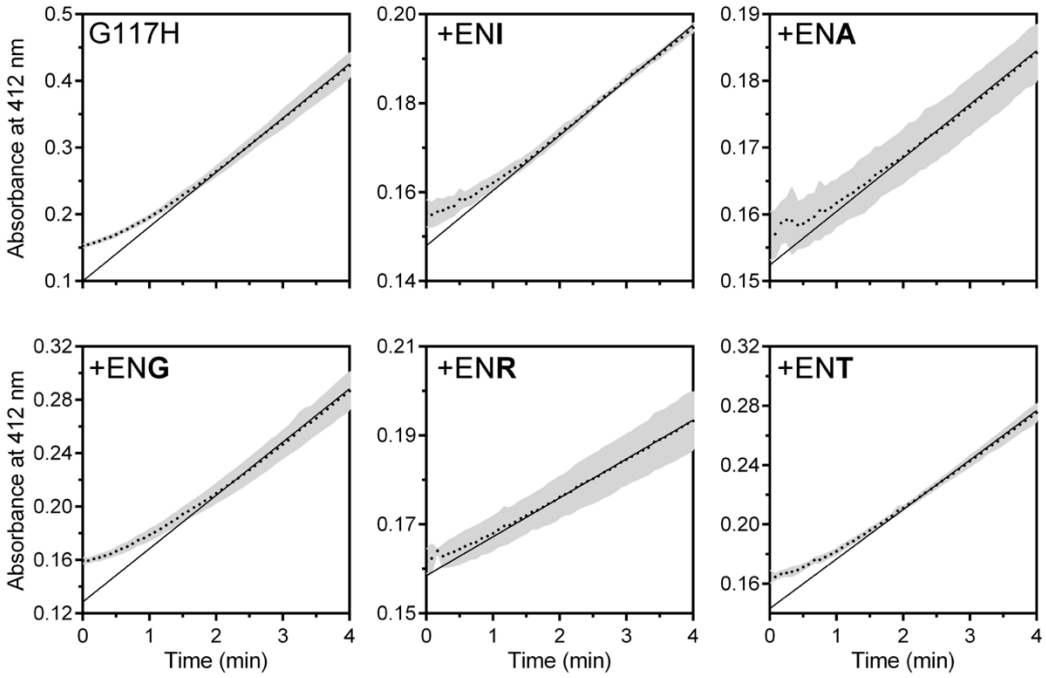

Figure 4-9. Recovery of $BChE_{G117H}$ and loop mutant activity following exposure to EthP. Enzymes were incubated with 10 mM EthP for 1 minute prior to a 400-fold dilution into the substrate cocktail (containing 1 mM BTChI substrate, final) as described in section 4.2.7. The dotted line represents the mean value of the raw data points (n=3), while the solid line is the linear regression fit (between 2-7 minutes). The standard deviation of the raw data points is represented as the shaded grey area. Note that while the x-axes are on the same scale for each panel, the y-axes are different for each panel.

Table 4-2. Enzyme reactivation of $BChE_{G117H}$ and loop mutants with DFP. Enzymes were incubated with 10 mM DFP for 1 minute followed by a 400-fold dilution prior to measurement of activity using BTChI. Values are reported as mean and 95% confidence intervals, when appropriate (n=3).

	Enzyme Activity (mOD/min)		**% Reactivation**	k_3 (min^{-1})	
	Control	+DFP		Observed	Corrected[a]
G117H	236.5 (226.6 - 246.4)	159.2 (151.6 - 148.2)	67.3	2.38 (1.93 - 2.83)	1.60 (1.30 - 1.90)
+ENI	22.1 (21.5 - 22.7)	18.7 (18.5 - 18.9)	84.6	0.87 (0.50 - 1.23)	0.74 (0.42 - 1.04)
+ENA	23.8 (23.0 - 24.6)	17.1 (16.9 - 17.3)	71.8	2.64 (1.84 - 3.44)	1.90 (1.32 - 2.47)
+ENG	44.2 (43.8 - 44.7)	39.6 (38.9 - 40.2)	89.6	1.18 (0.47 - 1.88)	1.06 (0.42 - 1.68)
+ENR	24.3 (23.8 - 24.8)	23.5 (23.3 - 23.8)	96.7	0.89 (0.73 - 1.05)	N/A[b]
+ENT	47.2 (44.6 - 49.9)	35.0 (34.5 - 35.5)	74.2	1.63 (0.84 - 2.42)	1.21 (0.62 - 1.80)

[a] Corrected values were determined using the method described by Hovanec and colleagues, by multiplying the observed k_3 values by the determined percent reactivation values and dividing by 100 [315].

[b] A corrected k_3 value was not calculated for ENR as the 95% confidence intervals for the control and +DFP enzyme activities were overlapping, thus it was considered "completely" reactivated.

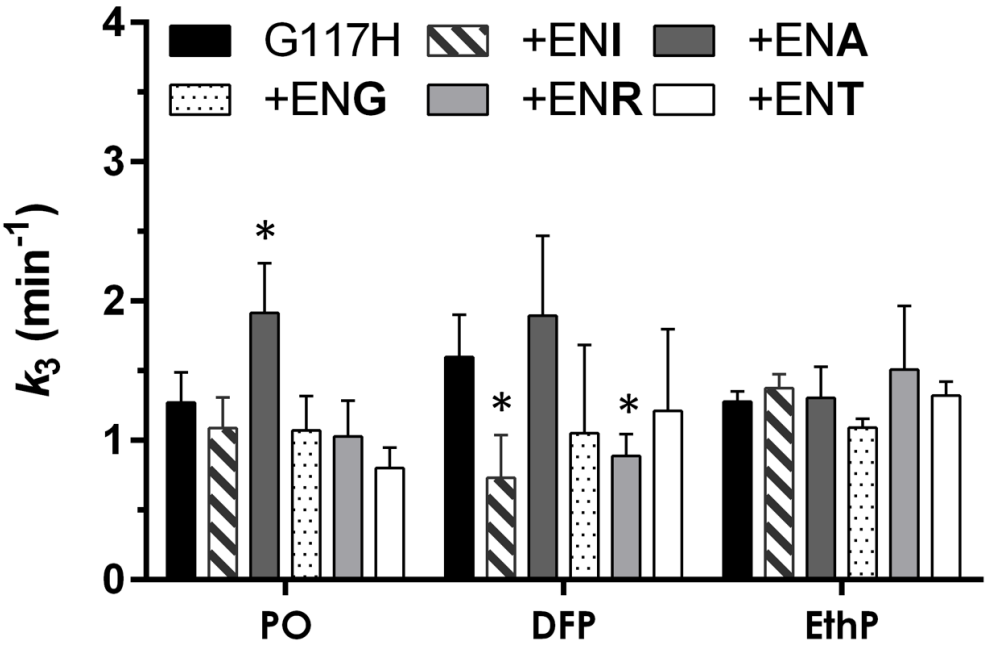

Figure 4-10. Reactivation rates (k_3) of $BChE_{G117H}$ and loop mutants following exposure to 10 mM of an OP compound (PO, DFP or EthP). Enzyme was allowed to react with the inhibitor for one minute and then diluted 400-fold into a solution containing substrate (BTChI, 1 mM). The data are reported as mean with 95% confidence interval bars (n=3). In the case of DFP, 100% reactivation was not achieved, thus reported k_3 values have been corrected based on Hovanec et al [315]. Asterisks indicate a significant difference compared to $BChE_{G117H}$.

4.3.5 Paraoxon Hydrolysis

As a statistically significant difference was noted with enzyme reactivation assays with paraoxon, we next conducted a direct hydrolysis assay using paraoxon as the substrate. The substrate kinetics assay suggested that all loop mutants had altered catalytic activity as compared to $BChE_{G117H}$ ($F_{(10,148)} = 46.76$, $p < 0.0001$)(Fig. 4-11). Table 4-3 compares substrate kinetics parameters among the different enzymes. Significant differences were detected in both k_{cat} ($F_{(5,148)} = 29.46$) and K_M ($F_{(5,148)} = 5.735$, $p < 0.0001$) values. *Post hoc* multiple comparisons indicated that k_{cat} was significantly lower than $BChE_{G117H}$ in all loop mutant enzymes ($p < 0.0001$ for all), and K_M was significantly lower in the ENA ($p = .0005$), ENG ($p = 0.001$), and ENT ($p = 0.0009$) mutants. The loop mutants ENA, ENG, and ENT showed a trend toward higher catalytic efficiency (k_{cat}/K_M) compared to $BChE_{G117H}$, but this appeared driven by the changes in K_M and not catalytic activity. Changes in substrate binding affinity could be critical in the kinetics of organophosphate hydrolysis.

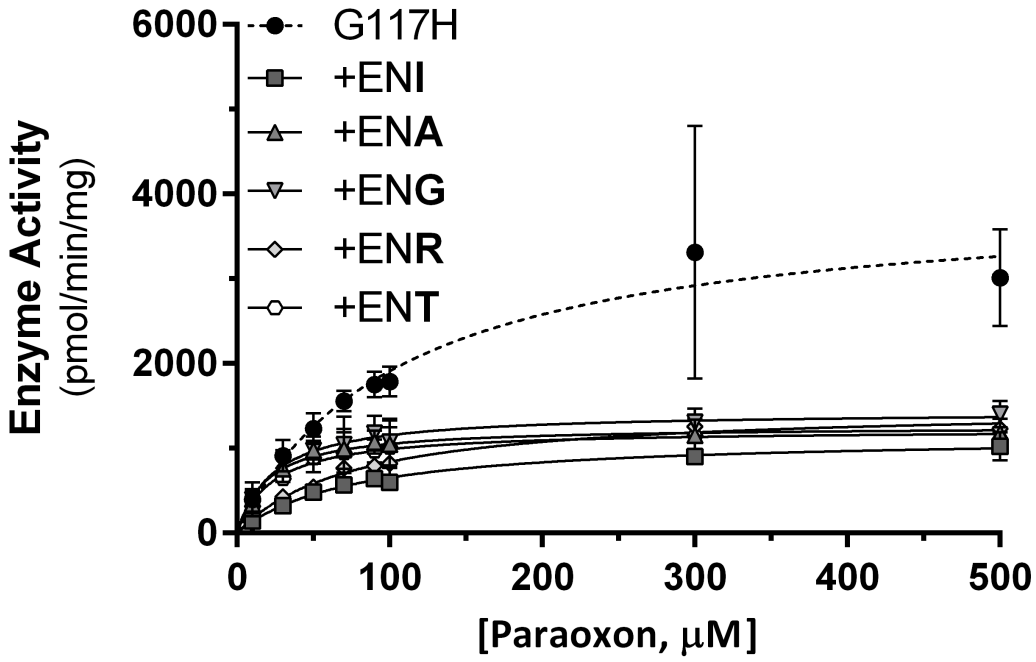

Figure 4-11. Concentration-dependent hydrolysis of PO by $BChE_{G117H}$ and loop mutants. Each enzyme preparation was incubated with paraoxon (10 μM - 500 μM) for 5 min at 37°C and activity quantified by the measurement of the hydrolysis product, p-nitrophenol (ΔA_{405}). Data represent mean ± SD determined from three to four independent replicates.

Table 4-3. Comparison of the substrate kinetics parameters of $BChE_{G117H}$ and loop mutants using PO**.** Kinetic analysis was determined using non-linear regression with the classic Michaelis-Menten equation. Mean values are reported with 95% confidence intervals in parentheses.

	k_{cat} (min^{-1})	K_M (mM)	k_{cat}/K_M ($min^{-1}M^{-1}$)
G117H	0.244 (0.19 - 0.30)	107.6 (50.3 - 164.9)	2.2×10^3
+ENI	0.071 * (0.065 - 0.078)	75.8 (56.9 - 94.8)	0.9×10^3
+ENA	0.078 * (0.068 - 0.087)	19.7 * (8.8 - 30.7)	3.9×10^3
+ENG	0.089 * (0.078 - 0.099)	24.2 * (11.8 - 36.6)	3.6×10^3
+ENR	0.092 * (0.081 - 0.103)	77.6 (52.3 - 103.0)	1.2×10^3
+ENT	0.076 * (0.066 - 0.085)	23.6 * (10.9 - 36.3)	3.2×10^3

* indicates a significant difference compared to $BChE_{G117H}$

4.4 DISCUSSION

The use of BChE as a prophylactic agent is hindered by its stoichiometric interaction with OP toxicants. From a functional standpoint, OP compounds irreversibly bind to ChEs, but molecularly, the interaction proceeds similar to that of substrates. The most pronounced difference between the different interactions is in the reactivation (k_3) step (refer to Fig. 2-2). Therefore, it is conceivable that re-engineering of BChE could increase the rate of reactivation, resulting in an efficient catalyst of OP compounds. While it is well established that enzymes' catalytic machinery is dependent on protein structural characteristics, recent research suggests that the dynamic motion of the protein is also important for catalysis [316]. Moreover, it has been suggested that enzyme structure and dynamics of certain surface loop regions enable thermodynamical coupling between the enzyme surface and active site residues by collecting energy from interactions with solvent molecules and relaying it to the active site through a network of residues. The current study sought to apply these principles to $BChE_{G117H}$, a previously-developed mutant which can slowly hydrolyze OP compounds, to better understand the role of surface peptide networks in catalysis, and study the structure-dynamics-activity relationships in catalytic degradation of OP compounds. Initial molecular dynamics simulations identified a dynamic surface loop on $BChE_{G117H}$ (278−285), and we hypothesized that a 3-residue insertion into this region would increase energy transfer to the active site, resulting in an increased rate of catalysis. To evaluate the effect of these insertions, we modeled the enzyme-substrate interactions in the active site and measured enzyme activity with choline and OP esters.

We first studied the catalytic interaction of the engineered loop mutants with BTChI. As native BChE is operating near the diffusion-limited rate with choline substrates, it is expected that the introducing mutations would if anything result in a decreased catalytic rate. This effect was observed with $BChE_{G117H}$ as compared to the wild-type enzyme [14]. We found that all of the produced loop mutants had a significantly reduced catalytic efficiency (k_{cat}/K_M) compared to $BChE_{G117H}$. Our data also suggested that binding of the substrate in the loop mutants was reduced relative to $BChE_{G117H}$. These findings suggest that the introduced changes in the surface peptide network were indeed influencing physiochemical interactions in the active site region, albeit in a negative manner relative to catalytic activity with BTChI.

We conducted two assays to elucidate the enzymes' interactions with the three OP compounds. The relative resistance to inhibition by a high concentration of PO, DFP, or EthP provided an initial perspective on the effect of our surface loop mutations. It should be noted that with this assay, the *mechanism* of resistance cannot be fully appreciated, but a change in resistance to inhibition may reflect a change in catalytic activity or substrate binding. When DFP and EthP were used, the loop mutants were relatively more resistant to inhibition compared to $BChE_{G117H}$. The resistance found with ENA and ENR was statistically significant with both OP compounds. In contrast, all loop mutants were significantly less resistant to inhibition by paraoxon compared to $BChE_{G117H}$, suggesting an important structure-dynamics-activity relationship. While paraoxon has the classical organophosphate structure (i.e. phosphate ester), DFP is a phosphorofluoridate and EthP is a phosphorothioate [317]. To further clarify the mechanism of altered interactions between the enzyme and substrates, we measured enzyme reactivation, which is

relatively unaffected by changes in substrate binding. Interestingly, the ENA mutant had a significantly increased reactivation rate compared to $BChE_{G117H}$ with paraoxon. However, we did not detect this effect in the direct paraoxon hydrolysis assay, where we found a significant decrease in the enzyme's turnover rate (k_{cat}). Taken together, these results suggested that the decreased K_M with paraoxon (seen in the direct hydrolysis assay and supported by the resistance to inhibition assay) had more impact on the enzyme's apparent efficiency than the small increase in reactivation rate. Reactivation data with DFP and EthP did not show significant increases in k_3, suggesting that the noted increase in loop mutant resistance to inhibition is also a reflection of altered binding. A direct hydrolysis assay with DFP and EthP may confirm this presumption.

Molecular dynamics simulations of $BChE_{G117H}$ and the engineered loop mutants with the choline ester substrate butyrylcholine and selected OP compounds provided insights into the observed experimental findings. While BCh had strong interactions with all enzymes tested, the OP compounds showed mostly weak interactions. The OP compounds frequently lost contact with the active site pocket in less than 50 nanoseconds. From this, it can be inferred that the enzyme has limited time for effective hydrolysis [242]. Interestingly, in some cases, loop mutations appeared to slightly improve the stability of PO and EthP in the active site pocket of $BChE_{G117H}$, through an unknown mechanism.

In conclusion, the results confirmed that surface peptide networks identified on this enzyme by molecular simulations can influence substrate-active site interactions and be potentially used to enhance the hydrolysis of catalytic bioscavengers. In particular, we observed a slight but significant increase in the dephosphylation rate constant with

paraoxon with one (ENA) loop mutant. While these changes were subtle, our data suggest that increasing the interaction of identified hypermobile surface loops with the solvent may potentially yield improved catalytic interactions between OP-hydrolyzing enzymes and their substrates. It is likely that significant improvements in the active site stability of OP compounds with BChE are necessary for significant improvement of catalytic rate. Due to this, the approach of targeting of surface loop dynamics may be better suited to native OP hydrolases (e.g., paraoxonase, phosphotriesterase) with higher intrinsic catalytic activity against OP compounds (and, presumably, more stable active site interactions). Understanding how surface loop networks and their dynamics contribute to catalysis may lead to further development of more effective catalytic bioscavengers for protection against OP toxicity.

CHAPTER V

IN VITRO AND *IN VIVO* EVALUATION OF TOXICOKINETICS/TOXICODYNAMICS OF FREE PYRIDOSTIGMINE AND PYRIDOSTIGMINE IN NANOCRYSTALLINE CELLULOSE HYDROGELS

5.1 INTRODUCTION

Pyridostigmine bromide is currently the only drug available for military use as a prophylactic against nerve agent exposure. PB is formulated for prophylactic use as 30 mg tablets. These tablets require refrigerated storage and must be discarded three months after distribution. Following oral dosing with these tablets, PB reaches its maximal blood concentration at two hours, and the half-life of PB is approximately three hours [318]. As a result, soldiers are required to take a dose every eight hours to achieve and retain protection (considered to be 20-40% blood AChE inhibition). In a retrospective study of Gulf War veterans, 61% of soldiers reported taking fewer than the recommended three pills daily [319]. Formulations which extend the pharmacokinetics of PB would decrease the recommended dosing schedule, thereby improving logistics and potentially increasing compliance.

Hydrogels are a type of drug delivery system constructed from crosslinked polymer chains, which release drugs *via* diffusion, controlled by the mesh/pore size of the

polymer network [320]. Nanocrystalline cellulose (NCC) is a material produced from cellulose fibers which can be used to create hydrogels for improved drug delivery [321]. *In vitro* evaluation of BSA-loaded CNC showed a biphasic release - a "burst" phase during the initial 8 hours, followed by gradual release up to 48 hours. By 48 hours, 90-100% of the BSA had been released from the hydrogel [322]. NCC is essentially non-toxic by oral delivery and can be produced renewably and inexpensively, making it an attractive drug delivery vehicle [321, 323].

The major goal of Aim 3 was to characterize how NCC-PB formulations alter the pharmacodynamic and pharmacokinetic interaction of PB and AChE. We hypothesized that NCC-PB hydrogel formulations would extend the time course of AChE inhibition in both *in vitro* and *in vivo* assays. Preparation of nanocrystalline cellulose is frequently conducted via sulfuric acid hydrolysis of cellulose fibers; however, another method of hydrolysis (TEMPO-oxidation) results in NCC which has carboxylic acid groups on its surface amenable to functionalization. Three NCC-PB hydrogel formulations were prepared using the "normal" method, wherein the crosslinking conditions were altered, and lyophilized prior to use. A final NCC-PB formulation was prepared using the TEMPO-oxidation methods to test the effect of differing surface chemistries. Using the rehydrated NCC hydrogels, we compared the time course of *in vitro* AChE inhibition during incubation with NCC-PB and free PB using mouse blood and intestinal homogenate. We then evaluated the comparative effects of one NCC-PB hydrogel formulation and free PB on the *in vivo* time course of AChE inhibition in mice.

5.2 MATERIALS AND METHODS

5.2.1 Chemicals

Nanocrystalline cellulose hydrogel-encapsulated PB was produced by InnoSense, LLC (Torrance, CA). NCC starting material was obtained from CelluForce (Montreal, QC, CA). Three hydrogel formulations were prepared using nanocrystalline cellulose sulfate particles which were crosslinked with epichlorohydrin for one (NCC-PB1), or ten (NCC-PB10) minutes prior to addition of PB into the mixture. The third formulation added PB immediately following addition of the crosslinking agent (NCC-PB0). All other preparation details were kept consistent. A fourth hydrogel formulation (TEMPO-PB) utilized a different form of cellulose, which was prepared using 2,2,6,6-tetramethylpiperidine-1-oxyl radical (TEMPO). Due to the altered surface chemistry of the TEMPO-oxidized gels, calcium chloride dihydrate was added to form metal-ion complexes (as opposed to chemical crosslinking by epichlorohydrin).

Tissue sources of ChE (small intestine and whole blood from CD1 mice) were obtained from Charles-River (Wilmington, MA). Upon receipt, tissues were homogenized or diluted in PBS and immediately frozen at -80°C until use. Free pyridostigmine bromide (3-(dimethylaminocarbonyloxy)-1-methylpyridinium bromine; PB) (100% purity by HPLC) used in *in vitro* and *in vivo* studies was purchased from Sigma-Aldrich (St. Louis, MO) and kept desiccated under nitrogen at room temperature until use. [^{3}H]Acetylcholine iodide (specific activity about 65.5 mCi/mmol) was purchased from Perkin-Elmer (Waltham, MA). Certified ACS grade toluene and iso-amyl alcohol were purchased from Fisher Scientific (Waltham, MA). POPOP (1,4-Bis[5-phenyl-2-oxazolyl] benzene), PPO (2,5-diphenyloxazole), potassium phosphate, and

other remaining chemicals and reagents were purchased from Sigma-Aldrich (St. Louis, MO).

5.2.2 Animals

All studies were conducted using 6-week-old, male, CD1 mice (35-40 g) purchased from Charles River and acclimated for at least one week prior to study initiation. Mice were kept in shoebox cages under a 12-12-hour light-dark cycle with *ad libitum* access to water and standard chow. All procedures were approved by Oklahoma State University's Institutional Animal Care and Use Committee.

5.2.3 Radiometric Cholinesterase Assay

In some cases, acetylcholinesterase activity was measured radiometrically using the method of Johnson and Russell [324]. This assay avoids complications regarding quantitation of cholinesterase activity in blood samples (which can be difficult using the photometric method), and it also allows use of highly concentrated tissue samples not possible with the photometric method (due to turbidity interference). The enzyme source (e.g. mouse blood, tissue homogenate) was diluted using phosphate buffered saline (PBS; 10 mM phosphate buffer containing 154 mM NaCl, pH 7.4) before use. Twenty µl of the enzyme source was added to 60 µl of potassium phosphate buffer (50 mM, pH 7.0), and the reaction started by addition of 20 µl [^{3}H]acetylcholine (1 mM final concentration). Reactions were allowed to proceed at 37°C until termination by addition of an acidified stop solution (1 M chloroacetic acid, 0.5 M NaOH, and 2 M NaCl) followed by extensive vortexing. A hydrophobic scintillation cocktail (0.5% PPO/0.03% POPOP/10% iso-amyl alcohol in toluene) was then added and the product ([^{3}H]acetic acid) was separated by

liquid-liquid exchange and then counted in a scintillation counter (Perkin Elmer Tri-Carb 2810 TR; 61% efficiency).

5.2.4 *In Vitro* Time Course of ChE Inhibition

Mouse blood or homogenized small intestine was diluted 1:10 in PBS to be used as the tissue/enzyme source. A pyridostigmine bromide solution (3 μM for whole blood; 6 μM for intestinal homogenate) was prepared in PBS in advance and kept on ice until use. Just before the assay, the contents of one vial containing lyophilized NCC-PB gel (provided by InnoSense, LLC) was ground using a small mortar and pestle, the powder transferred to a polypropylene tube and then rehydrated with 3 ml of PBS. The solution (putatively 5.745 mM pyridostigmine) was vortexed to ensure an even suspension prior to rapid serial dilution to obtain a 3 or 6 μM working concentration of PB in NCC-PB0, NCC-PB1, NCC-PB10 and TEMPO-PB. PBS, diluted pyridostigmine, or the gel working reagent (250 μl each) was then added to an equal volume of the diluted blood or intestinal sample (500 μl final volume). The vials were vortexed and then placed into a 37°C water bath with mild shaking. At specified time points (10, 20, 40, and 80 minutes), aliquots (20 μl) of the mixtures were withdrawn and assayed for AChE activity using the radiometric method described in section 5.2.3. All reactions were corrected for non-enzymatic substrate hydrolysis. Preliminary assays were conducted to determine the appropriate blood dilution and incubation time to capture a linear rate of substrate hydrolysis.

5.2.5 *In Vivo* Pharmacodynamic Evaluation

To evaluate comparative time-dependent inhibition of AChE by free PB and NCC-PB0, the maximum tolerated dose (MTD) was determined first. MTDs were estimated using the up-and-down method [325], which involved treating one to three

mice and observing cholinergic toxicity and lethality for 24 hours. If the treated animal(s) survived 24 hours, the previous dose was multiplied by a factor of 1.3. If the animal(s) did not survive 24 hours, the previous dose was divided by 1.3. This continued until an MTD estimate was determined. Functional signs were recorded and ranked according to the following scale: 0 = no signs, 1 = very slight signs such as possible fasciculations and piloerection, 2 = slight toxicity including fasciculations, salivation or lacrimation (i.e. SLUD signs), 3 = moderate signs including head and neck area tremors, tail "twitching" and more obvious fasciculations and/or SLUD signs, 4 = severe, notable whole body tremors, prostrate/reduced ambulation, extensive fasciculations and/or SLUD signs, occasional choreatic movements, and 5 = death.

Following MTD determination, the selected doses were utilized for subsequent time course studies. Animals were divided into two groups, free PB and NCC-PB0 (n = 5-6/group). Prior to dosing, baseline cholinesterase activity was determined for each animal by collecting a small blood sample (5 μl) *via* a tail snip procedure. A solution of free pyridostigmine bromide (13.33 mg/kg) was made in PBS and used for all PB dosing, adjusting the dosing volume accordingly for each dose. Contents of a vial of lyophilized NCC-PB0 gel (65 mg wet weight) containing 40 ± 5 mg pyridostigmine was homogenized using a small mortar and pestle and then rehydrated by adding 3 ml PBS to obtain a putative PB concentration of 13.33 mg/ml. Free PB and NCC-PB0 gel were administered by oral gavage, making sure that gavage treatments were completed as soon as possible after gel rehydration to minimize pyridostigmine release prior to dosing. Functional signs of cholinergic toxicity were recorded and ranked 1-5 according to the severity and presence of muscle fasciculations, tremors, and SLUD signs (i.e. salivation,

lacrimation, urination, defecation). At specified time points (45, 90, 180, 270, 380, 720, 1080, and 1440 minutes) small blood samples were collected from the tail to assay for cholinesterase activity as described in section 5.2.3.

5.2.6 Statistical Methods

For *in vitro* studies, data from three independent samples were normalized based on vehicle controls (100% activity). In both cases (*in vitro* and *in vivo*) ChE inhibition data were analyzed using a two-way repeated measures ANOVA, with time and formulation type as the main factors. When appropriate, t-tests were also used for pairwise comparison (noted in-text). If warranted, a *post hoc* Dunnett's multiple comparison test was used to determine statistical significance between conditions. Statistical significance was defined as a p-value < 0.05 in all cases, and p-values resulting from multiple comparisons analysis reported in-text are multiplicity adjusted. All statistical tests were conducted using GraphPad Prism software (La Jolla, CA), version 6.0.

5.3 RESULTS

5.3.1 *In Vitro* Evaluation of NCC-PB

Four nanocrystalline cellulose pyridostigmine formulations – NCC-PB0, NCC-PB1, NCC-PB10, and TEMPO-PB – were compared against free PB for their *in vitro* time-dependent anticholinesterase activity. A mixture of the PB gel and either small intestinal homogenate or whole blood was vortexed and incubated at 37°C. Aliquots were removed at specified time points for measurement of residual ChE activity (Figs. 5-1 and 5-2). In each case, the ChE inhibition progressively increased until about 1-2 hours, at which point a plateau was achieved, suggesting maximal ChE inhibition. A slight

increase in activity was noted at later time points, likely due to reactivation of PB-inhibited enzyme molecules.

Figure 5-3 shows the comparison of intestinal ChE inhibition by NCC-PB0, -PB1, and -PB10 at each time point. Two-way ANOVA of the intestinal cholinesterase data revealed a significant main effect of PB gel formulations ($F_{(3, 8)} = 7.176$, $p = 0.012$) as well as a significant interaction ($F_{(15, 40)} = 1.953$, $p = 0.046$). *Post hoc* multiple comparisons showed that the NCC-PB0 formulation was significantly different from free PB at the 10 ($p = 0.0001$), 30 ($p < 0.0001$), and 60 ($p = 0.0007$) minute time points. The NCC-PB10 formulation was significantly different from free PB at the 10 ($p = 0.02$) and 30 ($p = 0.02$) minute time points, while the NCC-PB1 formulation was not different at any time point. Figure 5-4 shows the comparison of each PB gel formulation's ability to inhibit blood ChE at each time point. When whole blood was used as the ChE source, the two-way ANOVA showed a similar main effect of PB gel formulations ($F_{(4,13)} = 62.67$, $p < 0.0001$) and a significant interaction ($F_{(20,65)} = 3.072$, $p = 0.0003$). The NCC-PB0 gel formulation was significantly different from free PB at the 10 ($p = 0.01$) and 30 ($p = 0.04$) minute time points. The TEMPO-PB gel was significantly different from free PB at all tested time points ($p < 0.0001$ in all cases). No significant differences were noted with the NCC-PB1 or -PB10 formulations.

Interestingly, the TEMPO gel formulation showed a higher plateau (28% activity remaining) compared to free PB (12% activity remaining) during the eight-hour incubation ($F_{(4, 118)} = 56.36$; $p < 0.0001$). Therefore, an extra time point at 24 hours was collected from the TEMPO gels and free PB (Fig. 5-5). The results from this incubation

showed that the residual activity remained relatively consistent until 24 hours, which was statistically significant between free PB and the TEMPO-PB gel (t-test; $p = 0.0001$)

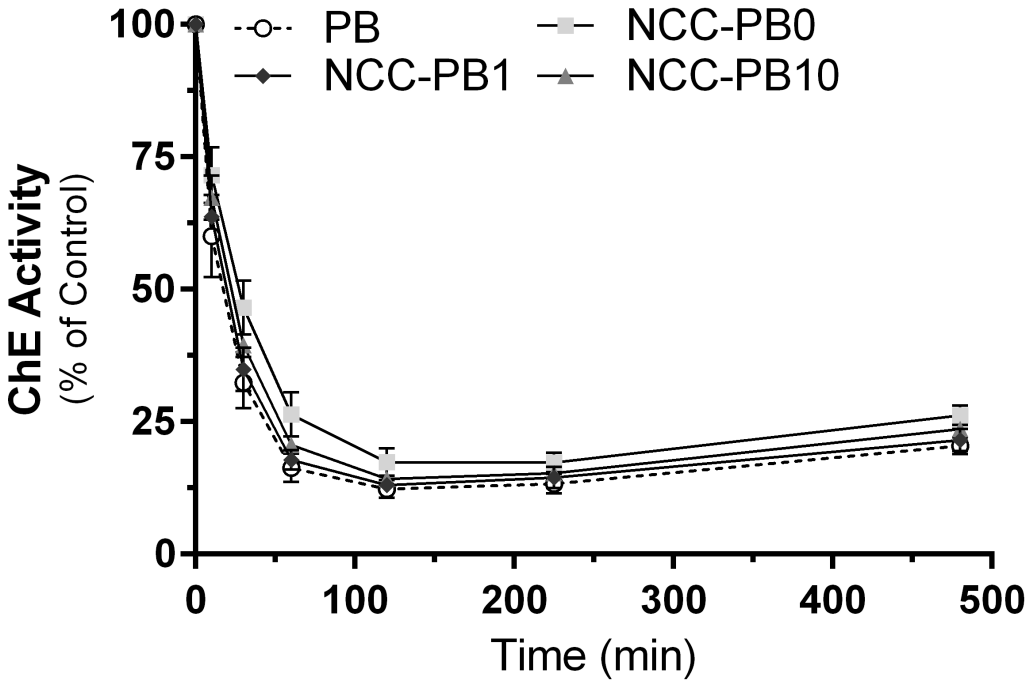

Figure 5-1. *In vitro* time course of intestinal ChE inhibition by PB or NCC-PB. Free PB or nanocrystalline cellulose formulated PB (NCC-PB0, NCC-PB1, NCC-PB10) (3 μM final) were incubated with intestinal homogenate (1:10 dilution) at 37°C with gentle shaking. At specified time points (10-480 min), 20 μl aliquots were removed and assayed for cholinesterase activity with [^{3}H] acetylcholine as described in section 5.2.3. Data are reported as percent of contemporaneous controls (no PB) and represent three independent replicates (mean ± SD).

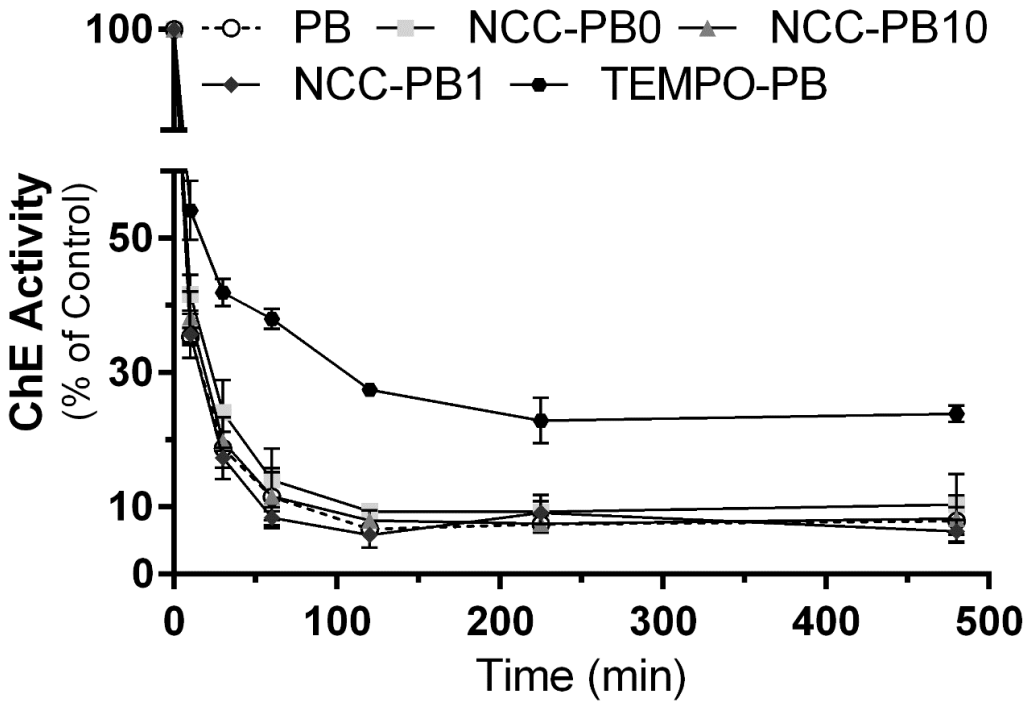

Figure 5-2. *In vitro* time course of whole blood ChE inhibition by PB or NCC-PB. Free PB or nanocrystalline cellulose formulated PB (NCC-PB0, NCC-PB1, NCC-PB10, TEMPO-PB) (1.5 μM final) was incubated with whole blood (1:10 dilution) at 37℃ with gentle shaking. At specified time points (10-480 min), 20 μl aliquots were removed and assayed for cholinesterase activity with [^{3}H] acetylcholine as described in section 5.2.3. Data are reported as percent of contemporaneous controls (no PB) and represent three independent replicates (mean ± SD).

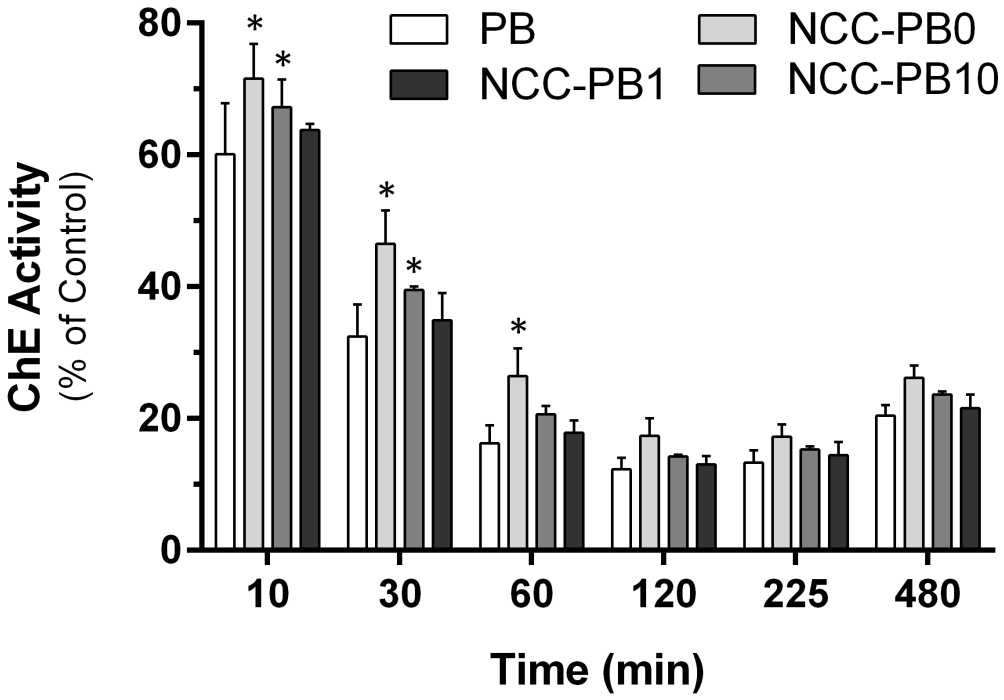

Figure 5-3. Comparison of intestinal ChE inhibition by PB or NCC-PB at selected time points. Free PB or nanocrystalline cellulose formulated PB (NCC-PB0, NCC-PB1, NCC-PB10) (3 μM final) was incubated with intestinal homogenate (1:10 dilution) at 37℃ with gentle shaking. At specified time points (10-480 min), 20 μl aliquots were removed and assayed for cholinesterase activity with [^{3}H] acetylcholine as described in section 5.2.3. Data are reported as percent of contemporaneous controls (no PB) and represent three independent replicates (mean ± SD). Asterisks indicate a significant difference compared to free PB.

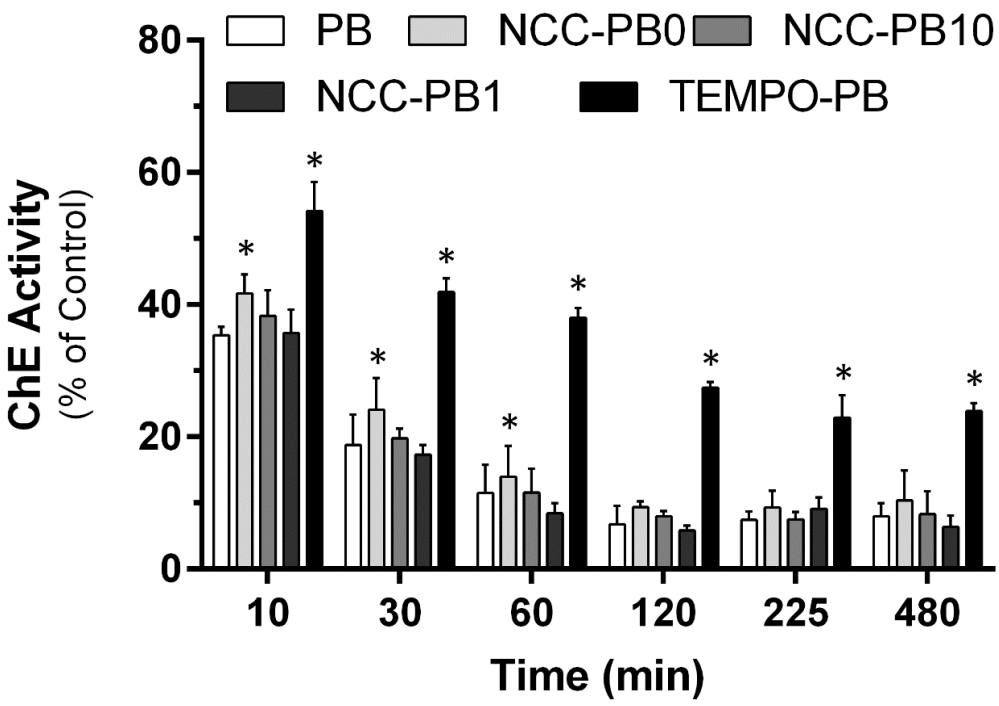

Figure 5-4. Comparison of whole blood ChE inhibition by PB NCC- PB at selected time points. Free PB or nanocrystalline cellulose formulated PB (NCC-PB0, NCC-PB1, NCC-PB10, TEMPO-PB) (1.5 μM final) was incubated with intestinal homogenate (1:10 dilution) at 37℃ with gentle shaking. At specified time points (10-480 min), 20 μl aliquots were removed and assayed for cholinesterase activity with [^{3}H] acetylcholine as described in section 5.2.3. Data are reported as percent of contemporaneous controls (no PB) and represent three independent replicates (mean ± SD). Asterisks indicate a significant difference compared to free PB.

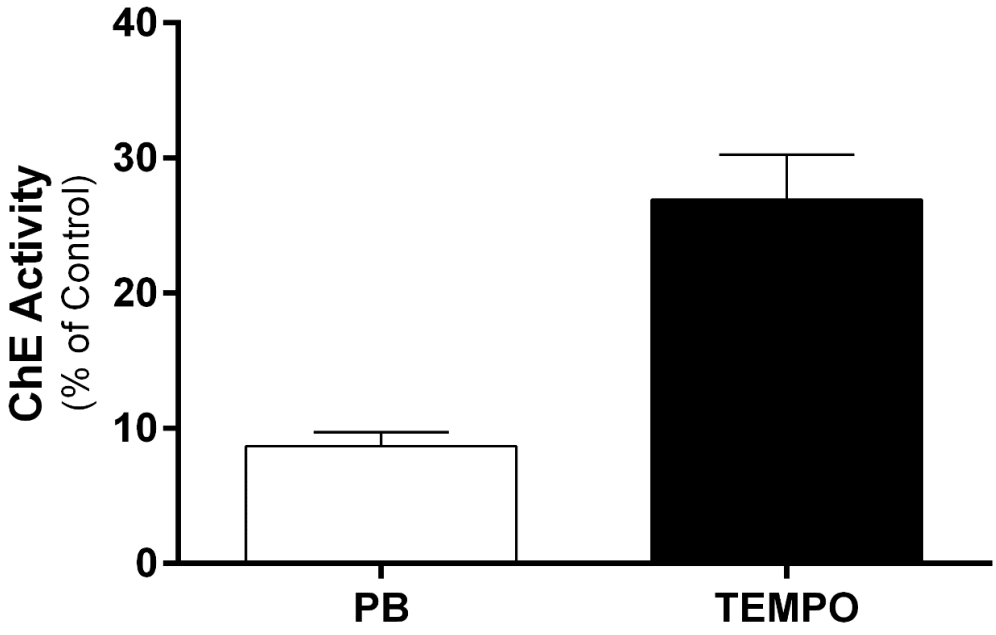

Figure 5-5. Comparison of whole blood ChE inhibition by PB or TEMPO-PB gel at 24 hours. Free PB or TEMPO-PB gel (1.5 μM final) was incubated with intestinal homogenate (1:10 dilution) at 37℃ with gentle shaking. After 24 hours of incubation, a 20 μl aliquot was removed and assayed for cholinesterase activity with [^{3}H] acetylcholine as described in section 5.2.3. Data are reported as percent of contemporaneous controls (no PB) and represent three independent replicates (mean ± SD).

5.3.2 *In Vivo* Evaluation of NCC-PB0

Prior to collecting cholinesterase inhibition data, we determined the maximum tolerated dose (MTD) of free PB and NCC-PB0 in CD1 mice based on functional signs data. We first treated one mouse with 112.7 mg/kg of free pyridostigmine, which caused severe signs and death within one minute. Due to the rapid, lethal reaction, we decreased the next dose by three "steps" (each step decreases the previous dose by a factor of 1.3) to 51.3 mg/kg. This dose resulted in a steady increase in signs until 60 minutes at which point death occurred. A dose of 39.5 mg/kg also resulted in death, though the animal survived until 4.5 hours. We decreased the dose to 20 mg/kg (between 2 and 3 "steps"), which caused moderate toxicity but not lethality. Therefore, the MTD for free PB was operationally defined as 20 mg/kg. For NCC-PB0, our first treatment dose was 39.5 which elicited moderate signs of toxicity but no lethality. The dose was increased to 51.3 mg/kg which also did not result in lethality. The next dose, 66.7 mg/kg, caused a steady increase in toxicity until death occurred around 4.5 hours. Therefore, the MTD for NCC-PB0 was operationally defined as 51.3 mg/kg. Figure 5-6 shows the functional signs data over time with free PB and NCC-PB0 animals.

Following the MTD studies, we treated a small group of animals (2-3/group) with half of the MTD dose (i.e. 10 mg/kg for free PB and 25.7 mg/kg for NCC-PB0), aiming to inhibit a non-lethal but substantial amount of ChE activity. A baseline blood sample was taken from mice prior to dosing, and then subsequent blood samples were taken between 45- and 360-minutes post-dosing. Figure 5-7 shows the time course of inhibition for free PB and NCC-PB0 (0.5 MTD). During this study, functional signs and some lethality (one NCC-PB0 animal) were noted; therefore, the next time course study was

conducted using a lower dose (0.3 x MTD) (Fig. 5-8). Analysis using two-way ANOVA did not identify a significant main effect of formulation type (i.e. free PB versus NCC-PB0)($p=0.14$). While the 6 mg/kg dose of free PB did not cause any functional signs of toxicity, the 15 mg/kg dose of NCC-PB0 resulted in cholinergic signs and lethality in two animals.

Due to the toxicity noted in NCC-PB0 treated animals at 0.5 and 0.3 x MTD, we compared the cholinesterase inhibition caused by equivalent doses (6 mg/kg), and followed the inhibition to 24 hours (Fig 5-9). No signs of toxicity were noted in either group at the 6 mg/kg dosing level, and no significant weight loss occurred over 24 hours (Fig. 5-10). Similar to previous doses, we observed an apparent burst release with both free PB and NCC-PB0 followed by slightly extended ChE inhibition. However, these differences failed to reach significance ($p=0.07$). If the initial absorption phase (0-180 min) is excluded from the analysis, however, there was a significant effect of formulation at the later time points ($p=0.01$). Pairwise comparisons of the elimination-only data identified a significant difference between PB and NCC-PB0 at the 380-minute timepoint ($p=0.03$). The area under the curve (AUC) is a measure of bioavailability. The AUC was 17,301 (CI = 11,623 - 22, 979) for free PB and 28,584 (CI = 17,600 - 39,569) for NCC-PB0 (t-test; $p = 0.08$).

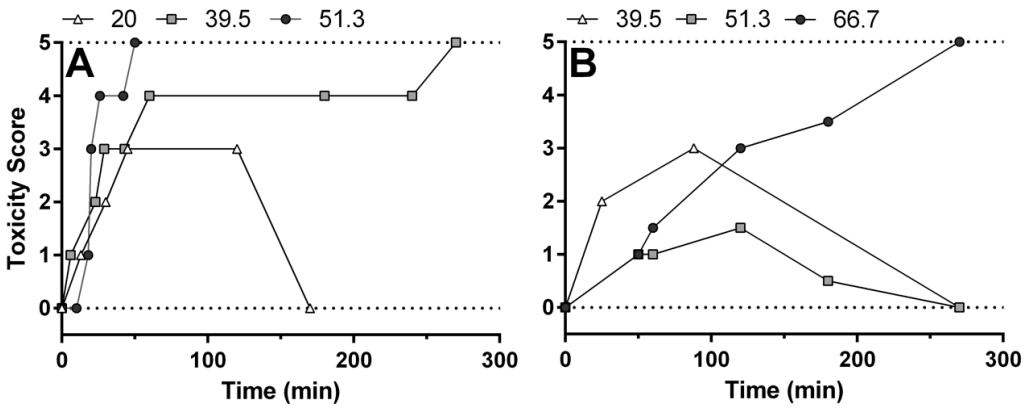

Figure 5-6. Comparison of acute toxicity following treatment with PB or NCC-PB0. CD1 mice were treated with free PB (20, 39.5, and 51.3 mg/kg, po; Panel A) or NCC-PB0 (39.5, 51.3 and 66.7 mg/kg, po; Panel B). Free PB was also given at 112.7 mg/kg, which led to severe signs of toxicity and death within one minute (data not plotted). Each line represents the toxicity scores noted from a single animal.

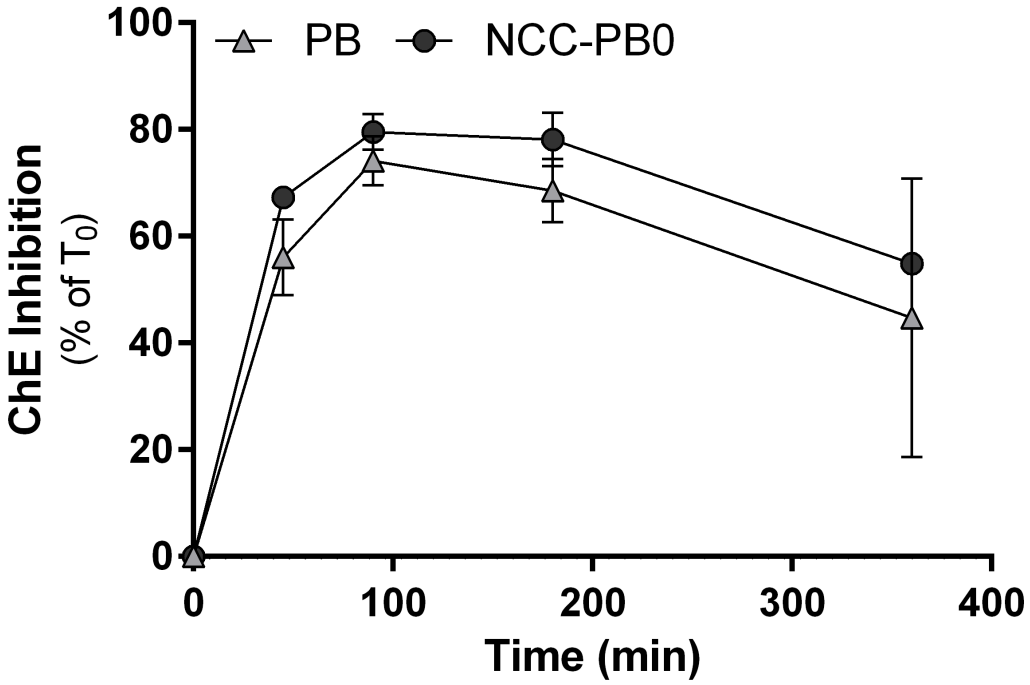

Figure 5-7. Comparison of whole blood ChE inhibition following *in vivo* exposure to 0.5 MTD of PB or NCC-PB0. CD1 mice were given free PB (10 mg/kg, po) or NCC-PB0 (25.7 mg/kg, po), which preliminary assays defined as the 0.5 maximum tolerated dose level (MTD). A small sample of whole blood was collected from mice at each time point from the tail tip, and the ChE activity was immediately measured using the radiometric method described in section 5.2.3. Data are reported as mean ± SD (n= 2-3 animals/group).

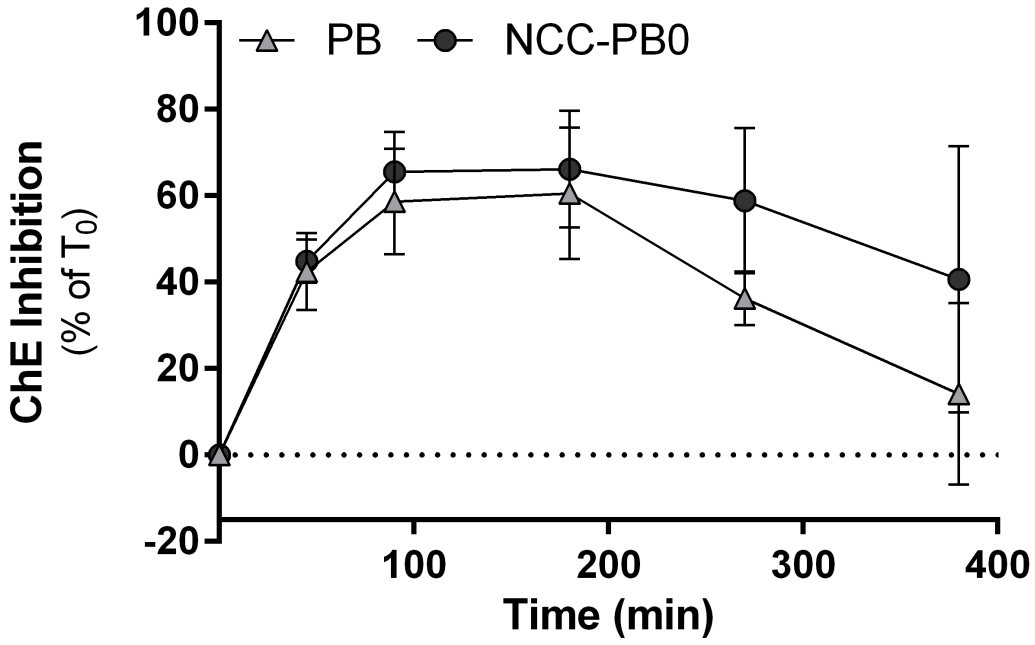

Figure 5-8. Comparison of whole blood ChE inhibition following *in vivo* exposure to 0.3 MTD of PB or NCC-PB0. CD1 mice were given free PB (6 mg/kg, po) or NCC-PB0 (15 mg/kg, po), which preliminary assays defined as the 0.3 maximum tolerated dose level (MTD). A small sample of whole blood was collected from mice at each time point from the tail tip, and the ChE activity was immediately measured using the radiometric method described in section 5.2.3. Data are reported as mean ± SD (n= 6 animals/group).

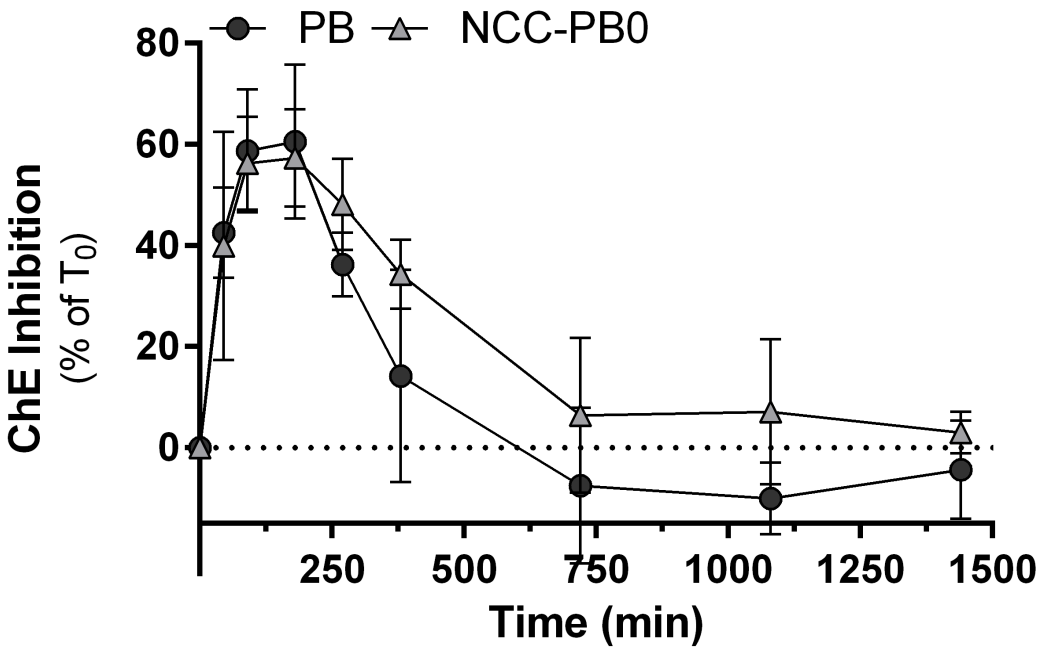

Figure 5-9. Twenty-four-hour time course of ChE inhibition following oral PB or NCC-PB0. CD1 mice were given free PB or NCC-PB0 (6 mg/kg, po). A small sample of whole blood (5-10 μl) was collected from mice at each time point from the tail tip, and the ChE activity was immediately measured using the radiometric method described in section 5.2.3. Data are reported as mean ± SD (n= 6 animals/group).

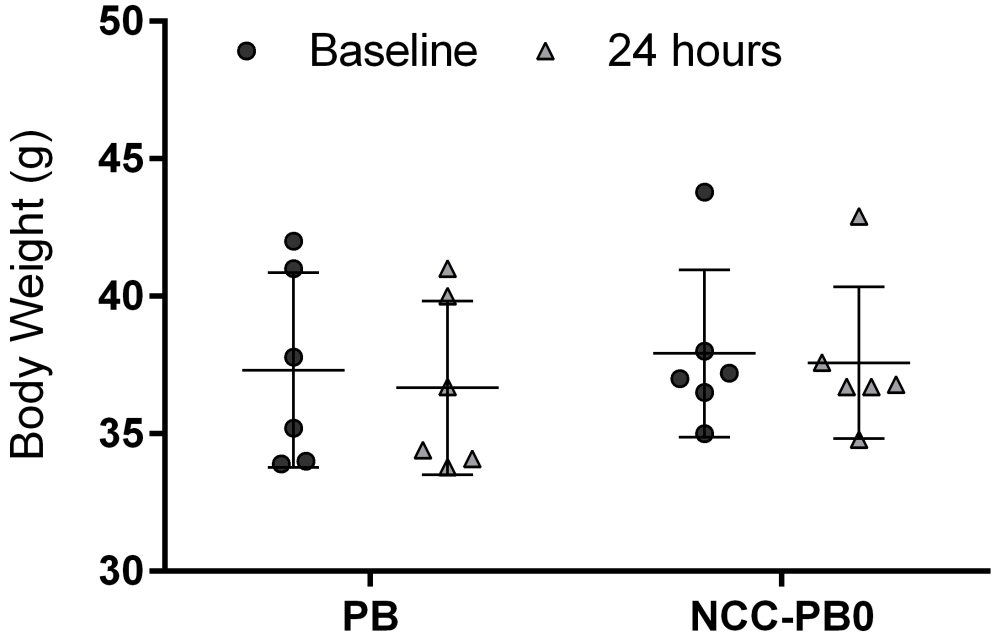

Figure 5-10. Twenty-four-hour body weight comparison of animals treated with PB or NCC-PB0. CD1 mice were given free PB or NCC-PB0 (6 mg/kg, po). All animals were weighed prior to dosing, and 24-hours later, the body weights were recorded again for comparison. Animals had free access to food and water following treatment. Data are reported as individual values with bars representing the mean ± SD (n= 6 animals/group).

5.4 DISCUSSION

Inhibitor-based prophylactics like pyridostigmine bromide have been available for military use since the 1990's. While enzyme-based prophylactics may be on the horizon, improved PB formulations could likely be implemented more quickly and would remain an inexpensive alternative to biological prophylactics. The current PB tablet formulation must be taken every 8 hours to retain the recommended 20-40% ChE inhibition levels. Improved pharmacokinetics of PB release and elimination would allow for sustained inhibition and thus an improved dosing schedule. PB formulated within nanocrystalline cellulose hydrogels may provide a mechanism for improved drug release. The goal of this study was to evaluate several NCC-PB formulations (NCC-PB0, NCC-PB10, NCC-PB1, and TEMPO-PB) based on *in vitro* ChE inhibition. One formulation, NCC-PB0, was also tested for its pharmacodynamic effect (*in vivo* blood ChE inhibition) compared to free PB.

Incubation of free PB and NCC-PB formulations supported our hypothesis that hydrogel formulations may prolong ChE inhibition. The NCC-PB0, NCC-PB10, and NCC-PB1 (which were differentiated by their crosslinking conditions) altered the time course of ChE inhibition minimally. The NCC-PB0 formulation inhibited significantly less ChE than free PB up to the 60-minute time point, after which "maximal" (i.e. same inhibition levels as free PB) were noted. This suggested that the NCC-PB0 formulation slightly retarded the release of PB. The NCC-PB10 formulation also marginally retarded release out to 30 minutes, while the NCC-PB1 formulation did not appear to alter PB release. These results are in agreement with another study which found that over 80% of the drug was released by 50 minutes when using a microcrystalline cellulose preparation

[17]. While our study did not directly evaluate PB release, we can estimate that most of the PB had been released from these formulations due to the levels of cholinesterase inhibition achieved.

The TEMPO-PB gel formulation was the most effective in altering the time course of *in vitro* ChE inhibition. ChE inhibition was significantly lower than with free PB at each time point tested until 24 hours, suggesting that formulation with a nanocrystalline hydrogel slowed the release of PB into solution. Interestingly, however, the ChE inhibition achieved by the TEMPO-PB formulation plateaued around 70% inhibition (as compared to ~90% inhibition with free PB) at about four hours of incubation. This effect could be achieved by two possible mechanisms. First, the TEMPO-PB formulation changed the maximal amount of PB which may be released from the gel (i.e. some PB is irreversibly contained within the gel). Incomplete release of loaded drug within cellulose formulation has been observed previously [17]. Second, following a "burst" release, the rate of PB released from TEMPO-PB gels proceeds slowly out to 24 hours, at a rate which closely equals the reactivation rate of PB-inhibited ChE. Carbamylated enzymes spontaneously reactivate with a half-life of 15-30 minutes *in vitro* [195]. If this were the case, the 70% inhibition level achieved should persist at later time points. Moreover, direct evaluation of PB release from the hydrogel formulations would provide insight into nature of the PB release rate.

The NCC-PB0 formulation was used for *in vivo* evaluation of the pharmacodynamic effect of PB release. While other studies have found that cellulose formulations alter oral absorption and bioavailability [326], we did not find any differences in these parameters between NCC-PB0 and free PB. The burst effect, wherein

a large bolus of drug releases prior to achieving a stable drug release rate, is a well-known phenomenon in controlled release research [327]. Methods such as excipient coating, decreasing pore size, altering surface hydrophobicity, and others have been incorporated into controlled release formulations to offset this effect [328-331]. It is therefore possible that further tuning of the hydrogel formulations, either by chemical or mechanical means, could result in more desirable release kinetics. Despite this, the NCC-PB0 preparation appeared to elicit slightly higher levels of inhibition following the absorption phase (Fig. 5-9). Analysis of the data after peak ChE inhibition was achieved (i.e. after three hours) showed ChE inhibition was increased at the 380-minute time point compared to free PB. This supports the suggestion that the effect of PB may be slightly extended by hydrogel formulation, similar to what was found in the *in vitro* studies.

Toxicity arising from PB overdose is another mechanism of evaluating differences in pharmacokinetic/pharmacodynamics of free PB and cellulose formulated PB. Soldiers taking PB during the Gulf War reported minor symptoms of anticholinesterase toxicity including frequent urination and gastrointestinal upset [204]. An extended release formulation may avoid some of these side effects as ChE inhibition is not expected to peak as sharply. Though our biochemical data did not support the goal of slower absorption or decreased maximal concentration, we observed that symptoms of toxicity were decreased in animals which had been given the NCC-PB0 formulation. The 51.3 mg/kg dosing level resulted in severe signs of toxicity and death within one hour for an animal given free PB, while the animal given the NCC-PB0 formulation survived after showing mild-to-moderate signs of toxicity. A similar result was also found at the 39.5 mg/kg dosing level. While animals were generally able to survive higher doses than free

PB, an accurate maximum tolerated dose for NCC-PB0 was difficult to determine. In our preliminary studies individual animals were able to survive doses up to 51.3 mg/kg, but in subsequent studies some lethality was noted at much lower doses (25.7 mg/kg and 15 mg/kg). This may be due to differences in individual animals' sensitivity to PB, an inconsistent pharmacodynamic effect of cellulose formulation, or a combination thereof.

Hydrogel formulation with nanocellulose has been used to successfully extend the release of certain small molecule and protein drugs. In this study we applied this formulation tactic on the prophylactic drug pyridostigmine. While some results were promising, tuning of the formulation to delay *in vivo* absorption and further extend ChE inhibition is necessary. Our *in vitro* studies suggested that altered surface chemistry (e.g. TEMPO-oxidized cellulose) may further alter release kinetics compared to other NCC-PB formulations, though other methods of hydrogel tuning (e.g. addition of other excipients) merit investigation. Overall, further *in vitro* and *in vivo* studies are necessary to completely characterize cellulose hydrogels as a method of delayed PB release formulation. An improved extended release formulation of PB would be beneficial for soldiers and other personnel at risk for exposure to OP toxicants.

CHAPTER VI

CONCLUSIONS

Although the agricultural use of organophosphorus compounds has been decreasing, they remain easy to obtain and relatively simple to manufacture. Moreover, while the Chemical Weapons Convention has seemingly been effective at reducing nerve agent stockpiles, several incidents involving nerve agents have occurred as recently as 2018. Individuals exposed to OP compounds, whether intentionally or inadvertently, may experience long-term neurological sequelae in addition to disabling acute toxicity and death. Improvements in post-exposure treatments are being investigated, with particular focus on preventing OP-induced seizures and lethality. Currently, however, prophylaxis against OP toxicity is the most effective method at avoiding serious complications of OP exposure. While this approach cannot be utilized by everyone, the potential benefit to soldiers and other high-risk personnel warrant further development of such drugs.

The two primary approaches to OP prophylaxis, inhibitor-based and enzyme-based, work by different mechanisms. Inhibitor-based approaches employ a carbamate, typically pyridostigmine, to "reversibly" inhibit a small proportion of AChE which creates a pool of enzyme which is protected from essentially irreversible OP inhibitors. In contrast,

enzyme-based approaches act as a molecular "sink" which is able to interact with OP molecules, essentially removing them from circulation (either through irreversible binding or catalytic destruction) before the target enzyme can be reached. The challenges associated with these two approaches have been discussed herein. This study evaluated several different approaches to improve the pharmacokinetics or pharmacodynamics of the stoichiometric scavenger butyrylcholinesterase, the slow catalytic bioscavenger $BChE_{G117H}$, and the reversible inhibitor pyridostigmine.

Complexation with PEG has been shown to improve BChE's pharmacokinetics. Furthermore, studies have demonstrated that circulation of drugs can be prolonged by red blood cell attachment, which PEG functionalization could facilitate. My studies evaluated the effect of PLL-g-PEG complexation on BChE enzyme characteristics. We found that complexation decreased the catalytic efficiency of the enzyme, but had variable effects on the OP binding capacity of the enzyme, which is more important for bioscavenger evaluation. We hypothesized that the binding capacity of C-BCs is less affected with lipophilic compounds as compared to hydrophilic compounds. However, more inhibitors would need to be evaluated to confirm this hypothesis, and whether or not this could have biological importance. Lastly, we determined that the complexation of the enzyme made it more resistant to inactivation by heat and proteases. Taken together, these findings suggest that copolymer-complexation results in both favorable and slightly unfavorable outcomes.

Next, we utilized computational re-engineering techniques aiming to improve the OP turnover rate of the mutant enzyme $BChE_{G117H}$. We successfully produced mutants of $BChE_{G117H}$ which had a three-residue insertion on a hyper-mobile surface loop (278-285)

of the enzyme. While the mutants were catalytically active, they exhibited decreased activity with both choline and OP substrates compared to $BChE_{G117H}$. Interestingly, some of the loop-mutant enzymes had increased binding affinity for paraoxon, an effect that was also observed *in silico*. Moreover, one of the tested loop-mutants, ENA, had an increased ability to reactivate after paraoxon exposure. Computational results suggested that all of the OP substrates tested were unstable within the active site, making significant improvements in the catalytic rate futile unless the binding pocket is made more secure. Previous literature has suggested, however, that this is not easily done. While the results of this study did not point to improved catalytic activity, they may provide proof-of-concept for catalytic improvement of other bioscavenging enzymes. We hypothesize that application of this method on a catalytic bioscavenger with higher intrinsic catalytic activity (e.g. paraoxonase) may lead to more relevant changes in catalysis as the active site is already optimized for catalysis of OP compounds.

Our final aim was focused on prophylaxis with the inhibitor pyridostigmine. We sought to develop an extended-release nanocrystalline cellulose hydrogel formulation of PB with the goal of improving upon the current recommended 8-hour dosing schedule. The cellulose formulation tested in this study did not decrease the absorption rate or maximal concentration achieved *in vivo,* but following this "peak", higher ChE inhibition was maintained during early time points. *In vitro* studies suggested that TEMPO-oxidized cellulose gels may have a better release profile than the original cellulose formulation; however, an *in vivo* study would be necessary to confirm this. Further pharmacokinetic improvements may be achieved with these cellulose formulations *via* gel modifications.

REFERENCES

1. Schmaltz, F.: Neurosciences and Research on Chemical Weapons of Mass Destruction in Nazi Germany. Journal of the History of the Neurosciences. 15, 186–209 (2006).
2. Macilwain, C.: Study Proves Iraq Used Nerve-Gas. Nature. 363, 3–3 (1993).
3. Paddock, R.C., Sang-Hun, C.: Kim Jong-nam Was Killed by VX Nerve Agent, Malaysians Say, https://nyti.ms/2md8bwy.
4. Vale, J.A., Marrs, T.C., Maynard, R.L.: Novichok: a murderous nerve agent attack in the UK. Clin Toxicol (Phila). 62, 1–5 (2018).
5. Holstege, C.P., Kirk, M., Sidell, F.R.: Chemical warfare. Nerve agent poisoning. Crit. Care. Clin. 13, 923–942 (1997).
6. Chen, Y.: Organophosphate-induced brain damage: mechanisms, neuropsychiatric and neurological consequences, and potential therapeutic strategies. Neurotoxicology. 33, 391–400 (2012).
7. Reed, B.A., Sabourin, C.L., Lenz, D.E.: Human butyrylcholinesterase efficacy against nerve agent exposure. J. Biochem. Mol. Toxicol. 31, (2017).
8. Saxena, A., Sun, W., Luo, C., Doctor, B.P.: Human serum butyrylcholinesterase: In vitro and in vivo stability, pharmacokinetics, and safety in mice. Chem. Biol. Interact. 157-158, 199–203 (2005).
9. Gaydess, A., Duysen, E.G., Li, Y., Gilman, V., Kabanov, A., Lockridge, O., Bronich, T.: Visualization of exogenous delivery of nanoformulated butyrylcholinesterase to the central nervous system. Chem. Biol. Interact. 187, 295–298 (2010).
10. Pope, C., Uchea, C., Flynn, N., Poindexter, K., Geng, L., Brimijoin, W.S., Hartson, S., Ranjan, A., Ramsey, J.D., Liu, J.: In vitro characterization of cationic copolymer-complexed recombinant human butyrylcholinesterase. Biochem. Pharmacol. 98, 531–539 (2015).
11. Harris, J.M., Chess, R.B.: Effect of pegylation on pharmaceuticals. Nature Reviews Drug Discovery. (2003).
12. Rodríguez-Martínez, J.A., Rivera-Rivera, I., Solá, R.J., Griebenow, K.: Enzymatic activity and thermal stability of PEG-alpha-chymotrypsin conjugates. Biotechnol. Lett. 31, 883–887 (2009).
13. Monfardini, C., Schiavon, O., Caliceti, P., Morpurgo, M., Harris, J.M., Veronese, F.M.: A Branched Monomethoxypoly(ethylene glycol) for Protein Modification. Bioconjugate Chem. 6, 62–69 (2002).
14. Lockridge, O., Blong, R.M., Masson, P., Froment, M.T., Millard, C.B., Broomfield, C.A.: A single amino acid substitution, Gly117His, confers

phosphotriesterase (organophosphorus acid anhydride hydrolase) activity on human butyrylcholinesterase. Biochemistry. 36, 786–795 (1997).
15. Agarwal, P.K., Schultz, C., Kalivretenos, A., Ghosh, B., Broedel, S.E.J.: Engineering a Hyper-catalytic Enzyme by Photoactivated Conformation Modulation. Journal of Physical Chemistry Letters. 3, 1142–1146 (2012).
16. Dunn, M.A., Hackley, B.E., Sidell, F.R.: Pretreatment for Nerve Agent Exposure. In: Sidell, F.R., Takafuji, E.T., and Franz, D.R. (eds.) Medical Aspects of Chemical and Biological Warfare. pp. 181–196. Office of the Surgeon General at TMM Publications, Washington, DC (1997).
17. Oprea, A.-M., Nistor, M.-T., Popa, M.I., Lupusoru, C.E., Vasile, C.: In vitro and in vivo theophylline release from cellulose/chondroitin sulfate hydrogels. Carbohydrate Polymers. 90, 127–133 (2012).
18. Gao, X., Cao, Y., Song, X., Zhang, Z., Zhuang, X., He, C., Chen, X.: Biodegradable, pH-Responsive Carboxymethyl Cellulose/Poly(Acrylic Acid) Hydrogels for Oral Insulin Delivery. Macromol. Biosci. 14, 565–575 (2014).
19. Tansey, E.M.: Henry Dale and the discovery of acetylcholine. C. R. Biol. 329, 419–425 (2006).
20. Everitt, B.J., Robbins, T.W.: Central cholinergic systems and cognition. Annu Rev Psychol. 48, 649–684 (1997).
21. Hrabovska, A., Krejci, E.: Reassessment of the Role of the Central Cholinergic System. J Mol Neurosci. 53, 352–358 (2013).
22. Picciotto, M.R., Higley, M.J., Mineur, Y.S.: Acetylcholine as a neuromodulator: cholinergic signaling shapes nervous system function and behavior. Neuron. 76, 116–129 (2012).
23. Carey, J.L., Dunn, C., Gaspari, R.J.: Central respiratory failure during acute organophosphate poisoning. Respiratory Physiology & Neurobiology. 189, 403–410 (2013).
24. Martyn, J.A.J., Fagerlund, M.J., Eriksson, L.I.: Basic principles of neuromuscular transmission. Anaesthesia. 64 Suppl 1, 1–9 (2009).
25. Atri, A., Chang, M.S., Strichartz, G.R.: Cholinergic Pharmacology. In: Golan, D.E., Armstrong, E.J., and Armstrong, A.W. (eds.) Principles of pharmacology: the pathophysiologic basis of drug therapy. pp. 127–149. Wolters-Kluwer (2017).
26. Taylor, P., Brown, J.H.: Acetylcholine. In: Siegel, G.J., Agranoff, B.W., Albers, W., Fisher, S.K., and Uhler, M.D. (eds.) Basic Neurochemistry. Lippincott-Raven, Philadelphia (1999).
27. Parsons, S.M., Bahr, B.A., Gracz, L.M., Kaufman, R., Kornreich, W.D., Nilsson, L., Rogers, G.A.: Acetylcholine transport: fundamental properties and effects of pharmacologic agents. Ann. N. Y. Acad. Sci. 493, 220–233 (1987).
28. Kramer, I.M.: Choinergic Signaling and Muscule Contraction. In: Audet, J. (ed.) Signal Transduction. pp. 263–327. Academic Press (2015).
29. Taylor, P., Radic, Z.: The cholinesterases: from genes to proteins. Annu. Rev. Pharmacol. Toxicol. 34, 281–320 (1994).
30. Haga, T.: Molecular properties of muscarinic acetylcholine receptors. Proceedings of the Japan Academy Series B-Physical and Biological Sciences. 89, 226–256 (2013).

31. Caulfield, M.: Muscarinic receptors—characterization, coupling and function. Pharmac. Ther. 58, 319–379 (1993).
32. Thiele, A.: Muscarinic Signaling in the Brain. http://dx.doi.org/10.1146/annurev-neuro-062012-170433. 36, 271–294 (2013).
33. Abrams, P., Andersson, K.-E., Buccafusco, J.J., Chapple, C., Groat, W.C., Fryer, A.D., Kay, G., Laties, A., Nathanson, N.M., Pasricha, P.J., Wein, A.J.: Muscarinic receptors: their distribution and function in body systems, and the implications for treating overactive bladder. British Journal of Pharmacology. 148, 565–578 (2006).
34. Miledi, R., Molinoff, P., Potter, L.T.: Isolation of the cholinergic receptor protein of Torpedo electric tissue. Nature. 229, 554–557 (1971).
35. Mishina, M., Takai, T., Imoto, K., Noda, M., Takahashi, T., Numa, S., Methfessel, C., Sakmann, B.: Molecular distinction between fetal and adult forms of muscle acetylcholine receptor. Nature. 321, 406–411 (1986).
36. Skok, V.I.: Nicotinic acetylcholine receptors in autonomic ganglia. Auton Neurosci. 97, 1–11 (2002).
37. Wonnacott, S.: Presynaptic nicotinic ACh receptors. Trends Neurosci. 20, 92–98 (1997).
38. Jones, S., Sudweeks, S., Yakel, J.L.: Nicotinic receptors in the brain: correlating physiology with function. Trends Neurosci. 22, 555–561 (1999).
39. Plazas, P.V., Katz, E., Gomez-Casati, M.E., Bouzat, C., Elgoyhen, A.B.: Stoichiometry of the alpha9alpha10 nicotinic cholinergic receptor. J. Neurosci. 25, 10905–10912 (2005).
40. Colović, M.B., Krstić, D.Z., Lazarević-Pašti, T.D., Bondžić, A.M., Vasić, V.M.: Acetylcholinesterase inhibitors: pharmacology and toxicology. Curr Neuropharmacol. 11, 315–335 (2013).
41. Richman, D.P., Agius, M.A.: Treatment of autoimmune myasthenia gravis. Neurology. 61, 1652–1661 (2003).
42. Hampel, H., Mesulam, M.M., Cuello, A.C., Farlow, M.R., Giacobini, E., Grossberg, G.T., Khachaturian, A.S., Vergallo, A., Cavedo, E., Snyder, P.J., Khachaturian, Z.S.: The cholinergic system in the pathophysiology and treatment of Alzheimer's disease. Brain. 141, 1917–1933 (2018).
43. Pope, C.N., Brimijoin, S.: Cholinesterases and the fine line between poison and remedy. Biochem. Pharmacol. 153, 205–216 (2018).
44. Connolly, B.S., Lang, A.E.: Pharmacological Treatment of Parkinson Disease. JAMA. 311, 1670–14 (2014).
45. Gibbons, A., Dean, B.: The Cholinergic System: An Emerging Drug Target for Schizophrenia. Curr. Pharm. Des. 22, 2124–2133 (2016).
46. Dulawa, S.C., Janowsky, D.S.: Cholinergic regulation of mood: from basic and clinical studies to emerging therapeutics. Mol Psychiatry. 24, 694–709 (2018).
47. Alles, G.A., Hawes, R.C.: CHOLINESTERASES IN THE BLOOD OF MAN. J. Biol. Chem. 133, 375–390 (1940).
48. Mendel, B., Rudney, H.: Studies on cholinesterase: 1. Cholinesterase and pseudo-cholinesterase. Biochem. J. 37, 59–63 (1943).
49. Mendel, B., Rudney, H.: ON THE TYPE OF CHOLINESTERASE PRESENT IN BRAIN TISSUE. Science. 98, 201–202 (1943).

50. Hawkins, R.D., Gunter, J.M.: Studies on cholinesterase: 5. The selective inhibition of pseudo-cholinesterase in vivo. Biochem. J. 40, 192–197 (1946).
51. Lockridge, O.: Review of human butyrylcholinesterase structure, function, genetic variants, history of use in the clinic, and potential therapeutic uses. Pharmacol. Ther. 148, 34–46 (2015).
52. Reid, G.A., Chilukuri, N., Darvesh, S.: Butyrylcholinesterase and the cholinergic system. Neuroscience. 234, 53–68 (2013).
53. Chatonnet, F., Boudinot, E., Chatonnet, A., Taysse, L., Daulon, S., Champagnat, J., Foutz, A.S.: Respiratory survival mechanisms in acetylcholinesterase knockout mouse. Eur. J. Neurosci. 18, 1419–1427 (2003).
54. Duysen, E.G., Li, B., Darvesh, S., Lockridge, O.: Sensitivity of butyrylcholinesterase knockout mice to (−)-huperzine A and donepezil suggests humans with butyrylcholinesterase deficiency may not tolerate these Alzheimer's disease drugs and indicates butyrylcholinesterase function in neurotransmission. Toxicology. 233, 60–69 (2007).
55. Kalow, W., Gunn, D.R.: The Relation Between Dose of Succinylcholine and Duration of Apnea in Man. J. Pharmacol. Exp. Ther. 120, 203–214 (1957).
56. Masson, P., Froment, M.T., Fortier, P.L., Visicchio, J.E., Bartels, C.F., Lockridge, O.: Butyrylcholinesterase-catalysed hydrolysis of aspirin, a negatively charged ester, and aspirin-related neutral esters. Biochim. Biophys. Acta. 1387, 41–52 (1998).
57. Stewart, D.J., Inaba, T., Tang, B.K., Kalow, W.: Hydrolysis of cocaine in human plasma by cholinesterase. Life Sci. 20, 1557–1563 (1977).
58. Lockridge, O., Mottershaw-Jackson, N., Eckerson, H.W., La Du, B.N.: Hydrolysis of diacetylmorphine (heroin) by human serum cholinesterase. J. Pharmacol. Exp. Ther. 215, 1–8 (1980).
59. Lockridge, O., Quinn, D.M.: Esterases. In: McQueen, C.A. (ed.) Comprehensive Toxicology. pp. 243–273. Elsevier (2010).
60. Casida, J.E., Quistad, G.B.: Organophosphate toxicology: safety aspects of nonacetylcholinesterase secondary targets. Chem. Res. Toxicol. 17, 983–998 (2004).
61. Yanagi, S., Sato, T., Kangawa, K., Nakazato, M.: The Homeostatic Force of Ghrelin. Cell Metab. 27, 786–804 (2018).
62. Wittekind, D.A., Kluge, M.: Ghrelin in psychiatric disorders - A review. Psychoneuroendocrinology. 52, 176–194 (2015).
63. Pradhan, G., Samson, S.L., Sun, Y.: Ghrelin: much more than a hunger hormone. Curr Opin Clin Nutr Metab Care. 16, 619–624 (2013).
64. Chen, V.P., Gao, Y., Geng, L., Brimijoin, S.: Radiometric assay of ghrelin hydrolase activity and 3H-ghrelin distribution into mouse tissues. Biochem. Pharmacol. 98, 732–739 (2015).
65. Schopfer, L.M., Lockridge, O., Brimijoin, S.: Pure human butyrylcholinesterase hydrolyzes octanoyl ghrelin to desacyl ghrelin. Gen. Comp. Endocrinol. 224, 61–68 (2015).
66. Chen, V.P., Gao, Y., Geng, L., Brimijoin, S.: Butyrylcholinesterase regulates central ghrelin signaling and has an impact on food intake and glucose homeostasis. International Journal of Obesity 2017 41:9. 41, 1413–1419 (2017).

67. Li, B., Duysen, E.G., Lockridge, O.: The butyrylcholinesterase knockout mouse is obese on a high-fat diet. Chem. Biol. Interact. 175, 88–91 (2008).
68. Chen, V.P., Gao, Y., Geng, L., Stout, M.B., Jensen, M.D., Brimijoin, S.: Butyrylcholinesterase Deficiency Promotes Adipose Tissue Growth and Hepatic Lipid Accumulation in Male Mice on High-Fat Diet. Endocrinology. 157, 3086–3095 (2016).
69. Zheng, X., Deng, J., Zhang, T., Yao, J., Zheng, F., Zhan, C.-G.: Potential anti-obesity effects of a long-acting cocaine hydrolase. Chem. Biol. Interact. 259, 99–103 (2016).
70. Chen, V.P., Gao, Y., Geng, L., Parks, R.J., Pang, Y.-P., Brimijoin, S.: Plasma butyrylcholinesterase regulates ghrelin to control aggression. Proc. Natl. Acad. Sci. U.S.A. 112, 2251–2256 (2015).
71. Li, B., Duysen, E.G., Carlson, M., Lockridge, O.: The butyrylcholinesterase knockout mouse as a model for human butyrylcholinesterase deficiency. J. Pharmacol. Exp. Ther. 324, 1146–1154 (2008).
72. Lockridge, O., Norgren, R.B., Johnson, R.C., Blake, T.A.: Naturally Occurring Genetic Variants of Human Acetylcholinesterase and Butyrylcholinesterase and Their Potential Impact on the Risk of Toxicity from Cholinesterase Inhibitors. Chem. Res. Toxicol. 29, 1381–1392 (2016).
73. Manoharan, I., Boopathy, R., Darvesh, S., Lockridge, O.: A medical health report on individuals with silent butyrylcholinesterase in the Vysya community of India. Clin. Chim. Acta. 378, 128–135 (2007).
74. Lockridge, O., Bartels, C.F., Vaughan, T.A., Wong, C.K., Norton, S.E., Johnson, L.L.: Complete amino acid sequence of human serum cholinesterase. J. Biol. Chem. 262, 549–557 (1987).
75. Lockridge, O., Adkins, S., La Du, B.N.: Location of disulfide bonds within the sequence of human serum cholinesterase. J. Biol. Chem. 262, 12945–12952 (1987).
76. Blong, R.M., Bedows, E., Lockridge, O.: Tetramerization domain of human butyrylcholinesterase is at the C-terminus. Biochem. J. 327 (Pt 3), 747–757 (1997).
77. Li, H., Schopfer, L.M., Masson, P., Lockridge, O.: Lamellipodin proline rich peptides associated with native plasma butyrylcholinesterase tetramers. Biochem. J. 411, 425–432 (2008).
78. Leung, M.R., van Bezouwen, L.S., Schopfer, L.M., Sussman, J.L., Silman, I., Lockridge, O., Zeev-Ben-Mordehai, T.: Cryo-EM structure of the native butyrylcholinesterase tetramer reveals a dimer of dimers stabilized by a superhelical assembly. Proc Natl Acad Sci USA. 115, 13270–13275 (2018).
79. Haupt, H., Heide, K., Zwisler, O., Schwick, H.G.: [Isolation and physico-chemical characterization of cholinesterase in human serum]. Blut. 14, 65–75 (1966).
80. Østergaard, D., Viby-Mogensen, J., Hanel, H.K., Skovgaard, L.T.: Half-life of plasma cholinesterase. Acta Anaesthesiologica Scandinavica. 32, 266–269 (1988).

81. Saxena, A., Ashani, Y., Raveh, L., Stevenson, D., Patel, T., Doctor, B.P.: Role of oligosaccharides in the pharmacokinetics of tissue-derived and genetically engineered cholinesterases. Mol Pharmacol. 53, 112–122 (1998).
82. CHITLARU, T., Kronman, C., Velan, B., Shafferman, A.: Effect of human acetylcholinesterase subunit assembly on its circulatory residence. Biochem. J. 354, 613–625 (2001).
83. Nicolet, Y., Lockridge, O., Masson, P., Fontecilla-Camps, J.C., Nachon, F.: Crystal structure of human butyrylcholinesterase and of its complexes with substrate and products. J. Biol. Chem. 278, 41141–41147 (2003).
84. Sussman, J.L., Harel, M., Frolow, F., Oefner, C., Goldman, A., Toker, L., Silman, I.: Atomic structure of acetylcholinesterase from Torpedo californica: a prototypic acetylcholine-binding protein. Science. 253, 872–879 (1991).
85. Masson, P., Legrand, P., Bartels, C.F., Froment, M.T., Schopfer, L.M., Lockridge, O.: Role of aspartate 70 and tryptophan 82 in binding of succinyldithiocholine to human butyrylcholinesterase. Biochemistry. 36, 2266–2277 (1997).
86. Nachon, F., Ehret-Sabatier, L., Loew, D., Colas, C., van Dorsselaer, A., Goeldner, M.: Trp82 and Tyr332 are involved in two quaternary ammonium binding domains of human butyrylcholinesterase as revealed by photoaffinity labeling with [3H]DDF. Biochemistry. 37, 10507–10513 (1998).
87. Masson, P., Xie, W., Froment, M.-T., Levitsky, V., Fortier, P.-L., Albaret, C., Lockridge, O.: Interaction between the peripheral site residues of human butyrylcholinesterase, D70 and Y332, in binding and hydrolysis of substrates. Biochimica et Biophysica Acta (BBA) - Protein Structure and Molecular Enzymology. 1433, 281–293 (1999).
88. Lockridge, O., Duysen, E.G.: Butyrylcholinesterase: Overview, Structure, and Function. In: Satoh, T. and Gupta, R.C. (eds.) Acetylcholinesterase Pesticides Metabolism, Neurotoxicity, and Epidemiology. pp. 25–41. Anticholinesterase …, Hoboken (2011).
89. Ashima Saxena, Ann M G Redman, Xuliang Jiang, Lockridge, O., Doctor, B.P.: Differences in Active Site Gorge Dimensions of Cholinesterases Revealed by Binding of Inhibitors to Human Butyrylcholinesterase†. American Chemical Society (1997).
90. Vellom, D.C., Radic, Z., Li, Y., Pickering, N.A., Camp, S.: Amino acid residues controlling acetylcholinesterase and butyrylcholinesterase specificity. Biochemistry. 32, 12–17 (1993).
91. Shafferman, A., Kronman, C., Flashner, Y., Leitner, M., Grosfeld, H., Ordentlich, A., Gozes, Y., Cohen, S., Ariel, N., Barak, D.: Mutagenesis of human acetylcholinesterase. Identification of residues involved in catalytic activity and in polypeptide folding. J. Biol. Chem. 267, 17640–17648 (1992).
92. Suárez, D., Díaz, N., Fontecilla-Camps, J., Field, M.J.: A Computational Study of the Deacylation Mechanism of Human Butyrylcholinesterase. Biochemistry. 45, 7529–7543 (2006).
93. Kovach, I.M.: Structure and dynamics of serine hydrolase-organophosphate adducts. J. Enzym. Inhib. 2, 199–208 (1988).

94. Kovach, I.M.: Stereochemistry and secondary reactions in the irreversible inhibition of serine hydrolases by organophosphorus compounds. J. Phys. Org. Chem. 17, 602–614 (2004).
95. Zhang, Y., Kua, J., McCammon, J.A.: Role of the Catalytic Triad and Oxyanion Hole in Acetylcholinesterase Catalysis: An ab initio QM/MM Study. J. Am. Chem. Soc. 124, 10572–10577 (2002).
96. Ordentlich, A., Barak, D., Kronman, C., Ariel, N., Segall, Y., Velan, B., Shafferman, A.: Functional characteristics of the oxyanion hole in human acetylcholinesterase. J. Biol. Chem. 273, 19509–19517 (1998).
97. Atwood, D., Paisley-Jones, C.: Pesticide Industry Sales and Usage.
98. FAOSTAT, http://www.fao.org/faostat/en/#data/RP.
99. Wei, G.-L., Li, D.-Q., Zhuo, M.-N., Liao, Y.-S., Xie, Z.-Y., Guo, T.-L., Li, J.-J., Zhang, S.-Y., Liang, Z.-Q.: Organophosphorus flame retardants and plasticizers: Sources, occurrence, toxicity and human exposure. Environ. Pollut. 196, 29–46 (2015).
100. van der Veen, I., de Boer, J.: Phosphorus flame retardants: Properties, production, environmental occurrence, toxicity and analysis. Chemosphere. 88, 1119–1153 (2012).
101. Johnson, N.H., Larsen, J.C., Meek, E.: Historical Perspective of Chemical Warfare Agents. In: Gupta, R.C. (ed.) Handbook of Toxicology of Chemical Warfare Agents. pp. 7–15. Academic Press (2015).
102. Barnaby, F.: Iran-Iraq War: the use of chemical weapons against the Kurds. Ambio. 17, 407–408 (1988).
103. Pita, R., Domingo, J.: The use of chemical weapons in the Syrian conflict. Toxics. 2, 391–402 (2014).
104. John, H., van der Schans, M.J., Koller, M., Spruit, H.E.T., Worek, F., Thiermann, H., Noort, D.: Fatal sarin poisoning in Syria 2013: forensic verification within an international laboratory network. Forensic Toxicol. 36, 61–71 (2018).
105. Nepovimova, E., Kuca, K.: Chemical warfare agent NOVICHOK - mini-review of available data. Food and Chemical Toxicology. 121, 343–350 (2018).
106. Evolution of the Status of Participation in the Convention, https://www.opcw.org/evolution-status-participation-convention.
107. Syria and the OPCW, https://www.opcw.org/media-centre/featured-topics/syria-and-opcw.
108. OPCW by the Numbers, https://www.opcw.org/media-centre/opcw-numbers.
109. Country Profiles, https://www.nti.org/learn/countries/.
110. Jokanović, M.: Biotransformation of organophosphorus compounds. Toxicology. 166, 139–160 (2001).
111. Freed, V.H., Schmedding, D., Kohnert, R., Haque, R.: Physical Chemical Properties of Several Organophosphates: Some Implication in Environmental and Biological Behavior. Pesticide Biochemistry and Physiology. 10, 203–211 (1979).
112. John, H., Balszuweit, F., Kehe, K., Worek, F., Thiermann, H.: Toxicokinetic Aspects of Nerve Agents and Vesicants. In: Gupta, R.C. (ed.) Handbook of Toxicology of Chemical Warfare Agents. pp. 817–856. Academic Press (2015).

113. Mason, H.J., Sams, C., Stevenson, A.J., Rawbone, R.: Rates of spontaneous reactivation and aging of acetylcholinesterase in human erythrocytes after inhibition by organophosphorus pesticides. Hum Exp Toxicol. 19, 511–516 (2000).
114. Reiner, E.: Spontaneous reactivation of phosphorylated and carbamylated cholinesterases. Bull. World Health Organ. 44, 109–112 (1971).
115. Langenberg, J.P., De Jong, L.P., Otto, M.F., Benschop, H.P.: Spontaneous and oxime-induced reactivation of acetylcholinesterase inhibited by phosphoramidates. Arch. Toxicol. 62, 305–310 (1988).
116. Worek, F., Diepold, C., Eyer, P.: Dimethylphosphoryl-inhibited human cholinesterases: inhibition, reactivation, and aging kinetics. Arch. Toxicol. 73, 7–14 (1999).
117. Worek, F., Thiermann, H., Szinicz, L., Eyer, P.: Kinetic analysis of interactions between human acetylcholinesterase, structurally different organophosphorus compounds and oximes. Biochem. Pharmacol. 68, 2237–2248 (2004).
118. Harris, L.W., Heyl, W.C., Stitcher, D.L., Broomfield, C.A.: Effects of 1,1'-oxydimethylene bis-(4-tert-butylpyridinium chloride) (SAD-128) and decamethonium on reactivation of soman- and sarin-inhibited cholinesterase by oximes. Biochem. Pharmacol. 27, 757–761 (1978).
119. Mew, E.J., Padmanathan, P., Konradsen, F., Eddleston, M., Chang, S.-S., Phillips, M.R., Gunnell, D.: The global burden of fatal self-poisoning with pesticides 2006-15: Systematic review. Journal of Affective Disorders. 219, 93–104 (2017).
120. Dawson, A.H., Eddleston, M., Senarathna, L., Mohamed, F., Gawarammana, I., Bowe, S.J., Manuweera, G., Buckley, N.A.: Acute Human Lethal Toxicity of Agricultural Pesticides: A Prospective Cohort Study. PLoS Med. 7, e1000357–10 (2010).
121. Lin, T.J., Walter, F.G., Hung, D.Z., Tsai, J.L., Hu, S.C., Chang, J.S., Deng, J.-F., Chase, P.B., Denninghoff, K., Chan, H.M.: Epidemiology of organophosphate pesticide poisoning in Taiwan. Clinical Toxicology. 46, 794–801 (2008).
122. Srinivas Rao, C., Venkateswarlu, V., Surender, T., Eddleston, M., Buckley, N.A.: Pesticide poisoning in south India: opportunities for prevention and improved medical management. Trop. Med. Int. Health. 10, 581–588 (2005).
123. Eddleston, M., Eyer, P., Worek, F., Mohamed, F., Senarathna, L., Meyer, von, L., Juszczak, E., Hittarage, A., Azhar, S., Dissanayake, W., Sheriff, M.R., Szinicz, L., Dawson, A.H., Buckley, N.A.: Differences between organophosphorus insecticides in human self-poisoning: a prospective cohort study. The Lancet. 366, 1452–1459 (2005).
124. Pope, C.N.: Organophosphorus pesticides: do they all have the same mechanism of toxicity? J Toxicol Environ Health B Crit Rev. 2, 161–181 (1999).
125. Casida, J.E., Quistad, G.B.: Serine hydrolase targets of organophosphorus toxicants. Chem. Biol. Interact. 157-158, 277–283 (2005).
126. Richardson, R.J., Hein, N.D., Wijeyesakere, S.J., Fink, J.K., Makhaeva, G.F.: Neuropathy target esterase (NTE): overview and future. Chem. Biol. Interact. 203, 238–244 (2013).

127. Quistad, G.B., Sparks, S.E., Segall, Y., Nomura, D.K., Casida, J.E.: Selective inhibitors of fatty acid amide hydrolase relative to neuropathy target esterase and acetylcholinesterase: toxicological implications. Toxicol. Appl. Pharmacol. 179, 57–63 (2002).
128. Quistad, G.B., Liang, S.N., Fisher, K.J., Nomura, D.K., Casida, J.E.: Each lipase has a unique sensitivity profile for organophosphorus inhibitors. Toxicol. Sci. 91, 166–172 (2006).
129. Costa, L.G.: Current issues in organophosphate toxicology. Clin. Chim. Acta. 366, 1–13 (2006).
130. Bardin, P.G., van Eeden, S.F., Joubert, J.R.: Intensive care management of acute organophosphate poisoning. A 7-year experience in the western Cape. S. Afr. Med. J. 72, 593–597 (1987).
131. Hayes, M.M., van der Westhuizen, N.G., Gelfand, M.: Organophosphate poisoning in Rhodesia. A study of the clinical features and management of 105 patients. S. Afr. Med. J. 54, 230–234 (1978).
132. Yurumez, Y., Yavuz, Y., Saglam, H., Durukan, P., Ozkan, S., Akdur, O., Yucel, M.: Electrocardiographic Findings of Acute Organophosphate Poisoning. JEM. 36, 39–42 (2009).
133. Saadeh, A.M., Farsakh, N.A., Al-Ali, M.K.: Cardiac manifestations of acute carbamate and organophosphate poisoning. Heart. 77, 461–464 (1997).
134. Karki, P., Ansari, J.A., Bhandary, S., Koirala, S.: Cardiac and electrocardiographical manifestations of acute organophosphate poisoning. Singapore Med J. 45, 385–389 (2004).
135. Vijayakumar, S., Fareedullah, M., Ashok Kumar, E., Mohan Rao, K.: A Prospective Study on Electrocardiographic Findings of Patients with Organophosphorus Poisoning. Cardiovasc Toxicol. 11, 113–117 (2011).
136. Okumura, T., Takasu, N., Ishimatsu, S., Miyanoki, S., Mitsuhashi, A., Kumada, K., Tanaka, K., Hinohara, S.: Report on 640 victims of the Tokyo subway sarin attack. Ann Emerg Med. 28, 129–135 (1996).
137. Taylor, P.: Anticholinesterase Agents. In: Hardman, J.G., Limbird, L.E., and Gilman, A.G. (eds.) Goodman & Gilman's The Pharmacological Basis of Therapeutics. pp. 175–191. McGraw-Hill (2001).
138. De Candole, C.A., Douglas, W.W., Evans, C.L., Holmes, R., Spencer, K.E., Torrance, R.W., Wilson, K.M.: The failure of respiration in death by anticholinesterase poisoning. Br J Pharmacol Chemother. 8, 466–475 (1953).
139. Rickett, D.L., Glenn, J.F., Beers, E.T.: Central respiratory effects versus neuromuscular actions of nerve agents. Neurotoxicology. 7, 225–236 (1986).
140. Houze, P., Pronzola, L., Kayouka, M., Villa, A., Debray, M., Baud, F.J.: Ventilatory effects of low-dose paraoxon result from central muscarinic effects. Toxicol. Appl. Pharmacol. 233, 186–192 (2008).
141. Bird, S.B., Gaspari, R.J., Dickson, E.W.: Early death due to severe organophosphate poisoning is a centrally mediated process. Acad Emerg Med. 10, 295–298 (2003).
142. Shih, T.M., Koviak, T.A., Capacio, B.R.: Anticonvulsants for poisoning by the organophosphorus compound soman: pharmacological mechanisms. Neurosci Biobehav Rev. 15, 349–362 (1991).

143. McDonough, J.H., Shih, T.M.: Neuropharmacological mechanisms of nerve agent-induced seizure and neuropathology. Neurosci Biobehav Rev. 21, 559–579 (1997).
144. Karalliedde, L.D., Edwards, P., Marrs, T.C.: Variables influencing the toxic response to organophosphates in humans. Food and Chemical Toxicology. 41, 1–13 (2003).
145. Sidell, F.R.: Nerve Agents. In: Sidell, F.R., Takafuji, E.T., and Franz, D.R. (eds.) Medical Aspects of Chemical and Biological Warfare. pp. 129–179. Office of the Surgeon General at TMM Publications, Washington, DC (1997).
146. Holstege, C.P., Dobmeier, S.G.: Nerve Agent Toxicity and Treatment. Curr Treat Options Neurol. 7, 91–98 (2005).
147. Bardin, P.G., van Eeden, S.F.: Organophosphate poisoning: grading the severity and comparing treatment between atropine and glycopyrrolate. Crit. Care Med. 18, 956–960 (1990).
148. Kventsel, I., Berkovitch, M., Reiss, A., Bulkowstein, M., Kozer, E.: Scopolamine Treatment for Severe Extra-Pyramidal Signs Following Organophosphate (Chlorpyrifos) Ingestion. Clinical Toxicology. 43, 877–879 (2009).
149. Hulse, E.J., Davies, J.O.J., Simpson, A.J., Sciuto, A.M., Eddleston, M.: Respiratory complications of organophosphorus nerve agent and insecticide poisoning. Implications for respiratory and critical care. Am. J. Respir. Crit. Care Med. 190, 1342–1354 (2014).
150. Sheridan, R.D., Smith, A.P., Turner, S.R., Tattersall, J.E.H.: Nicotinic antagonists in the treatment of nerve agent intoxication. J R Soc Med. 98, 114–115 (2005).
151. Dhanarisi, J., Shihana, F., Harju, K., Mohamed, F., Verma, V., Shahmy, S., Vanninen, P., Kostiainen, O., Gawarammana, I., Eddleston, M.: A pilot clinical study of the neuromuscular blocker rocuronium to reduce the duration of ventilation after organophosphorus insecticide poisoning. Clinical Toxicology. 43, 1–8 (2019).
152. Marrs, T.C., Rice, P., Vale, J.A.: The role of oximes in the treatment of nerve agent poisoning in civilian casualties. Toxicol. Rev. 25, 297–323 (2006).
153. Rahimi, R., Nikfar, S., Abdollahi, M.: Increased morbidity and mortality in acute human organophosphate-poisoned patients treated by oximes: a meta-analysis of clinical trials. Hum Exp Toxicol. 25, 157–162 (2006).
154. Peter, J.V., Moran, J.L., Graham, P.: Oxime therapy and outcomes in human organophosphate poisoning: An evaluation using meta-analytic techniques. Crit. Care Med. 34, 502–510 (2006).
155. Wani, T., Gurcoo, S., Farooqui, A., Nisa, W., Sofi, K., Syed, S.: Is the World Health Organization-recommended dose of pralidoxime effective in the treatment of organophosphorus poisoning? A randomized, double-blinded and placebo-controlled trial. Saudi J Anaesth. 9, 49–9 (2015).
156. Pawar, K.S., Bhoite, R.R., Pillay, C.P., Chavan, S.C., Malshikare, D.S., Garad, S.G.: Continuous pralidoxime infusion versus repeated bolus injection to treat organophosphorus pesticide poisoning: a randomised controlled trial. The Lancet. 368, 2136–2141 (2006).

157. Wandhammer, M., de Koning, M., van Grol, M., Loiodice, M., Saurel, L., Noort, D., Goeldner, M., Nachon, F.: A step toward the reactivation of aged cholinesterases--crystal structure of ligands binding to aged human butyrylcholinesterase. Chem. Biol. Interact. 203, 19–23 (2013).
158. Zhuang, Q., Young, A., Callam, C.S., McElroy, C.A., Ekici, Ö.D., Yoder, R.J., Hadad, C.M.: Efforts toward treatments against aging of organophosphorus-inhibited acetylcholinesterase. Ann. N. Y. Acad. Sci. 1374, 94–104 (2016).
159. Quinn, D., Topczewski, J., Yasapala, N., Lodge, A.: Why is Aged Acetylcholinesterase So Difficult to Reactivate? Molecules. 22, 1464–6 (2017).
160. Marrs, T.C.: The role of diazepam in the treatment of nerve agent poisoning in a civilian population. Toxicol. Rev. 23, 145–157 (2004).
161. Eddleston, M., Juszczak, E., Buckley, N.A., Senarathna, L., Mohamed, F., Dissanayake, W., Hittarage, A., Azher, S., Jeganathan, K., Jayamanne, S., Sheriff, M.R., Warrell, D.A.: Multiple-dose activated charcoal in acute self-poisoning: a randomised controlled trial. The Lancet. 371, 579–587 (2008).
162. Li, Y., Tse, M.L., Gawarammana, I., Buckley, N., Eddleston, M.: Systematic review of controlled clinical trials of gastric lavage in acute organophosphorus pesticide poisoning. Clinical Toxicology. 47, 179–192 (2009).
163. Schultz, M.K., Wright, L.K.M., de Araujo Furtado, M., Stone, M.F., Moffett, M.C., Kelley, N.R., Bourne, A.R., Lumeh, W.Z., Schultz, C.R., Schwartz, J.E., Lumley, L.A.: Caramiphen edisylate as adjunct to standard therapy attenuates soman-induced seizures and cognitive deficits in rats. Neurotoxicol Teratol. 44, 89–104 (2014).
164. Lallement, G., Clarençon, D., Galonnier, M., Baubichon, D., Burckhart, M.-F., Peoc'h, M.: Acute soman poisoning in primates neither pretreated nor receiving immediate therapy: value of gacyclidine (GK-11) in delayed medical support. Arch. Toxicol. 73, 115–122 (1999).
165. Lallement, G., Baubichon, D., Clarençon, D., Galonnier, M., Peoch, M., Carpentier, P.: Review of the value of gacyclidine (GK-11) as adjuvant medication to conventional treatments of organophosphate poisoning: primate experiments mimicking various Scenarios of Military or Terrorist Attack by Soman. Neurotoxicology. 20, 675–684 (1999).
166. Raveh, L., Eisenkraft, A., Ben Avi Weissman: Caramiphen edisylate: An optimal antidote against organophosphate poisoning. Toxicology. 325, 115–124 (2014).
167. Myhrer, T., Enger, S., Jonassen, M., Aas, P.: Enhanced efficacy of anticonvulsants when combined with levetiracetam in soman-exposed rats. Neurotoxicology. 32, 923–930 (2011).
168. Myhrer, T., Enger, S., Aas, P.: Pharmacological therapies against soman-induced seizures in rats 30 min following onset and anticonvulsant impact. Eur. J. Pharmacol. 548, 83–89 (2006).
169. Krishnan, J.K.S., Figueiredo, T.H., Moffett, J.R., Arun, P., Appu, A.P., Puthillathu, N., Braga, M.F., Flagg, T., Namboodiri, A.M.: Brief isoflurane administration as a post-exposure treatment for organophosphate poisoning. Neurotoxicology. 63, 84–89 (2017).

170. Shemesh, I., Bourvin, A., Gold, D., Kutscherowsky, M.: Chlorpyrifos poisoning treated with ipratropium and dantrolene: a case report. J. Toxicol. Clin. Toxicol. 26, 495–498 (1988).
171. Kaur, S., Singh, S., Chahal, K.S., Prakash, A.: Potential pharmacological strategies for the improved treatment of organophosphate-induced neurotoxicity. Can. J. Physiol. Pharmacol. 92, 893–911 (2014).
172. de Araujo Furtado, M., Rossetti, F., Chanda, S., Yourick, D.: Exposure to nerve agents: From status epilepticus to neuroinflammation, brain damage, neurogenesis and epilepsy. Neurotoxicology. 33, 1476–1490 (2012).
173. Myhrer, T., Enger, S., Mariussen, E., Aas, P.: Two medical therapies very effective shortly after high levels of soman poisoning in rats, but only one with universal utility. Toxicology. 314, 221–228 (2013).
174. Myhrer, T., Mariussen, E., Enger, S., Aas, P.: Supralethal poisoning by any of the classical nerve agents is effectively counteracted by procyclidine regimens in rats. Neurotoxicology. 50, 142–148 (2015).
175. Kadar, T., Cohen, G., Sahar, R., Alkalai, D., SHAPIRA, S.: Long-term study of brain lesions following soman, in comparison to DFP and metrazol poisoning. Hum Exp Toxicol. 11, 517–523 (1992).
176. Myhrer, T., Enger, S., Aas, P.: Determination of anti-convulsant and life-preserving capacities of three types of auto-injector therapies against soman intoxication in rats. Drug Test Anal. 5, 693–701 (2013).
177. McDonough, J.H., Smith, R.F., Smith, C.D.: Behavioral correlates of soman-induced neuropathology: deficits in DRL acquisition. Neurobehav Toxicol Teratol. 8, 179–187 (1986).
178. Hymowitz, N., Ploshnick, A., Laemle, L., Brezenoff, H.: Effects of repeated administration of soman on schedule-controlled behavior and brain in the rat. Neurotoxicol Teratol. 12, 47–56 (1990).
179. Raffaele, K., Hughey, D., Wenk, G., Olton, D., Modrow, H., McDonough, J.: Long-term behavioral changes in rats following organophosphonate exposure. Pharmacol. Biochem. Behav. 27, 407–412 (1987).
180. Choi, E.-K., Park, D., Yon, J.-M., Hur, G.-H., Ha, Y.-C., Che, J.-H., Kim, J., Shin, S., Jang, J.Y., Hwang, S.-Y., Seong, Y.-H., Kim, D.J., Kim, J.-C., Kim, Y.-B.: Protection by sustained release of physostigmine and procyclidine of soman poisoning in rats. Eur. J. Pharmacol. 505, 83–91 (2004).
181. Myhrer, T., Andersen, J.M., Nguyen, N.H.T., Aas, P.: Soman-induced convulsions in rats terminated with pharmacological agents after 45 min: neuropathology and cognitive performance. Neurotoxicology. 26, 39–48 (2005).
182. Murata, K., Araki, S., Yokoyama, K., Okumura, T., Ishimatsu, S., Takasu, N., White, R.F.: Asymptomatic sequelae to acute sarin poisoning in the central and autonomic nervous system 6 months after the Tokyo subway attack. J. Neurol. 244, 601–606 (1997).
183. Yokoyama, K., Araki, S., Murata, K., Nishikitani, M., Okumura, T., Ishimatsu, S., Takasu, N.: Chronic neurobehavioral and central and autonomic nervous system effects of Tokyo subway sarin poisoning. J. Physiol. Paris. 92, 317–323 (1998).

184. Okumura, T., Hisaoka, T., Naito, T., Isonuma, H., Okumura, S., Miura, K., Maekawa, H., Ishimatsu, S., Takasu, N., Suzuki, K.: Acute and chronic effects of sarin exposure from the Tokyo subway incident. Environ. Toxicol. Pharmacol. 19, 447–450 (2005).
185. Miyaki, K., Nishiwaki, Y., Maekawa, K., Ogawa, Y., Asukai, N., Yoshimura, K., Etoh, N., Matsumoto, Y., Kikuchi, Y., Kumagai, N., Omae, K.: Effects of sarin on the nervous system of subway workers seven years after the Tokyo subway sarin attack. J Occup Health. 47, 299–304 (2005).
186. Fenske, R.A., Farahat, F.M., Galvin, K., Fenske, E.K., Olson, J.R.: Contributions of inhalation and dermal exposure to chlorpyrifos dose in Egyptian cotton field workers. International Journal of Occupational and Environmental Health. 18, 198–209 (2013).
187. Mancini, F., Van Bruggen, A.H.C., Jiggins, J.L.S., Ambatipudi, A.C., Murphy, H.: Acute Pesticide Poisoning among Female and Male Cotton Growers in India. International Journal of Occupational and Environmental Health. 11, 221–232 (2005).
188. Singleton, S.T., Lein, P.J., Dadson, O.A., McGarrigle, B.P., Farahat, F.M., Farahat, T., Bonner, M.R., Fenske, R.A., Galvin, K., Lasarev, M.R., Anger, W.K., Rohlman, D.S., Olson, J.R.: Longitudinal assessment of occupational exposures to the organophosphorous insecticides chlorpyrifos and profenofos in Egyptian cotton field workers. International Journal of Hygiene and Environmental Health. 218, 203–211 (2015).
189. Abdel Rasoul, G.M., Abou Salem, M.E., Mechael, A.A., Hendy, O.M., Rohlman, D.S., Ismail, A.A.: Effects of occupational pesticide exposure on children applying pesticides. Neurotoxicology. 29, 833–838 (2008).
190. Farahat, T.M.: Neurobehavioural effects among workers occupationally exposed to organophosphorous pesticides. Occupational and Environmental Medicine. 60, 279–286 (2003).
191. Ismail, A.A., Wang, K., Olson, J.R., Bonner, M.R., Hendy, O., Abdel Rasoul, G., Rohlman, D.S.: The impact of repeated organophosphorus pesticide exposure on biomarkers and neurobehavioral outcomes among adolescent pesticide applicators. J. Toxicol. Environ. Health Part A. 80, 542–555 (2017).
192. Roldán-Tapia, L., Parrón, T., Sánchez-Santed, F.: Neuropsychological effects of long-term exposure to organophosphate pesticides. Neurotoxicol Teratol. 27, 259–266 (2005).
193. Rohlman, D.S., Lasarev, M., Anger, W.K., Scherer, J., Stupfel, J., McCauley, L.: Neurobehavioral performance of adult and adolescent agricultural workers. Neurotoxicology. 28, 374–380 (2007).
194. Koster, R.: Synergisms and antagonisms between physostigmine and di-isopropyl fluorophosphate in cats. J. Pharmacol. Exp. Ther. 88, 39–46 (1946).
195. Eckert, S., Eyer, P., Mückter, H., Worek, F.: Kinetic analysis of the protection afforded by reversible inhibitors against irreversible inhibition of acetylcholinesterase by highly toxic organophosphorus compounds. Biochem. Pharmacol. 72, 344–357 (2006).

196. Gordon, J.J., Leadbeater, L., Maidment, M.P.: The protection of animals against organophosphate poisoning by pretreatment with a carbamate. Toxicol. Appl. Pharmacol. 43, 207–216 (1978).
197. Leadbeater, L., Inns, R.H., Rylands, J.M.: Treatment of poisoning by soman. Fundam. Appl. Toxicol. 5, S225–31 (1985).
198. Kassa, J., Vachek, J.: A comparison of the efficacy of pyridostigmine alone and the combination of pyridostigmine with anticholinergic drugs as pharmacological pretreatment of tabun-poisoned rats and mice. Toxicology. 177, 179–185 (2002).
199. Koplovitz, I., Harris, L.W., Anderson, D.R., Lennox, W.J., Stewart, J.R.: Reduction by Pyridostigmine Pretreatment of the Efficacy of Atropine and 2-Pam Treatment of Sarin and Vx Poisoning in Rodents. Fundam. Appl. Toxicol. 18, 102–106 (1992).
200. Worek, F., Szinicz, L.: Cardiorespiratory function in nerve agent poisoned and oxime + atropine treated guinea-pigs: effect of pyridostigmine pretreatment. Arch. Toxicol. 69, 322–329 (1995).
201. Aquilonius, S.M., Eckernäs, S.A., Hartvig, P., Lindström, B., Osterman, P.O.: Pharmacokinetics and oral bioavailability of pyridostigmine in man. Eur. J. Clin. Pharmacol. 18, 423–428 (1980).
202. Breyer-Pfaff, U., Maier, U., Brinkmann, A.M., Schumm, F.: Pyridostigmine kinetics in healthy subjects and patients with myasthenia gravis. Clin. Pharmacol. Ther. 37, 495–501 (1985).
203. Madsen, J.M., Hurst, C.G., MacIntosh, R., Romano, J.A., Jr: Clinical Considerations in the Use of Pyridostigmine Bromide as Pretreatment for Nerve-agent Exposure. Aberdeen Proving Ground (2003).
204. Keeler, J.R., Hurst, C.G., Dunn, M.A.: Pyridostigmine used as a nerve agent pretreatment under wartime conditions. JAMA. 266, 693–695 (1991).
205. Golomb, B.A.: Acetylcholinesterase inhibitors and Gulf War illnesses. Proc. Natl. Acad. Sci. U.S.A. 105, 4295–4300 (2008).
206. Kerr, K.J.: Gulf War illness: an overview of events, most prevalent health outcomes, exposures, and clues as to pathogenesis. Rev Environ Health. 30, 273–286 (2015).
207. Tuovinen, K., Kaliste-Korhonen, E., Raushel, F.M., Hänninen, O.: Success of pyridostigmine, physostigmine, eptastigmine and phosphotriesterase treatments in acute sarin intoxication. Toxicology. 134, 169–178 (1999).
208. Harris, L., Stitcher, D.: Protection against diisopropylfluorophosphate intoxication by pyridostigmine and physostigmine in combination with atropine and mecamylamine. Naunyn Schmiedebergs Arch. Pharmacol. 327, 64–69 (1984).
209. Walter, K., Muller, M., Barkworth, M.F., Nieciecki, A.V., Stanislaus, F.: Pharmacokinetics of Physostigmine in Man Following a Single Application of a Transdermal System. Br J Clin Pharmacol. 39, 59–63 (1995).
210. Aracava, Y., Pereira, E.F.R., Akkerman, M., Adler, M., Albuquerque, E.X.: Effectiveness of Donepezil, Rivastigmine, and ( )Huperzine A in Counteracting the Acute Toxicity of Organophosphorus Nerve Agents: Comparison with Galantamine. J. Pharmacol. Exp. Ther. 331, 1014–1024 (2009).

211. Lavon, O., Eisenkraft, A., Blanca, M., Raveh, L., Ramaty, E., Krivoy, A., Atsmon, J., Grauer, E., Brandeis, R.: Is rivastigmine safe as pretreatment against nerve agents poisoning? A pharmacological, physiological and cognitive assessment in healthy young adult volunteers. Neurotoxicology. 49, 36–44 (2015).
212. Albuquerque, E.X., Pereira, E.F.R., Aracava, Y., Fawcett, W.P., Oliveira, M., Randall, W.R., Hamilton, T.A., Kan, R.K., Romano, J.A., Adler, M.: Effective countermeasure against poisoning by organophosphorus insecticides and nerve agents. Proc. Natl. Acad. Sci. U.S.A. 103, 13220–13225 (2006).
213. Gullapalli, R.P., Aracava, Y., Zhuo, J., Neto, E.H., Wang, J., Makris, G., Merchenthaler, I., Pereira, E.F.R., Albuquerque, E.X.: Magnetic resonance imaging reveals that galantamine prevents structural brain damage induced by an acute exposure of guinea pigs to soman. Neurotoxicology. 31, 67–76 (2010).
214. Plotnik, R., Mollenauer, S., Snyder, E.: Fear reduction in the rat following central cholinergic blockade. J Comp Physiol Psychol. 86, 1074–1082 (1974).
215. Clark, M.G., Sun, W., Myers, T.M., Bansal, R., Doctor, B.P., Saxena, A.: Effects of physostigmine and human butyrylcholinesterase on acoustic startle reflex and prepulse inhibition in C57BL/6J mice. Pharmacol. Biochem. Behav. 81, 497–505 (2005).
216. Myhrer, T., Enger, S., Aas, P.: Behavioral side effects in rats treated with acetylcholinesterase inhibitors suggested used as prophylactics against nerve agents. Pharmacol. Biochem. Behav. 95, 338–343 (2010).
217. Wolfe, A.D., Rush, R.S., Doctor, B.P., Koplovitz, I., Jones, D.: Acetylcholinesterase prophylaxis against organophosphate toxicity. Fundam. Appl. Toxicol. 9, 266–270 (1987).
218. Broomfield, C.A., Maxwell, D.M., Solana, R.P., Castro, C.A., Finger, A.V., Lenz, D.E.: Protection by butyrylcholinesterase against organophosphorus poisoning in nonhuman primates. J. Pharmacol. Exp. Ther. 259, 633–638 (1991).
219. Ashani, Y., Rothschild, N., Segall, Y., Levanon, D., Raveh, L.: Prophylaxis against organophsphate poisoning by an enzyme hydrolysing organophosphorus compounds in mice. Life Sci. 49, 367–374 (1991).
220. Masson, P.: Catalytic Bioscavengers. In: Gupta, R.C. (ed.) Handbook of Toxicology of Chemical Warfare Agents. pp. 1107–1123. Academic Press (2015).
221. Ashani, Y., SHAPIRA, S., LEVY, D., Wolfe, A.D., Doctor, B.P., Raveh, L.: Butyrylcholinesterase and Acetylcholinesterase Prophylaxis Against Soman Poisoning in Mice. Biochem. Pharmacol. 41, 37–41 (1991).
222. Masson, P., Nachon, F., Broomfield, C.A., Lenz, D.E., Verdier, L., Schopfer, L.M., Lockridge, O.: A collaborative endeavor to design cholinesterase-based catalytic scavengers against toxic organophosphorus esters. Chem. Biol. Interact. 175, 273–280 (2008).
223. Cohen, O., Kronman, C., Raveh, L., Mazor, O., Ordentlich, A., Shafferman, A.: Comparison of polyethylene glycol-conjugated recombinant human acetylcholinesterase and serum human butyrylcholinesterase as bioscavengers of organophosphate compounds. Mol Pharmacol. 70, 1121–1131 (2006).

224. Kronman, C., Cohen, O., Raveh, L., Mazor, O., Ordentlich, A., Shafferman, A.: Polyethylene-glycol conjugated recombinant human acetylcholinesterase serves as an efficacious bioscavenger against soman intoxication. Toxicology. 233, 40–46 (2007).
225. Maxwell, D.M., Castro, C.A., Denise, M., Gentry, M.K.: Protection of rhesus monkeys against soman and prevention of performance decrement by pretreatment with acetylcholinesterase. Toxicology and applied …. 115, 44–49 (1992).
226. Hatfield, M.J., Umans, R.A., Hyatt, J.L., Edwards, C.C., Wierdl, M., Tsurkan, L., Taylor, M.R., Potter, P.M.: Carboxylesterases: General detoxifying enzymes. Chem. Biol. Interact. 259, 327–331 (2016).
227. Maxwell, D.M., Brecht, K.M., O'Neill, B.L.: The effect of carboxylesterase inhibition on interspecies differences in soman toxicity. Toxicol. Lett. 39, 35–42 (1987).
228. Ellin, R.I.: Anomalies in theories and therapy of intoxication by potent organophosphorus anticholinesterase compounds. Pharmac. Ther. 13, 457–466 (1982).
229. Maxwell, D.M., Brecht, K.M.: Carboxylesterase: specificity and spontaneous reactivation of an endogenous scavenger for organophosphorus compounds. J Appl Toxicol. 21, S103–S107 (2002).
230. Lenz, D.E., Maxwell, D.M., Koplovitz, I., Clark, C.R., Capacio, B.R., Cerasoli, D.M., Federko, J.M., Luo, C., Saxena, A., Doctor, B.P., Olson, C.: Protection against soman or VX poisoning by human butyrylcholinesterase in guinea pigs and cynomolgus monkeys. Chem. Biol. Interact. 157-158, 205–210 (2005).
231. Saxena, A., Sun, W., Fedorko, J.M., Koplovitz, I., Doctor, B.P.: Prophylaxis with human serum butyrylcholinesterase protects guinea pigs exposed to multiple lethal doses of soman or VX. Biochem. Pharmacol. 81, 164–169 (2011).
232. Allon, N., Raveh, L., Gilat, E., Cohen, E., Grunwald, J., Ashani, Y.: Prophylaxis against soman inhalation toxicity in guinea pigs by pretreatment alone with human serum butyrylcholinesterase. Toxicol. Sci. 43, 121–128 (1998).
233. Lenz, D.E., Clarkson, E.D., Schulz, S.M., Cerasoli, D.M.: Butyrylcholinesterase as a therapeutic drug for protection against percutaneous VX. Chem. Biol. Interact. 187, 249–252 (2010).
234. Saxena, A., Sun, W., Dabisch, P.A., Hulet, S.W., Hastings, N.B., Jakubowski, E.M., Mioduszewski, R.J., Doctor, B.P.: Efficacy of human serum butyrylcholinesterase against sarin vapor. Chem. Biol. Interact. 175, 267–272 (2008).
235. Raveh, L., Grauer, E., Grunwald, J., Cohen, E., Ashani, Y.: The stoichiometry of protection against soman and VX toxicity in monkeys pretreated with human butyrylcholinesterase. Toxicol. Appl. Pharmacol. 145, 43–53 (1997).
236. Genovese, R.F., Doctor, B.P.: Behavioral and pharmacological assessment of butyrylcholinesterase in rats. Pharmacol. Biochem. Behav. 51, 647–654 (1995).
237. Myers, T.M., Sun, W., Naik, R.S., Clark, M.G., Doctor, B.P., Saxena, A.: Characterization of human serum butyrylcholinesterase in rhesus monkeys: behavioral and physiological effects. Neurotoxicol Teratol. 34, 323–330 (2012).

238. Genovese, R.F., Sun, W., Johnson, C.C., diTargiani, R.C., Doctor, B.P., Saxena, A.: Safety of administration of human butyrylcholinesterase and its conjugates with soman or VX in rats. Basic Clin. Pharmacol. Toxicol. 106, 428–434 (2010).
239. Järv, J.: Stereochemical aspects of cholinesterase catalysis. Bioorganic Chemistry. 12, 259–278 (1984).
240. Millard, C.B., Lockridge, O., Broomfield, C.A.: Design and expression of organophosphorus acid anhydride hydrolase activity in human butyrylcholinesterase. Biochemistry. 34, 15925–15933 (1995).
241. Geyer, B.C., Kannan, L., Garnaud, P.-E., Broomfield, C.A., Cadieux, C.L., Cherni, I., Hodgins, S.M., Kasten, S.A., Kelley, K., Kilbourne, J., Oliver, Z.P., Otto, T.C., Puffenberger, I., Reeves, T.E., Robbins, N., Woods, R.R., Soreq, H., Lenz, D.E., Cerasoli, D.M., Mor, T.S.: Plant-derived human butyrylcholinesterase, but not an organophosphorous-compound hydrolyzing variant thereof, protects rodents against nerve agents. Proc. Natl. Acad. Sci. U.S.A. 107, 20251–20256 (2010).
242. Lushchekina, S.V., Schopfer, L.M., Grigorenko, B.L., Nemukhin, A.V., Varfolomeev, S.D., Lockridge, O., Masson, P.: Optimization of Cholinesterase-Based Catalytic Bioscavengers Against Organophosphorus Agents. Front Pharmacol. 9, 211 (2018).
243. Mackness, M., Mackness, B.: Human paraoxonase-1 (PON1): Gene structure and expression, promiscuous activities and multiple physiological roles. Gene. 567, 12–21 (2015).
244. Masson, P., Josse, D., Lockridge, O., Viguie, N., Taupin, C., Buhler, C.: Enzymes hydrolyzing organophosphates as potential catalytic scavengers against organophosphate poisoning. J. Physiol. Paris. 92, 357–362 (1998).
245. Valiyaveettil, M., Alamneh, Y., Biggemann, L., Soojhawon, I., Doctor, B.P., Nambiar, M.P.: Efficient hydrolysis of the chemical warfare nerve agent tabun by recombinant and purified human and rabbit serum paraoxonase 1. Biochem. Biophys. Res. Commun. 403, 97–102 (2010).
246. Rochu, D., Chabriere, E., Masson, P.: Human paraoxonase: A promising approach for pre-treatment and therapy of organophosphorus poisoning. Toxicology. 233, 47–59 (2007).
247. Hodgins, S.M., Kasten, S.A., Harrison, J., Otto, T.C., Oliver, Z.P., Rezk, P., Reeves, T.E., Chilukuri, N., Cerasoli, D.M.: Assessing protection against OP pesticides and nerve agents provided by wild-type HuPON1 purified from Trichoplusia ni larvae or induced via adenoviral infection. Chem. Biol. Interact. 203, 177–180 (2013).
248. Valiyaveettil, M., Alamneh, Y., Rezk, P., Biggemann, L., Perkins, M.W., Sciuto, A.M., Doctor, B.P., Nambiar, M.P.: Protective efficacy of catalytic bioscavenger, paraoxonase 1 against sarin and soman exposure in guinea pigs. Biochem. Pharmacol. 81, 800–809 (2011).
249. Amitai, G., Gaidukov, L., Adani, R., Yishay, S., Yacov, G., Kushnir, M., Teitlboim, S., Lindenbaum, M., Bel, P., Khersonsky, O., Tawfik, D.S., Meshulam, H.: Enhanced stereoselective hydrolysis of toxic organophosphates by directly evolved variants of mammalian serum paraoxonase. FEBS J. 273, 1906–1919 (2006).

250. Goldsmith, M., Ashani, Y., Simo, Y., Ben-David, M., Leader, H., Silman, I., Sussman, J.L., Tawfik, D.S.: Evolved stereoselective hydrolases for broad-spectrum G-type nerve agent detoxification. Chem. Biol. 19, 456–466 (2012).
251. Worek, F., Seeger, T., Goldsmith, M., Ashani, Y., Leader, H., Sussman, J.S., Tawfik, D., Thiermann, H., Wille, T.: Efficacy of the rePON1 mutant IIG1 to prevent cyclosarin toxicity in vivo and to detoxify structurally different nerve agents in vitro. Arch. Toxicol. 88, 1257–1266 (2014).
252. Masson, P., Nachon, F.: Cholinesterase reactivators and bioscavengers for pre- and post-exposure treatments of organophosphorus poisoning. Journal of Neurochemistry. 142 Suppl 2, 26–40 (2017).
253. Nachon, F., Brazzolotto, X., Trovaslet, M., Masson, P.: Progress in the development of enzyme-based nerve agent bioscavengers. Chem. Biol. Interact. 206, 536–544 (2013).
254. diTargiani, R.C., Chandrasekaran, L., Belinskaya, T., Saxena, A.: In search of a catalytic bioscavenger for the prophylaxis of nerve agent toxicity. Chem. Biol. Interact. 187, 349–354 (2010).
255. Rezk, P.E., Zdenka, P., Sabnekar, P., Kajih, T., Mata, D.G., Wrobel, C., Cerasoli, D.M., Chilukuri, N.: An in vitro and in vivo evaluation of the efficacy of recombinant human liver prolidase as a catalytic bioscavenger of chemical warfare nerve agents. 38, 37–43 (2015).
256. Wales, M.E., Reeves, T.E.: Organophosphorus hydrolase as an in vivo catalytic nerve agent bioscavenger. Drug Test Anal. 4, 271–281 (2012).
257. Hoskin, F.C.G., Walker, J.E., Dettbarn, W.-D., Wild, J.R.: Hydrolysis of tetriso by an enzyme derived from Pseudomonas diminuta as a model for the detoxication of O-ethyl S-(2-diisopropylaminoethyl) methylphosphonothiolate (VX). Biochem. Pharmacol. 49, 711–715 (1995).
258. Dumas, D.P., Durst, H.D., Landis, W.G., Raushel, F.M., Wild, J.R.: Inactivation of organophosphorus nerve agents by the phosphotriesterase from Pseudomonas diminuta. Arch. Biochem. Biophys. 277, 155–159 (1990).
259. Rastogi, V.K., DeFrank, J.J., Cheng, T.-C., Wild, J.R.: Enzymatic hydrolysis of Russian-VX by organophosphorus hydrolase. Biochem. Biophys. Res. Commun. 241, 294–296 (1997).
260. Raveh, L., Segall, Y., LEADER, H., Rothschild, N., Levanon, D., HENIS, Y., Ashani, Y.: Protection Against Tabun Toxicity in Mice by Prophylaxis with an Enzyme Hydrolyzing Organophosphate Esters. Biochem. Pharmacol. 44, 397–400 (1992).
261. Kuo, J.M., Chae, M.Y., Raushel, F.M.: Perturbations to the active site of phosphotriesterase. Biochemistry. 36, 1982–1988 (1997).
262. Tsai, P.-C., Fox, N., Bigley, A.N., Harvey, S.P., Barondeau, D.P., Raushel, F.M.: Enzymes for the homeland defense: optimizing phosphotriesterase for the hydrolysis of organophosphate nerve agents. Biochemistry. 51, 6463–6475 (2012).
263. Cherny, I., Greisen, P.J., Ashani, Y., Khare, S.D., Oberdorfer, G., Leader, H., Baker, D., Tawfik, D.S.: Engineering V-Type Nerve Agents Detoxifying Enzymes Using Computationally Focused Libraries. ACS Chem. Biol. 8, 2394–2403 (2013).

264. Worek, F., Seeger, T., Reiter, G., Goldsmith, M., Ashani, Y., Leader, H., Sussman, J.L., Aggarwal, N., Thiermann, H., Tawfik, D.S.: Post-exposure treatment of VX poisoned guinea pigs with the engineered phosphotriesterase mutant C23: A proof-of-concept study. 1–10 (2014).
265. Hiblot, J., Gotthard, G., Chabriere, E., Elias, M.: Characterisation of the organophosphate hydrolase catalytic activity of SsoPox. Sci. Rep. 2, 779 (2012).
266. Jackson, C.J., Carville, A., Ward, J., Mansfield, K., Ollis, D.L., Khurana, T., Bird, S.B.: Use of OpdA, an organophosphorus (OP) hydrolase, prevents lethality in an African green monkey model of acute OP poisoning. Toxicology. 317, 1–5 (2014).
267. Gotthard, G., Hiblot, J., Gonzalez, D., Elias, M., Chabriere, E.: Structural and enzymatic characterization of the phosphotriesterase OPHC2 from Pseudomonas pseudoalcaligenes. PLoS ONE. 8, e77995 (2013).
268. Ashani, Y., Pistinner, S.: Estimation of the upper limit of human butyrylcholinesterase dose required for protection against organophosphates toxicity: a mathematically based toxicokinetic model. Toxicol. Sci. 77, 358–367 (2004).
269. Ilyushin, D.G., Haertley, O.M., Bobik, T.V., Shamborant, O.G., Surina, E.A., Knorre, V.D., Masson, P., Smirnov, I.V., Gabibov, A.G., Ponomarenko, N.A.: Recombinant human butyrylcholinesterase as a new-age bioscavenger drug: development of the expression system. Acta Naturae. 5, 73–84 (2013).
270. Brazzolotto, X., Wandhammer, M., Ronco, C., Trovaslet, M., Jean, L., Lockridge, O., Renard, P.-Y., Nachon, F.: Human butyrylcholinesterase produced in insect cells: huprine-based affinity purification and crystal structure. FEBS J. 279, 2905–2916 (2012).
271. Huang, Y.-J., Huang, Y., Baldassarre, H., Wang, B., Lazaris, A., Leduc, M., Bilodeau, A.S., Bellemare, A., Côté, M., Herskovits, P., Touati, M., Turcotte, C., Valeanu, L., Lemée, N., Wilgus, H., Bégin, I., Bhatia, B., Rao, K., Neveu, N., Brochu, E., Pierson, J., Hockley, D.K., Cerasoli, D.M., Lenz, D.E., Karatzas, C.N., Langermann, S.: Recombinant human butyrylcholinesterase from milk of transgenic animals to protect against organophosphate poisoning. Proc. Natl. Acad. Sci. U.S.A. 104, 13603–13608 (2007).
272. Chilukuri, N., Parikh, K., Sun, W., Naik, R., Tipparaju, P., Doctor, B.P., Saxena, A.: Polyethylene glycosylation prolongs the circulatory stability of recombinant human butyrylcholinesterase. Chem. Biol. Interact. 157-158, 115–121 (2005).
273. Duysen, E.G., Bartels, C.F., Lockridge, O.: Wild-type and A328W mutant human butyrylcholinesterase tetramers expressed in Chinese hamster ovary cells have a 16-hour half-life in the circulation and protect mice from cocaine toxicity. J. Pharmacol. Exp. Ther. 302, 751–758 (2002).
274. Caliceti, P., Veronese, F.M.: Pharmacokinetic and biodistribution properties of poly (ethylene glycol)–protein conjugates. Adv. Drug Deliv. Rev. (2003).
275. Sahoo, K., Koralege, R.S.H., Flynn, N., Koteeswaran, S., Clark, P., Hartson, S., Liu, J., Ramsey, J.D., Pope, C., Ranjan, A.: Nanoparticle Attachment to Erythrocyte Via the Glycophorin A Targeted ERY1 Ligand Enhances Binding without Impacting Cellular Function. Pharm. Res. 33, 1191–1203 (2016).

276. Doctor, B.P., Raveh, L., Wolfe, A.D., Maxwell, D.M., Ashani, Y.: Enzymes as pretreatment drugs for organophosphate toxicity. Neurosci Biobehav Rev. 15, 123–128 (1991).
277. Novikov, B.N., Grimsley, J.K., Kern, R.J., Wild, J.R., Wales, M.E.: Improved pharmacokinetics and immunogenicity profile of organophosphorus hydrolase by chemical modification with polyethylene glycol. Journal of Controlled Release. 146, 318–325 (2010).
278. Heiss, D.R., Zehnder, D.W., Jett, D.A., Platoff, G.E., Yeung, D.T., Brewer, B.N.: Synthesis and Storage Stability of Diisopropylfluorophosphate. J. Chem. 2016, 1–5 (2016).
279. Flynn, N., Topal, Ç.Ö., Hikkaduwa Koralege, R.S., Hartson, S., Ranjan, A., Liu, J., Pope, C., Ramsey, J.D.: Effect of cationic grafted copolymer structure on the encapsulation of bovine serum albumin. Mater. Sci. Eng. C Mater. Biol. Appl. 62, 524–531 (2016).
280. Ellman, G.L., Courtney, K.D., Andres, V., Featherstone, R.M.: A New and Rapid Colorimetric Determination of Acetylcholinesterase Activity. Biochem. Pharmacol. 7, 88–95 (1961).
281. Pope, C., Hester, K., Sultatos, L.: In Vitro Evaluation of Serine Hydrolase Inhibitors. In: Methods in Pharmacology and Toxicology. pp. 1–31. Humana Press, Totowa, NJ (2018).
282. Wolf, D., Ebner, E., Hinze, H.: Inactivation, stabilization and some properties of ATP: glutamine synthetase adenylyltransferase from Escherichia coli B. Eur. J. Biochem. 25, 239–244 (1972).
283. Finn, T.E., Nunez, A.C., Sunde, M., Easterbrook-Smith, S.B.: Serum albumin prevents protein aggregation and amyloid formation and retains chaperone-like activity in the presence of physiological ligands. J. Biol. Chem. 287, 21530–21540 (2012).
284. Richardson, R.J., Worden, R.M., Makhaeva, G.F.: Biomarkers and biosensors of delayed neuropathic agents. In: Gupta, R.C. (ed.) Handbook of Toxicology of Chemical Warfare Agents. pp. 859–876. Academic Press, Amsterdam (2009).
285. Wei, Y., Peng, A.-Y., Huang, J.: Inhibition of porcine liver carboxylesterase by phosphorylated flavonoids. Chem. Biol. Interact. 204, 75–79 (2013).
286. Gall, M.G., Nobili, A., Pavlidis, I.V., Bornscheuer, U.T.: Improved thermostability of a Bacillus subtilis esterase by domain exchange. Appl. Microbiol. Biotechnol. 98, 1719–1726 (2013).
287. Karnovsky, M.J., Roots, L.: A “Direct-Coloring” Thiocholine Method for Cholinesterases. J. Histochem. Cytochem. 12, 219–221 (1964).
288. Chang, B.S., Mahoney, R.R.: Enzyme thermostabilization by bovine serum albumin and other proteins: evidence for hydrophobic interactions. Biotechnology and Applied Biochemistry. 22 (Pt 2), 203–214 (1995).
289. Sweeney, P.J., Walker, J.M.: Pronase (EC 3.4.24.4). In: Burrell, M.M. (ed.) Methods in Molecular Biology. pp. 271–276. Humana Press, Totowa (1993).
290. Hester, K., Liu, J., Flynn, N., Sultatos, L.G., Geng, L., Brimijoin, S., Ramsey, J.D., Hartson, S., Ranjan, A., Pope, C.: Polyionic complexes of butyrylcholinesterase and poly-l-lysine-g-poly(ethylene glycol): Comparative

kinetics of catalysis and inhibition and in vitro inactivation by proteases and heat. Chem. Biol. Interact. 275, 86–94 (2017).
291. Alconcel, S., Baas, A.S., Maynard, H.D.: FDA-approved poly (ethylene glycol)–protein conjugate drugs. Polymer Chemistry. (2011).
292. Chilukuri, N., Sun, W., Naik, R.S., Parikh, K., Tang, L., Doctor, B.P., Saxena, A.: Effect of polyethylene glycol modification on the circulatory stability and immunogenicity of recombinant human butyrylcholinesterase. Chem. Biol. Interact. 175, 255–260 (2008).
293. Melzer, M., Heidenreich, A., Dorandeu, F., Gäb, J., Kehe, K., Thiermann, H., Letzel, T., Blum, M.-M.: In vitro and in vivo efficacy of PEGylated diisopropyl fluorophosphatase (DFPase). Drug Test Anal. 4, 262–270 (2011).
294. Kotzia, G.A., Lappa, K., Labrou, N.E.: Tailoring structure–function properties of L-asparaginase: engineering resistance to trypsin cleavage. Biochem. J. 404, 337–343 (2007).
295. Masson, P.: Time-dependent kinetic complexities in cholinesterase-catalyzed reactions. Biochemistry Mosc. 77, 1147–1161 (2012).
296. Stojan, J.: The significance of low substrate concentration measurements for mechanistic interpretation in cholinesterases. Chem. Biol. Interact. 203, 44–50 (2013).
297. EPA, U.S.: Estimation Programs Interface Suite for Microsoft Windows.
298. Raveh, L., Grunwald, J., Marcus, D., Papier, Y.: Human butyrylcholinesterase as a general prophylactic antidote for nerve agent toxicity: in vitro and in vivo quantitative characterization. Biochemical …. 45, 2465–2474 (1993).
299. Arrhenius, S.: Über die Dissociationswärme und den Einfluss der Temperatur auf den Dissociationsgrad der Elektrolyte. Z. Phys. Chem. 4, 96–116 (1889).
300. Tsutsumi, Y., Kihira, T., Tsunoda, S., Kamada, H., Nakagawa, S., Kaneda, Y., Kanamori, T., Mayumi, T.: Molecular design of hybrid tumor necrosis factor-alpha III: polyethylene glycol-modified tumor necrosis factor-alpha has markedly enhanced antitumor potency due to longer plasma half-life and higher tumor accumulation. J. Pharmacol. Exp. Ther. 278, 1006–1011 (1996).
301. Veronese, F.M., Caliceti, P., Schiavon, O.: Branched and linear poly(ethylene glycol): Influence of the polymer structure on enzymological, pharmacokinetic, and immunological properties of protein conjugates. Journal of Bioactive and Compatible Polymers. 12, 196–207 (1997).
302. Kaminskas, L.M., Boyd, B.J., Karellas, P., Krippner, G.Y., Lessene, R., Kelly, B., Porter, C.J.H.: The impact of molecular weight and PEG chain length on the systemic pharmacokinetics of PEGylated poly l-lysine dendrimers. Mol. Pharmaceutics. 5, 449–463 (2008).
303. Agarwal, P.K.: Enzymes: An integrated view of structure, dynamics and function. Microb. Cell Fact. 5, 2 (2006).
304. Ramanathan, A., Agarwal, P.K.: Evolutionarily conserved linkage between enzyme fold, flexibility, and catalysis. PLoS Biol. 9, e1001193 (2011).
305. Case, D.A., Cheatham, T.E., Darden, T., Gohlke, H., Luo, R., Merz, K.M., Onufriev, A., Simmerling, C., Wang, B., Woods, R.J.: The Amber biomolecular simulation programs. J Comput Chem. 26, 1668–1688 (2005).

306. Maier, J.A., Martinez, C., Kasavajhala, K., Wickstrom, L., Hauser, K.E., Simmerling, C.: ff14SB: Improving the Accuracy of Protein Side Chain and Backbone Parameters from ff99SB. J. Chem. Theory Comput. 11, 3696–3713 (2015).
307. Salomon-Ferrer, R., Götz, A.W., Poole, D., Le Grand, S., Walker, R.C.: Routine Microsecond Molecular Dynamics Simulations with AMBER on GPUs. 2. Explicit Solvent Particle Mesh Ewald. J. Chem. Theory Comput. 9, 3878–3888 (2013).
308. Narayanan, C., Bernard, D.N., Bafna, K., Gagné, D., Chennubhotla, C.S., Doucet, N., Agarwal, P.K.: Conservation of Dynamics Associated with Biological Function in an Enzyme Superfamily. Structure. 26, 426–436.e3 (2018).
309. Nachon, F., Carletti, E., Ronco, C., Trovaslet, M., Nicolet, Y., Jean, L., Renard, P.-Y.: Crystal structures of human cholinesterases in complex with huprine W and tacrine: elements of specificity for anti-Alzheimer's drugs targeting acetyl- and butyryl-cholinesterase. Biochem. J. 453, 393–399 (2013).
310. Raves, M.L., Harel, M., Pang, Y.P., Silman, I., Kozikowski, A.P., Sussman, J.L.: Structure of acetylcholinesterase complexed with the nootropic alkaloid, (-)-huperzine A. Nat. Struct. Biol. 4, 57–63 (1997).
311. Agarwal, P.K.: Cis/trans isomerization in HIV-1 capsid protein catalyzed by cyclophilin A: insights from computational and theoretical studies. Proteins. 56, 449–463 (2004).
312. Ramanathan, A., Agarwal, P.K.: Computational identification of slow conformational fluctuations in proteins. J Phys Chem B. 113, 16669–16680 (2009).
313. Shukla, S., Bafna, K., Gullett, C., Myles, D.A.A., Agarwal, P.K., Cuneo, M.J.: Differential Substrate Recognition by Maltose Binding Proteins Influenced by Structure and Dynamics. Biochemistry. 57, 5864–5876 (2018).
314. Wang, Y., Schopfer, L.M., Duysen, E.G., Nachon, F., Masson, P., Lockridge, O.: Screening assays for cholinesterases resistant to inhibition by organophosphorus toxicants. Anal. Biochem. 329, 131–138 (2004).
315. Hovanec, J.W., Broomfield, C.A., Steinberg, G.M., Lanks, K.W., Lieske, C.N.: Spontaneous reactivation of acetylcholinesterase following organophosphate inhibition. I. An analysis of anomalous reactivation kinetics. Biochim. Biophys. Acta. 483, 312–319 (1977).
316. Agarwal, P.K.: A Biophysical Perspective on Enzyme Catalysis. Biochemistry. 58, 438–449 (2019).
317. Gupta, R.C.: Classification and Uses of Organophosphates and Carbamates. In: Gupta, R.C. (ed.) Toxicology of Organophosphate & Carbamate Compounds. pp. 5–24. Elsevier (2006).
318. Pyridostigmine Bromide [Package Insert]. Defense Supply Center. (2003).
319. Schumm, W.R., Reppert, E.J., Jurich, A.P., Bollman, S.R., Webb, F.J., Castelo, C.S., Stever, J.C., Kaufman, M., Deng, L.-Y., Krehbiel, M., Owens, B.L., Hall, C.A., Brown, B.F.C., Lash, J.F., Fink, C.J., Crow, J.R., Bonjour, G.N.: Pyridostigmine bromide and the long-term subjective health status of a sample of

over 700 male Reserve Component Gulf War era veterans. Psychol Rep. 90, 707–721 (2002).
320. Tibbitt, M.W., Dahlman, J.E., Langer, R.: Emerging Frontiers in Drug Delivery. J. Am. Chem. Soc. 138, 704–717 (2016).
321. Sheikhi, A., Hayashi, J., Eichenbaum, J., Gutin, M., Kuntjoro, N., Khorsandi, D., Khademhosseini, A.: Recent advances in nanoengineering cellulose for cargo delivery. Journal of Controlled Release. 294, 53–76 (2019).
322. Müller, A., Ni, Z., Hessler, N., Wesarg, F., Müller, F.A., Kralisch, D., Fischer, D.: The Biopolymer Bacterial Nanocellulose as Drug Delivery System: Investigation of Drug Loading and Release using the Model Protein Albumin. J Pharm Sci. 102, 579–592 (2013).
323. Roman, M.: Toxicity of Cellulose Nanocrystals: A Review. Industrial Biotechnology. 11, 25–33 (2015).
324. Johnson, C.D., Russell, R.L.: Rapid, Simple Radiometric Assay for Cholinesterase, Suitable for Multiple Determinations. Anal. Biochem. 64, 229–238 (1975).
325. Bruce, R.D.: A Confirmatory Study of the Up-and-Down Method for Acute Oral Toxicity Testing. Fundam. Appl. Toxicol. 8, 97-100 (1987).
326. Bhandari, J., Mishra, H., Mishra, P.K., Wimmer, R., Ahmad, F.J., Talegaonkar, S.: Cellulose nanofiber aerogel as a promising biomaterial for customized oral drug delivery. Int J Nanomedicine. 12, 2021–2031 (2017).
327. Huang, X., Brazel, C.S.: On the importance and mechanisms of burst release in matrix-controlled drug delivery systems. Journal of Controlled Release. 73, 121–136 (2001).
328. Wheatley, M.A., Chang, M., Park, E., Langer, R.: Coated alginate microspheres: Factors influencing the controlled delivery of macromolecules. Journal of Applied Polymer Science. 43, 2123–2135 (1991).
329. Pekarek, K.J., Jacob, J.S., Mathiowitz, E.: Double-walled polymer microspheres for controlled drug release. Nature. 367, 258–260 (1994).
330. Brazel, C.S., Peppas, N.A.: Mechanisms of solute and drug transport in relaxing, swellable, hydrophilic glassy polymers. Polymer. 40, 3383–3398 (1999).
331. Kishida, A., Murakami, K., Goto, H., Akashi, M., Kubota, H., Endo, T.: Polymer Drugs and Polymeric Drugs X: Slow Release of 5-Fluorouracil from Biodegradable Poly(γ-Glutamic Acid) and its Benzyl Ester Matrices:. Journal of Bioactive and Compatible Polymers. 13, 270–278 (1998).

VITA

Kirstin Paige Hester

Candidate for the Degree of

Doctor of Philosophy

Dissertation: ENHANCING INHIBITOR- AND ENZYME-BASED STRATEGIES FOR PROPHYLAXIS AGAINST ORGANOPHOSPHATE TOXICITY

Major Field: Veterinary Biomedical Sciences

Biographical:

Personal: Born in Norman, Oklahoma on December 21st, 1992, the daughter of John P and Karen L Poindexter.

Education: Completed the requirements for the Doctor of Philosophy in Veterinary Biomedical Sciences at Oklahoma State University, Stillwater, Oklahoma in December, 2019.

Received a Bachelor of Science in Microbiology/Cell & Molecular Biology *cum laude* at Oklahoma State University, Stillwater, Oklahoma in May 2015.

Experience: Raised in Broken Arrow, Oklahoma; employed as a veterinary kennel technician during high school; employed by Oklahoma State University's College of Arts and Sciences Technical Services as a Student Computer Technician; employed by Oklahoma State University Department of Physiological Sciences as an undergraduate research assistant; employed by Oklahoma State University Department of Physiological Sciences as a graduate research assistant

Professional Memberships: Society of Toxicology, American Association for the Advancement of Science, Phi Kappa Phi Honor Society